universität wien

DIPLOMARBEIT

Titel der Diplomarbeit

Synergistic anticancer activity of arsenic trioxide and the EGFR inhibitor erlotinib

Verfasser

Kushtrim Kryeziu

angestrebter akademischer Grad

Magister der Naturwissenschaften (Mag.rer.nat.)

Wien, 2011

Studienkennzahl lt. Studienblatt:	A 441
Studienrichtung lt. Studienblatt:	Diplomstudium Genetik - Mikrobiologie
Betreuerin:	Univ. – Prof. Mag. Dr. Renée Schröder

This diploma thesis was conducted at the

Medical University of Vienna

Department of Medicine I

Institute of Cancer Research

and was supervised by

Univ. – Prof. Mag. Dr. Renée Schröder

Ao. Univ. Prof. Dr. Walter Berger

Univ. Ass. Mag. Dr. Petra Heffeter

Danksagung

Sehr lange habe ich diesem Moment nachgefiebert und konnte es mir kaum vorstellen wie es sein könnte meine Diplomarbeit in meinen Händen zu halten. Nun ist es soweit. Ein Kapitel meines Lebens, welches meine Persönlichkeit, Wissen und Fähigkeiten sehr geprägt hat, ist zu Ende gegangen und ein neues wurde geschaffen.

Ich möchte mich an dieser Stelle bei den Personen bedanken, die mich bei der Erarbeitung dieser Diplomarbeit unterstützt haben.

Danke an ...

Prof. Walter Berger und **Dr. Petra Heffeter**, die mir während meiner Diplomarbeit unerschöpft zur Seite gestanden sind und die großartige Betreuung. Sie haben mir nicht nur wertvolle Tipps gegeben, sondern auch zu gleich mir ermöglicht meinen Horizont in verschiedenen Bereichen zu erweitern. Des weiteren möchte ich mich bei Dr. Petra Heffeter bedanken, dass sie mir die Freiheit gab, meine Arbeit nach meinen eigenen Wünschen und Vorstellungen zu entwickeln.

Prof. Renée Schröder vom Institut für Biochemie und Zellbiologie für die Betreuung und Begutachtung dieser Diplomarbeit.

all meinen KollegenInnen, **Christine Pirker, Ute Jungwirth, Walter Miklos, Daniela Lötsch, Mir Ali Reza Hoda, Bahil Ghanim, Theresa Tuder, Gerhard Zeitler** und **Johannes Gojo**, die mir in verschiedenen Situationen geholfen haben und immer eine Antwort für mich parat hatten und einfach für das tolle Arbeitsklima im Labor.

Christian Barcalek und **Vera Bachinger**, die mir im Labor immer hilfreich gewesen sind und den vielen netten Gespräche.

Prof. Michael Grusch und den MitarbeiterInnen am Institut für Krebsforschung für die gute Zusammenarbeit.

meinen Bruder **Atdhe**, der mit vielen künstlerischen Graphiken meine Diplomarbeit verbildlicht hat.

Nicht zuletzt gilt mein Dank meiner Familie, besonders meinen Eltern, die mich nicht nur finanziell unterstützt haben, sondern auch immer ein offenes Ohr für mich hatten und meine Anliegen zur ihr eigen machten. ``*Ju jeni arsya e vetme që unë jam ktu sot dhe jeni gjithashtu ata që beni të plotë botën time. Prandaj edhe ua dedikoj ketë diplomë. Ju lus të më falni nëse ju kam shkaktue mërzi edhe mall për gjithë këto vite që nuk ishim bashkë*``.

Abschließend bedanke ich mich herzlichst bei meiner Frau, für ihr Verständnis und die Liebe, die sie mir in dieser Zeit immer wieder entgegen gebracht hat.

Table of contents

Summary

1a

Arsenic is considered as the oldest remedy in the world which has been used for more than 2400 years. After rediscovery of anti-leukemic effects in the late 20th century, arsenic trioxide (ATO) has been approved for the treatment of relapsed or refractory acute promyelocytic leukemia (APL).

Aim of the here presented study was the investigation of a combination therapy of ATO and the EGFR inhibitor erlotinib against various malignancies but also to gain more insights into the molecular mechanisms underlying the synergistic action of this drug combination. In general, the drug combination was shown to act synergically against non-hematological malignancies as well as in chemotherapy-resistant cell lines *in vitro* and a xenograft A549 lung cancer model *in vivo*. These potent anticancer effects of the combination were found to be multifactorial and based on cytostatic (DNA synthesis stop and enhanced cell cycle arrest in G2/M phase) as well as cytotoxic effects (enhanced apoptosis induction). With regard to the underlying molecular mechanisms, we found that a functional and active wild-type EGFR pathway is necessary for the synergistic activity of ATO with erlotinib. Thus, no synergism was observed in cells resistant to erlotinib based on Met overexpression or hypersensitive to erlotinib due to a mutation which leads to constitutive activity of the EGFR. Synergistic effects of ATO were also observed (although always to a lesser extent) in combination with other EGFR inhibitors (gefitinib, lapatinib) as well as some other tyrosine kinase inhibitors (TKI) such as sorafenib, the p38 inhibitor SB203580 and especially the Akt inhibitor MK-2206. Notably, accumulation experiments revealed that erlotinib co-treatment distinctly enhanced the intracellular accumulation of ATO, probably by inhibition of multidrug resistance-related protein 1 (MRP1)-mediated efflux of ATO.

Taken together, out data reveal a potent synergistic activity of ATO in combination with erlotinib which is based on several molecular mechanisms. Consequently, this drug combination seems very promising for further (pre)clinical development especially in ATO-resistant cancer cell types.

Zusammenfassung

1b

Arsen gilt als eine der ältesten Arzneimittel, das seit über 2400 Jahren Verwendung findet. Die Wirksamkeit von Arsen gegen humane Krebszellen wurde Ende des 20. Jahrhunderts wiederendeckt und schließlich in Form von Arsentrioxid (ATO) zur Behandlung von Patienten mit rezidivierender beziehungsweise refraktärer Akuter Promyelozyten Leukämie (APL) zugelassen.

Ziel der hier präsentierten Studie war, die Wirksamkeit von ATO in Kombination mit dem neuen EGFR Hemmer Erlotinib zu untersuchen. Die Aktivitäten dieser Therapiekombination wurden in verschiedene maligne Zelllinien aus unterschiedlichen Ursprungsgeweben getestet und erforscht. Eine bemerkenswerte synergistische Aktivität von ATO und Erlotinib wurde sowohl in nicht-hämatologischen als auch in cisplatin-resistenten Krebszellen in der Zellkultur beobachtet. Die Substanzkombination zeigte eine synergistische Wirkung auch in nicht-kleinzelligen Lungenkrebs (NSCLC) Xenograft A549 in der Maus. Weiterführende Experimente ergaben, dass dieser Synergismus ein Ergebnis von verschiedenen Wirkungsmechanismen ist: 1) Die Substanzkombination zeigt zytostatische Effekte basierend auf einem DNA Synthesestopp und einem ausgeprägten Zellzyklus Arrest in G2/M, 2) die zytotoxische Wirksamkeit der Substanzkombination führte zu erhöhter Apoptoseinduktion. Generell hat sich herausgestellt, dass für einen erfolgreichen Synergismus ein funktionierender wild-typ EGFR Signalweg notwendig ist. Daher könnten die Effekte die Folge einer Interaktion der getesteten Substanzen mit dem EGFR Signaltransduktion sein. Diese Hypothese bestätigend, konnte kein Synergismus mit erlotinib-resistenten NSCLC Zellen (Met Amplifikation) oder erlotinib-hypersensitive Zellmodellen (aufgrund einer aktivierenden EGFR Mutation) festgestellt werden. ATO zeigte auch synergistische Wirkung sowohl mit anderen EGFR Inhibitoren (wenn auch in einem geringem Ausmaß), wie Gefitinib und Lapatinib, als auch mit anderen Tyrosinkinase Inhibitoren (TKI) (Multikinase-Inhibitor Sorafenib, p38 Inhibitor SB203580 und besonders mit Akt Inhibitor MK-2206). Bemerkenswerterweise konnte zusätzlich zur Blockade des EGFR Signalwegs gezeigt werden, dass Co-Inkubation mit Erlotinib zur Erhöhung der intrazellulären ATO Mengen führt. Diese hemmende Funktion beruht vermutlich auf Interaktion von Erlotinib mit den Multidrug Resistance-Related Protein 1 (MRP1), welches in Export von ATO aus der Zelle beteiligt ist.

Zusammengefasst zeigen unsere Ergebnisse eine synergistische Aktivität von ATO mit Erlotinib *in vitro* und *in vivo*, die auf mehreren molekularen Mechanismen beruht. Diese Kombination stellt dementsprechend eine vielversprechende Option besonders für die Therapie von ATO-resistenten Tumoren dar und sollte dringend weiter untersucht werden.

Introduction

2

2.1. Cancer: Incidence and mortality

All mammalian cells share similar molecular communication networks that constantly control the balance of cell division, differentiation or cell death. Cancer develops a degree of autonomy from these signals and is characterized by an enhanced proliferation of malignant cells. This abnormal state is caused by multiple changes in gene expression leading to deregulated balance of cell proliferation and cell death as well as the ability to invade tissues and metastasize to distant sites in the body[1]. Cancer is the leading cause of death worldwide and the second cause of death in Europe after cardiovascular diseases (Figure 1). In developed countries, the lifetime risk of developing cancer is more than one in three people, and one in four dies from it.

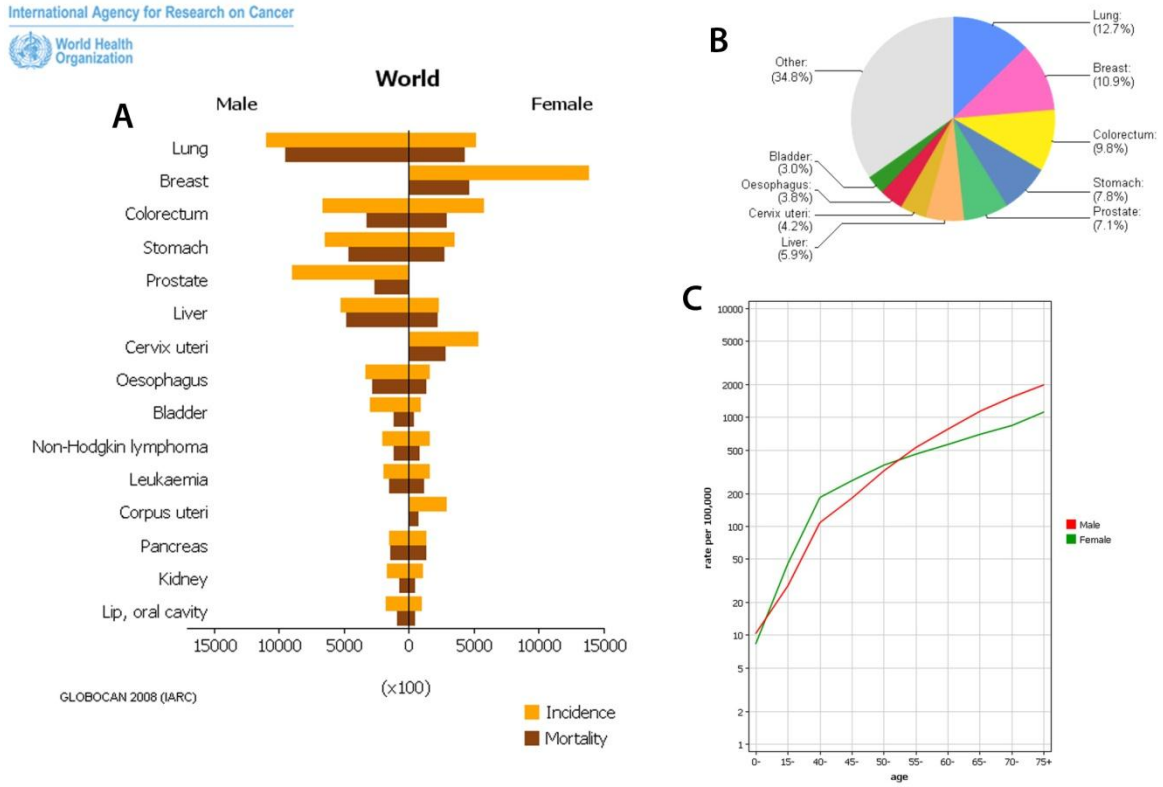

Figure 1. ***Cancer incidence and mortality. A*** *- Diagram showing cancer incidence (orange) and mortality (brown) of the top 15 leading cancers in the world.* ***B*** *- Pie diagram shows the percentage of various cancer incidences in both sexes.* ***C*** *- Age related cancer incidence in both sexes*[2].

The highest world incidence rates were seen in cases with lung, breast, colorectal, stomach, and prostate cancers, whereas lung, stomach, and liver showed the highest mortality rates. More than 70% of all cancer deaths occurred in low- and middle-income countries. Overall, predicted mortality from cancer worldwide shows a continuous rise with an estimated 12

million cases in 2020 (WHO, 2011[3]). Cancer can occur in persons of every age, but the incidence increases in elderly people (Figure 1 - C). Sixty percent of new cases and two thirds of cancer deaths occur in persons older than 65 years[4]. Moreover, incidence cancer rates are also influenced from human ethnology and gender. As example, prostate cancer is the most frequent cancer in males, but rates are 1.5 times higher in afro-caribbean men than in white. Similarly, the leading cancer in women is breast cancer with 20% higher incidence rates in white than in afro-caribbean woman[5]. Nearly 90-95% of all cancer cases can be attributed at least mainly to the environment and lifestyle. Heritable genetic defects are responsible only for 5–10% of all cancer cases (Figure 2).

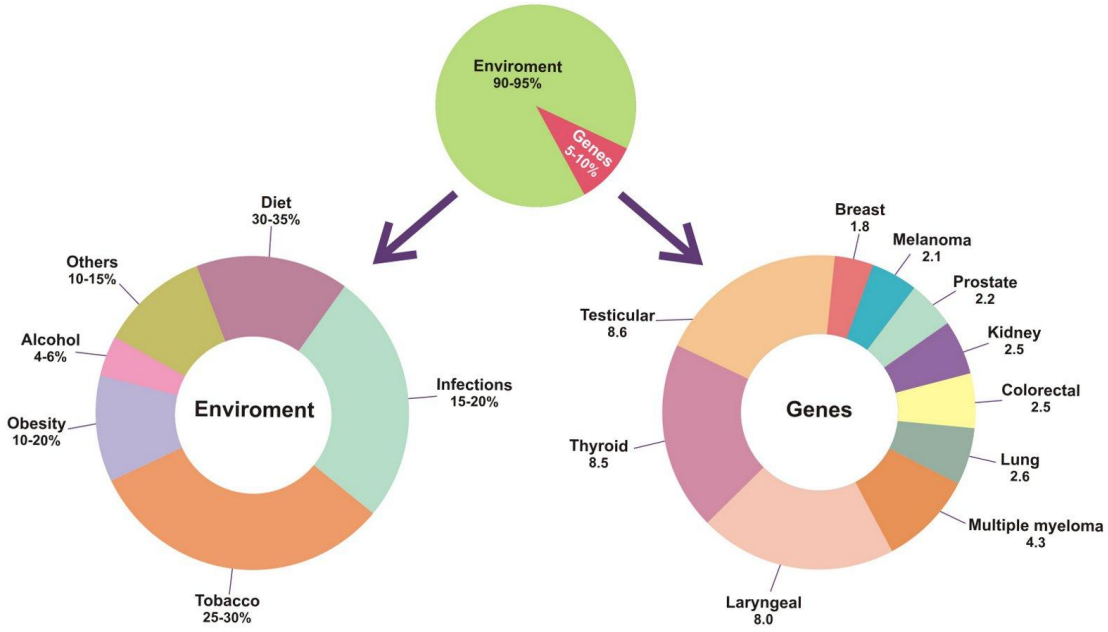

Figure 2. ***The role of genes and environment in the development of cancer. A -*** *The percentage contribution of genetic and environmental factors to cancer.* ***B -*** *Percentage contribution of each environmental factor.* ***C -*** *Family risk ratios for selected cancers. The numbers represent familial risk ratios, defined as the risk to a given type of relative of an affected individual divided by the population prevalence (Adapted from ref.[6]).*[7]

Lifestyle factors involved in cancer incidence include cigarette smoking, diet (fried foods, red meat), alcohol, environmental pollutants, sun exposure, infections, obesity, stress, and lack of physical activity. The evidence indicates that of all cancer-related deaths, almost 25–30% are due to tobacco, as many as 30–35% are linked to diet, about 15–20% are due to infections, and the remaining percentage are due to other factors like radiation, stress, low physical activity, environmental pollutants etc.[6].

2.1.1. Mechanisms of cancer development

The origin of cancer usually dates a long time back in the past, before the disease becomes clinically detectable. The incidence of leukemia in Hiroshima and Nagasaki showed a marked rise 5 years after the explosion of the atomic bombs, or the incidence of lung cancer rises significantly after around 10 to 20 years of heavy smoking[8]. During this long incubation period, cancer cells undergo a set of molecular changes. It is already known that genes contribute to common conditions of many types of malignancies and, thus, cancer might be considered also as a genetic disease. Currently, identified "cancer genes" include more than 1% of all human genes, of which approximately 90% exhibit somatic mutations in cancer, 20% bear germ-line mutations that predispose to cancer, and 10% show both somatic and germ-line mutations[5]. Cancer development can be summarized in three main stages: initiation, promotion, and progression (Figure 3).

In general, cancer is behaved to start with a mutational event in a single cell also known as tumor initiation. During tumor promotion, a clonally expansion of initiated cell follows as a result of released growth and proliferation factors from regenerating tissues. Accumulation of initiated cells form a neoplastic mass represents a pre-stage of cancer development with a high malignancy risk[5,9]. The progression stage of carcinogenesis is an extension of the tumor promotion stage and results from cell proliferation caused by promoting agents that allows the cellular damage to propagate and lead to the production of more genetic alterations. In addition, further alterations in the genome of the neoplastic cells during the progression phase lead to increased growth rate, invasiveness, metastatic capability and, finally, to a clinically detectable disease[1].

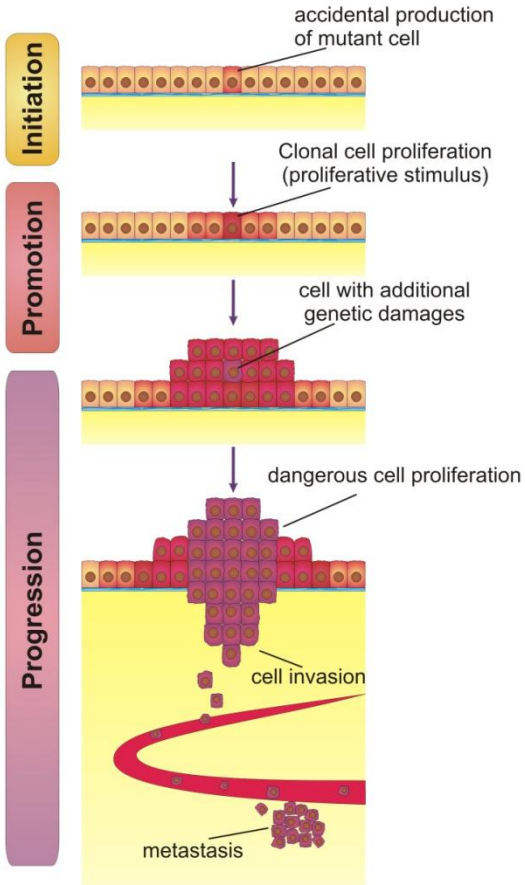

Figure 3. ***Three main stages in cancer development***[7]

The number of mutational hits minimally necessary for a malignant phenotype varies from one to six or more. Chronic myleogenous leukemia (CML) is an example with one hit event. This single hit is the chromosomal translocation between chromosomes 9 and 22 (philadelphia chromosome). As a result, a chimeric active tyrosine kinase called Bcr/Abl is produced which promotes cell proliferation[1]. A two mutational hit phenomenon is retinoblastoma, a cancer that develops from the loss of functional tumor suppressor gene (*RB*) in cells of retina (Knudson's ''two hit'' model). Inheritance of this tumor predisposition is associated with the loss of the 13q14 chromosome region, were the *RB* is normally located. Heterozygous loss of *RB* could be inherited, whereas the second mutation occurs somatically during embryogenesis or early in life that finally leads to the homozygous *RB* loss and disease[10].

Proto-oncogenes, tumor-suppressor genes, and caretaker genes like DNA repair genes play a key role in tumor initiation. Combinations of mutations from those three types of genes can lead to tumor development[5]. Proto-oncogenes are normal genes, whose products are proteins involved in cell growth and differentiation. Mutations or increased expression of proto-oncogenes lead to pathological activation of oncogenes and, subsequently, in enhanced survival or proliferation of normal cells as well as malignant transformation. The activation process of proto-oncogenes to oncogenes can include structural alterations from point mutations in a single gene to chromosomal translocations, and gene amplification, leading to overexpression of the oncogene[5] (Figure 4).

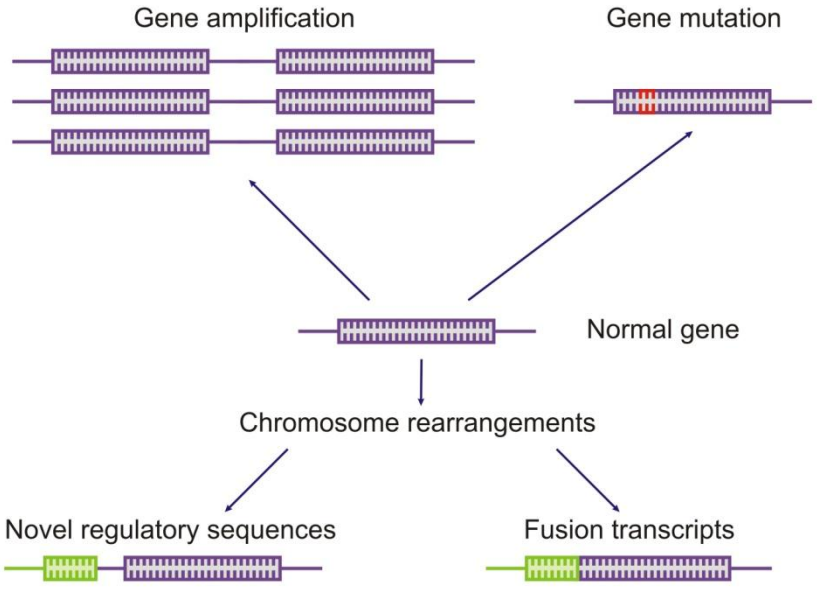

Figure 4. ***Schematic representation of the main mechanisms of proto-oncogene activation to an oncogene (Adapted from ref.[11])[7].***

One of the acquired abilities of a transformed cell is modulation of cell cycle checkpoints. The cell cycle is defined as the sequence of events that regulate cell division[12]. There are two main phases of the cell cycle in non-reproductive cells: Interphase and cell division (mitosis (M)). Interphase is than subdivided in three stages (gap 1 (G1), DNA synthesis (S), and gap 2 (G2)) (Figure 5).

Check points are sequences in eukaryotic cell cycle where further progression can be stopped until conditions are suitable for the cell to proceed to the next stage. Oncogenes can allow check points to be overcome and drive the cell cycle forward, typically causing cells to proceed from G1 to S phase or from G2 to mitosis. Regulators of the cell cycle like cyclin-dependent kinases (CDKs) and their activators (cyclins) are some of the candidate proteins targeted from oncogenes. Therefore, instead of staying within a G phase, a transformed cell with activated oncogenes continues to progress through the cell cycle, leading to uncontrolled cell division.

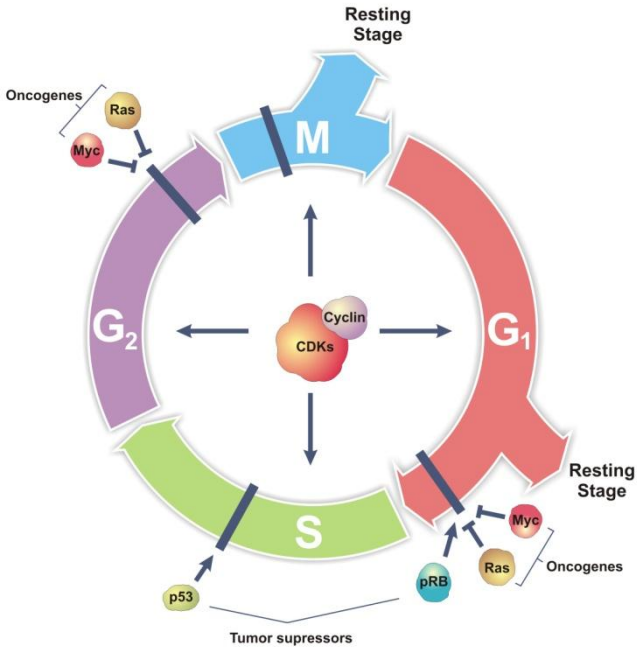

Figure 5. ***Cell cycle and regulation:*** *Checkpoints are depicted as thick red bars. The stages of the cell cycle (G1: Gap 1, S: DNA synthesis, G2: Gap 2, and M: mitosis) are indicated. Tumor suppressors act to maintain checkpoints (arrows) whereas oncogenes allow for checkpoints to be overcome (stop lines) (Adapted from Kopnin 2000)*[7]

Tumor suppressor genes are the cell-governors of proliferation. Many of those genes monitor DNA damage and help to repair the damage before cells undergo further cell division[5]. Additionally, tumor suppressor genes encode proteins whose absence, repression, inactivation of expression, or mutation promotes oncogenesis[10]. Typical tumor suppressor genes are found to be involved at the two DNA damage checkpoints of the cell cycle: G1/S and G2/M (Figure 5). This enables cells to check the integrity of the chromosomes before proceeding into S phase or mitosis. Loss of tumor-suppressor function releases the cell cycle from these checkpoints. As a result, DNA damage is not repaired and cells accumulate mutations that ultimately can lead to cancer progression[5]. *RB* was the first tumor suppressor

gene identified in retinoblastoma (see above), and together with the transcription factor p53 encoded by the *TP53* gene are the best known examples in controlling growth arrest, differentiation, and apoptosis. As already mentioned loss of RB function induces cell proliferation because RB mediates control of G1/S transition. RB has many serine and threonine phosphorylation sites. Active RB is not phosphorylated and binds E2F that is important for G1/S transition. Growth stimulation signals induce the expression of cyclin D and cyclin E which activate CDKs. Those cyclin-CDK complexes phosporylate RB and further release E2F to start the synthesis of S phase proteins. In contrast, growth inhibition signals like TGFβ induce the expression of phosphates that specifically inhibit CDKs and thereby keep the cell cycle in G1[9]. Tumor suppressor p53 receives inputs from stress and abnormality sensors like genomic damage or availability of nucleotides, glucose, and oxygenation. Therefore, p53 stops the cell cycle progression until these conditions have been normalized. Otherwise, signals of irreparable damage from those conditions can trigger p53 mediated apoptosis[13]. P53 is permanently degraded and, thus, very small amounts of this protein are detectable in undamaged cells. DNA damage stabilizes and activates p53 by releasing it from Mdm2 protein. Active p53 induces the expression of p21waf that inhibits the cyclin E/CDK2 and cyclin A/CDK2 complexs and further inhibits the G1/S transition. Furthermore, p53 induces the expression of DNA repairing enzymes. However, if DNA damage proves to be irreparable, p53 activates Bax which finally induces apoptosis[14]. *TP53* gene is often mutated in tumor cells. Mutations usually disrupt DNA binding domain that leads to accumulation of tumor cells with DNA damage.

2.1.2. Hallmarks of cancer

In fact, malignant tumors are more than insular masses of proliferating cancer cells. The proposed model ''The Hallmarks of Cancer'' from Hanahan and Weinberg in 2000, simplified the complexity of malignant cancer in six capabilities: self-suficiency in growth signals, insensitivity to anti-growth signals, tissue invasion and metastasis, limitless replicative potential, sustained angiogenesis, and impaired apoptosis[15]. Since then, the understanding of cancer complexity has further progressed. Recently, the same authors added four emerging hallmarks to their model: reprogramming of energy metabolism and avoidance of the destruction by the immune system as well as genome instability and tumor-promoting inflammation[13] (Figure 6).

Sustaining proliferative signals

Figure 6. ***Hallmarks of Cancer***[13]

Some tissues in the body have faster proliferation ratios than the others, and there are also tissues that stop their proliferation in a distinct developmental stage. Moreover, this proliferation is strictly regulated to accomplish the normal tissue architecture and function. Healthy cells need proliferative signals (mitogenic signals) to survive and fulfill their physiological functions. Mechanisms controlling the release and sources of those signals in normal tissues are poorly understood. In contrast, cancer mitogenic signaling is better understood. Proliferative control in cancer cells is usually disrupted, therefore cancer cells gain they own supervision over mitogenic signals. In general, there are different ways how cancer cells acquire the capability to sustain proliferative signaling. For example, autocrine stimulation by growth factor ligands, increase of the respective receptor proteins at the cancer cell surface or production of ligand-independent receptor molecules are attributes of various cancer cells. An alternative way for cancer cells to be supplied with growth factors is paracrine stimulation of normal cells to produce those factors for them[13,16]. Proliferative signaling depends not only on ligands and their receptors on the cell surface. Somatic mutations in certain tumor types can affect downstream transducers which can activate proliferation pathways independently from receptor activation. For example, activating mutations affecting the structure of b-Raf protein are present in more than ~60-70% of human melanomas. Activated b-Raf leads to constitutive signaling of MAP kinase pathway, important for proliferation (see MAPK signaling, section 2.4.1)[17-19].

Moreover, negative feedback loops are important in the repression of various types of signaling to ensure homeostatic regulation. In contrast, aberrant signal processing and feedback regulation mechanisms can lead to proliferative signaling enhancement[20]. An example of this type of regulation involves the Ras oncoprotein, part of a proliferation

signaling pathway. Ras GTPases have a high affinity for both guanosine triphosphate (GTP) and guanosine diphosphate (GDP). They work as binary switches by cycling between inactive GDP- and active GTP-bound conformations. Oncogenic mutations affecting *Ras* genes usually compromise Ras GTPase activity. The disrupted Ras GTPase protein is not able to fulfill the conformation change which normally operates as an intrinsic negative-feedback. As a result, the signal transmission continues permanently without interruption resulting in proliferation[10,13].

Evading growth suppressors

Long-living organisms like humans, have a large potential for somatic mutational load. As an example, point mutations that activate Ras occur in thousands of cells every day[5]. Without the powerful protection programs of healthy cells, the risk of cancer development would be much higher than it actually is. Another reason for enhanced proliferation typical for cancer cells is to overcome those programs that negatively regulate cell proliferation. Thus, tumor suppressor genes are frequently inactivated in human cancers (mentioned above). Dozens of tumor suppressors that operate in various ways to limit cell growth and proliferation have been discovered.

Cell-cell contacts formed by dense non-malignant cell populations are an important feature to regulate cells positional identity and achieve two-dimensional tissue architecture. Healthy cells show ''contact inhibition'' *in vitro* as a result of contact response with other cells and, finally, suppress further cell proliferation. This ability is lost in cancer cells. Thus, they continue to divide even in dense culture conditions.

One of the proteins that play important roles in stabilizing contact inhibition is Merlin (moesinezrin-radixin-like protein), encoded from Neurofibromatosis type 2 gene (NF2). Mutations of NF2 gene lead to human neurofibromatosis and were also found in several cancers like: thyroid cancer, mesothelioma, and melanoma[21]. Merlin stabilizes the contact inhibition via coupling cell surface adhesion molecules (e.g. E-cadherin) to transmembrane receptor tyrosine kinases (e.g. EGF receptor) and, thus, it serves as a key regulator of several important signaling pathways that regulate cell motility, proliferation, and survival. Such mechanisms that enable cells to construct and maintain architecturally complex tissues show an important way of suppression and counterbalance of proliferative signals[13].

Resisting cell death

Apoptosis or programmed cell death was initially recognized during healthy developmental processes[10]. Apoptosis represents a ''clean'' way of cell death that evokes inflammatory responses. It is characterized by cell shrinkage, chromatin condensation, nuclear fragmentation and appearance of plasma membrane surrounded apoptotic bodies that are easily removed by phagocytes. There are two main ways of apoptosis initiation. Cell signals may originate extracellularly, from cell surface receptors, such as Fas and tumor necrosis factor receptor-1 (TNFR1) (extrinsic pathway) or, intracellularly, by various genotoxic agents, metabolic insults or transcriptional cues (intrinsic pathway) (Figure 7)[22].

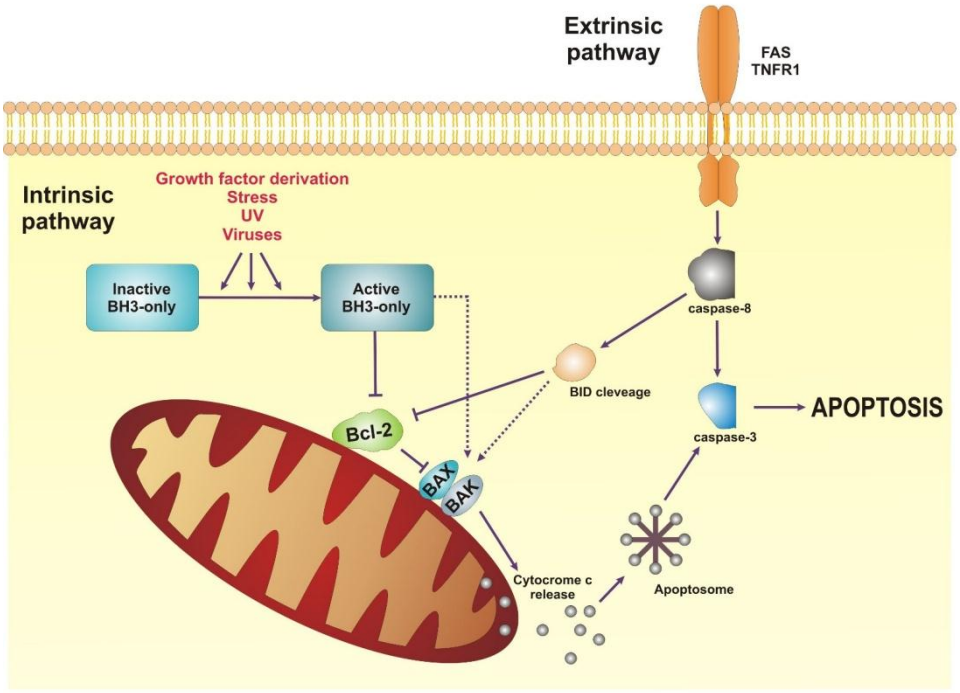

Figure 7. ***Apoptosis:*** *Intrinsic and extrinsic pathways (Adapted from ref.[22])*[7]

Also loss of cellular survival factors may initiate apoptosis[22]. The extrinsic pathway starts with death receptors FAS or TNFR1 which can activate caspase-8 through the adaptor protein Fas-associated death domain (FADD). Caspase-8 leads to mitochondrial-independent caspase-3 activation. Caspases in turn cleave a series of substrates, activate DNases and orchestrate the demolition of the cell.

Mitochondria play a critical role in promotion of intrinsic apoptotic signals. There are several BCL-2 protein family members that govern mitochondrial outer membrane permeabilization and can be either pro-apoptotic or anti-apoptotic. BCL-2 protein is controlled from BH3-only protein family who receives signals from different stimuli such as DNA damage, UV, viruses,

growth factor deprivation etc,. BCL-2 inhibits BAX and/or BAK activation. Once activated, BAX and BAK promote channel formation in the outer mitochondrial membrane following cytochrome c release and mitochondrial fission. Free cytochrome c in the cytoplasm leads to the recruitment of APAF1 into the apoptosome which, in turn, activates caspase-9 and further caspase-3 cleavage. BIM and PUMA (BH3-only proteins) are able to directly activate BAX and/or BAK, without BCL-2 inhibition. BID is another pro-apoptotic BCL-2 homologue and already a BH3-only protein with a unique role that links the intrinsic and extrinsic apoptosis pathways. BID can be activated through extrinsic caspase-8 cleavage. Therefore, the C-terminal form of BID (tBID) translocates to mitochondria and promotes further intrinsic caspase activation (caspase-9 and the effector caspase-3, -6 and 7)[23-24]. The common loss of p53 tumor suppressor function is one of the strategies that tumor cells have evolved to evade apoptosis (mentioned above). There are several proapoptotic transcriptional targets of p53, such as BAX, NOXA, and PUMA, that in case of p53-loss, cannot promote cytochrome c release from the mitochondria[10]. Otherwise, tumors can achieve apoptosis resistance by upregulation of anti-apoptotic regulators (Bcl-2, Bcl-xL) and survival signals (Igf1/2), or by downregulation of proapoptotic factors (Bax, Bim, Puma). Various apoptosis-avoiding mechanisms at the same time reflect the diversity of apoptosis-inducing signals that cancer cell populations encounter during their evolution to malignancy[13,25].

Autophagy represents an important cell-physiologic response to stress or starvation. During this process, portions of the cytoplasm and intracellular organelles like ribosomes and mitochondria are sequestered in double-membrane-bound structures known as autophagosomes. These autophagosomes fuse with lysosomes to form autolysosomes. The contents inside the autolysosomes can be energetically recycled after degradation by lysosomal hydrolases. The PI3K/Akt signaling pathway is induced by survival signals to block apoptosis (see PI3K/Akt signaling, section 2.4.2). Similarly, induction of the same pathway blocks autophagy. Autophagy and/or apoptosis can be induced after insufficient survival signals that lead to downregulation of PI3K signaling pathway[26]. Genetic studies have shown that Beclin-1 is necessary for autophagy induction, and already serves as another link between apoptosis and autophagy[26]. Beclin-1 as a member of the BH3-only subfamily of apoptotic regulatory proteins, binds the Bcl-2/Bcl-xL proteins. Stress-sensor-coupled BH3 proteins (e.g., Bid, Bad, Puma, etc.) can induce apoptosis and/or autophagy, depending on the physiologic state of the cell. Those proteins can release Beclin-1 from its association with

Bcl-2/Bcl-xL to trigger autophagy with a higher affinity, than they can release proapoptotic Bax and Bak to induce apoptosis[13]. Defective autophagy through allelic loss of *beclin-1* or deficiency in the activation of the PI3K pathway promotes tumorigenesis. This suggests that induction of autophagy can be seen as a mechanism that kills malignant cells. On the other hand, there are types of autophagy that promote cell survival of cancer cells after tumor development under conditions of poor nutrient supply[27]. Cancer cells after various stress conditions can shrink via autophagy to a state of reversible dormancy. This survival response may enable the persistence and eventual re-growth of some late stage tumors following treatment with potent anticancer agents[13]. Thus, paradoxically, it is so far unclear if autophagy represents a survival or a suicide mechanism for tumor cells[28].

In comparison to apoptosis and autophagy, necrosis (another type of cell death) is characterized with cell swelling and integrity loss of plasma membrane that leads to the exposure of cytoplasmic contents into the extracellular space (Figure 8).

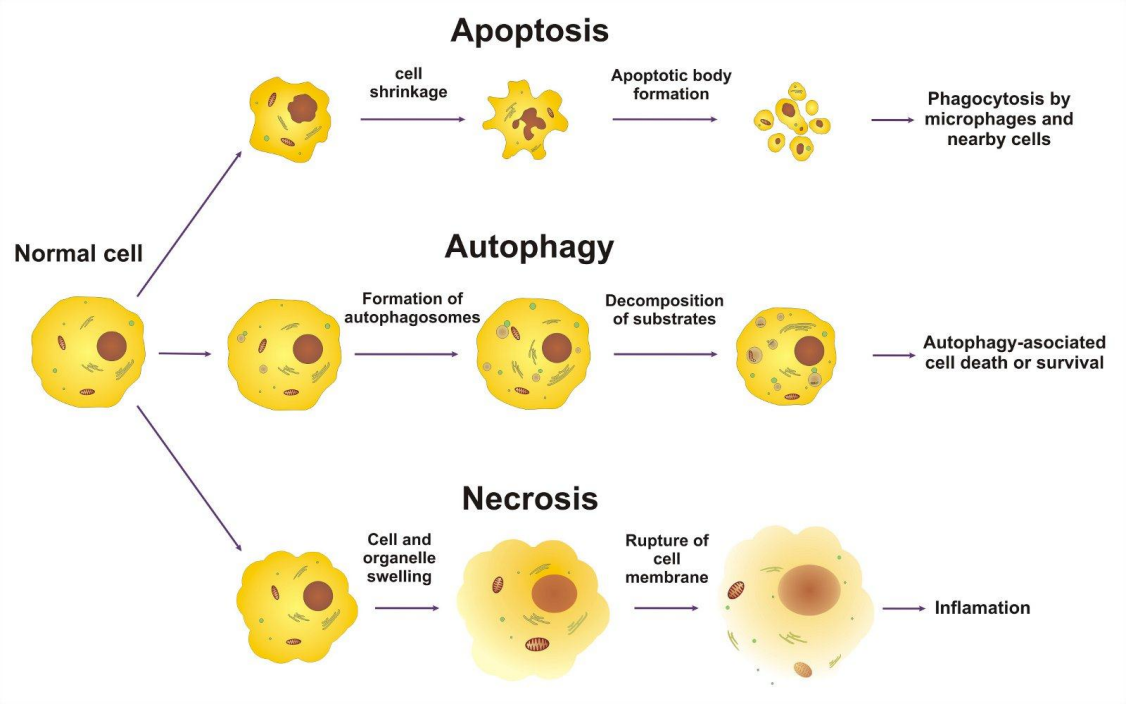

Figure 8. ***Three pathways of cell death*[7].**

Unlike apoptosis, the necrotic debris released in the local microenvironment is not consumed by phagocytes but recruits inflammatory cells. Those cells can trigger inflammation and in the context of neoplasia can be tumor promoting. Furthermore, necrotic cells can release regulatory factors like IL-1α, which can directly stimulate neighboring cells to proliferate. Once again, some degree of necrotic cell death could be used for starting neoplasias and

potentially invasive and metastatic tumors to progress as a result of recruited tumor-promoting inflammatory cells and their growth-stimulating factors[13,29].

Enabling replicative immortality

Non-malignant cells are characterized by limited replication potential. Thus, after about 50 generations they usually stop successive cell growth-and-division cycles and undergo an irreversible nonproliferative, but viable state that is also known as senescence. This process has been associated with various aspects of aging, but may also play an important role in preventing cancer[5]. Another barrier of proliferation in non-malignant cells is cell crisis which ends in apoptosis. Rarely, some cells overcome senescence and cell crisis to an immortalization state, characterized with unlimited replication potential. Telomere stabilizations are essential in the capacity for unlimited proliferation. Telomeres are located at the end of chromosomes, representing protein-protected open DNA-strands. Thus, they protect chromosomal shortening and end-to-end fusions[13]. The length of telomeres determines the number of cell divisions allowed for a given cell. In vertebrates, telomeres are made of tandem repeat sequences (TTAGGG) that are continuously lost during the incomplete replication of linear chromosomes by conventional DNA polymerases (end-replication problem). Telomerase is a reverse transcriptase that prevents constant loss of important DNA from chromosome ends by elongation of shortened TTAGGG sequences[30]. This enzyme is almost absent in somatic cells but expressed at high levels in germ cells as well as the majority of spontaneously immortalized cells, including human cancer cells. The presence of telomerase activity correlates with resistance to both senescence and apoptosis. In contrast, suppression of telomerase activity leads to activation of proliferative barriers. Recently, it has become apparent that telomerase has noncanonical functions that are relevant to cell proliferation but unrelated to telomere maintenance. For example, telomerase subunit TERT was shown to amplify signaling of cancerogenic Wnt pathway, by serving as a cofactor of the β-catenin/LEF transcription complex[31]. Other telomerase activities include enhancement of cell proliferation and/or resistance to apoptosis[32], involvement in DNA-damage repair[33], and RNA-dependent RNA polymerase function[34]. These additional functions of telomerase to tumorigenesis remain to be fully clarified[13].

Inducing angiogenesis

The vascular system of vertebrates continuously supplies almost all body tissues with oxygen and nutrients. At the same time, it eliminates metabolic waste products and carbon dioxide. Early in the development of the vertebrate embryo, blood vessels are formed from endothelial precursor cells (angioblasts) in a process called vasculogenesis. Later in the development, the growth of new blood vessels from existing vasculature is known as angiogenesis. This process is essential for growth of organs but also malignant tumors and their metastases[35]. Angiogenesis is remarkably quiescent in adult times, occurring mainly during menstruation and wound healing. In contrast, during tumor development and progression angiogenesis is almost always activated, causing normal quiescent vasculature to continually sprout new vessels that help tumors to expand in size[36]. When a tumor starts to produce angiogenic factors (also known as *angiogenic switch*), it activates endothelial cells in the vasculature of the surrounding tissue to initiate angiogenesis[37]. In the last 20 years many factors with pro- and anti-angiogenic activity have been identified and include growth factors, cytokines, chemokines etc. For example, the well-known vascular endothelial growth factor-A (VEGF-A) belongs to the inducers and thrombospondin-1 (TSP-1) to the inhibitors of angiogenesis[13]. VEGF and three of its receptors (VEGFR 1-3) orchestrate new blood vessel growth during embryogenesis and postnatal development. Additionally, other pro-angiogenic ligands such as members of the fibroblast growth factor family (FGF) were shown to be involved in tumor vascularization. They induce the production of proteases by endothelial cells and stimulate tube formation in three-dimensional cell culture systems. Angiogenic activity of FGFs is observed in all *in vivo* assays and is often used as a positive control in angiogenesis assays[37]. Suppressive signals from TSP-1 maintain a counterbalance in angiogenic switch[38]. TSP-1 binds to transmembrane receptors of endothelial cells and activates suppressive signals[39]. Other natural inhibitors like angiostatin and endostatin are selective and potent endogenous inhibitors of angiogenesis that show promise as future therapeutic agents[10]. The blood vessels produced within tumors induced by an unbalanced mix of proangiogenic signals are typically aberrant. They are usually characterized with premature capillary sprouting, convoluted and excessive vessel branching, distorted and enlarged vessels, erratic blood flow, micro hemorrhaging, leakiness, and abnormal levels of endothelial cell proliferation and apoptosis. Angiogenesis was previously seen to be important only in rapidly growing macroscopic tumors, but recently, it was indicated that

angiogenesis contributes also to the microscopic premalignant phase of neoplastic progression[13].

Activating invasion and metastasis

In most cases, cancer is diagnosed at late stages of the disease and is characterized by tumor invasion and metastasis. Unfortunately, patients with obvious or occult metastases always have a bad prognosis[37]. Invasion and metastasis is a multistep process that undergoes a sequence of discrete steps, often termed as the invasion-metastasis cascade[40]. Cell-biologic changes involved in this cascade begin with local cell invasion. This process is an active translocation of neoplastic cells across tissue boundaries and through host cellular- and ECM barriers. Invasive cancer cells acquire the ability to migrate, develop alterations in their shape and in attachment capability to other cells or to the extracellular matrix (ECM). E-cadherin is the prototypic protein that maintains cell–cell adhesions in the human epithelial tissues[41]. Increased expression of E-cadherin was well established as a suppressor of invasion and metastasis, whereas reduced expression was observed to potentiate these phenotypes[13,42]. Epithelial cancer cells can lose E-cadherin when they progress towards malignancy in several ways: 1) inherited- or spontaneous mutations of the responsive gene, 2) aberrant protein processing, 3) increased promoter methylation, and 4) induction of transcriptional repressors such as Snail and ZEB family members[41]. Epithelial-mesenchymal-transition (EMT) is another developmental regulatory program by which cancer cells down-modulate their cell-cell adhesion structures. Regarding cancer, during EMT, cells become isolated, motile, and resistant to apoptosis. EMT plays a key role in gastrulation (embryological event in vertebrates). Later in development, EMT participates in the formation of numerous organs and tissues. In adults, EMT-like processes occur during wound healing and pathological fibrosis. These multifaceted programs can also be activated transiently or stably during invasion and metastasis[43-44]. It has been shown that several transcriptional factors (Snail, Slug, Twist, and Zeb1/2) which orchestrate EMT during embryogenesis are also expressed in various combinations in malignant tumors. The same factors were shown to be important for programming invasion and metastasis[45-48]. Lack of EMT-inducing factors may revert carcinoma cells to a noninvasive state. The reverse process of EMT is called the mesenchymal-epithelial transition (MET) and may result in the formation of new tumor cell colonies of carcinoma cells similar to those in the primary tumor that never underwent an

EMT[49]. After ECM penetration, cancer cells enter nearby blood and lymphatic vessels. Cancer cells are then transported through the lymphatic and hematogenous systems. Metastases are clones of tumor cells in tissues distant from the primary tumor site, which follow the escape from the lumina of blood or lymphatic vessels into the parenchyma of distant tissues (extravasation). The process of metastasis starts with small nodules of cancer cells (micrometastases), which then develop to macroscopic tumors (colonization)[13].

Reprogramming energy metabolism

Transformed cells are characterized not only with rapid proliferation but also modified metabolic activity. Enhanced nutrient supply, energy production, and biosynthesis of various macromolecular building blocks are needed during each passage of proliferating cells[50]. In normal aerobic conditions, cells metabolize glucose first to pyruvate via glycolysis and then to carbon dioxide in a process known as oxidative phosphorylation. Thereby, 36 adenosine triphosphate (ATP) molecules per glucose are produced that supply metabolism with energy (Figure 9).

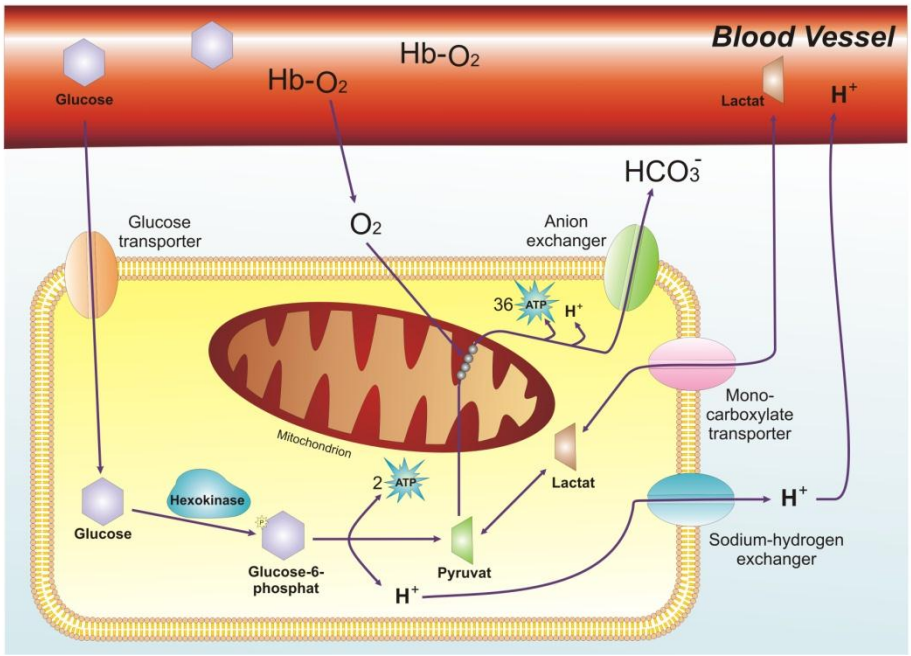

Figure 9. ***Glucose metabolism in mammalian cells*** *(Adapted from ref.[51])*[7]

Under anaerobic conditions, glycolysis ends with the production of lactate and only two ATP molecules. Interestingly, even in the presence of oxygen, proliferating cancer cells often limit their energy production largely to glycolysis. This metabolic switch, termed ''aerobic glycolysis'' was first observed by Otto Warburg in 1920s. Warburg published that rapidly

proliferating tumor cells consume glucose at a surprisingly high rate compared to normal cells and secrete most of the glucose-derived carbon as lactate rather than oxidizing it completely (Warburg-effect)[52].

The mechanism of aerobic glycolysis as a wasteful form of metabolism in proliferating cells presented a paradox for decades. It was observed that many tumor types upregulate the glucose transporter GLUT1, which increases glucose import into the cytoplasm[52]. Notably, if the glycolytic flux is sufficient, the amount of cellular ATP produced from glycolysis can even exceed the ATP amount of molecules produced from oxidative phosphorylation. Another advantage in anaerobic energy production is also minimized production of free radicals generated in oxidative metabolism, which are toxic to the cell[53]. Glycolytic flux has also been shown to be associated with hypoxic conditions (oxygen deficiency), activated oncogenes (e.g., Ras, Myc) and mutant tumor suppressors (e.g., p53). Furthermore, both Ras oncoprotein and hypoxia can independently increase the levels of transcription factors HIF1α and HIF2α, which in turn upregulate glycolysis[13]. Interestingly, there are tumors with two subpopulations of cancer cells which can act symbiotically in energy production even if they differ in their oxygenation capacity. On the one hand, a hypoxic cell subpopulation secretes lactate as waste product of glycolysis that might diffuse and be taken up by the oxygenated tumor cell subpopulation as their main energy source. On the other hand, preferential utilization of lactate for oxidative metabolism spares glucose which may in turn reach the hypoxic tumor cell population[13,54].

Evading immune destruction

Humans and animals which are born without a proper functional immune system or undergo immunosuppression suffer from multiple infections and usually die at early age. However, beside multiple infections, the immune system also prevents, or at least delays, the growth of many tumors[10]. The ''immune surveillance'' theory suggests that cells and tissues are constantly monitored by the immune system and that the majority of incipient cancer cells are recognized and eliminated. Various clinical and experimental data seem to be in accordance with the immune surveillance theory. Evidence, both from genetically engineered mice and from clinical epidemiology, suggests that both the innate and adaptive immune systems are able to contribute significantly as a barrier to tumor formation and progression[55]. Despite this, tumors do appear also in immune-competent individuals. Basically all clinically detectable tumors have managed to avoid detection by immune system or have been able to

limit the extent of immunological killing, thereby evade eradication[13]. Also infected humans with HIV (human immunodeficiency virus) or pharmacologically immunosuppressed patients, which are predominantly immunodeficient in the T- and B-cell compartments, exhibit a residual capability for an immunological defense against cancer that is mounted by NK cells and other innate immune cells[13]. The mechanisms by which tumor cells evade the immune system are multiple. For example, cancer cells may block the activity of immune cells and manipulate the host immunity by secretion of TGF-β or chemokine like CCL21[56-57]. TGF-β exerts systemic immune suppression and inhibits host immune surveillance. Furthermore, TGF-β inhibition enhances CD8+ T-cell- and NK-cell-mediated anti-tumor immune responses. Another escape mechanism from immune surveillance is recruitment of inflammatory cells with immunosuppressive activity induced by cancer cells. Those immunosuppressive cells include regulatory T-cells and myeloid-derived suppressor cells (MDSCs)[58-59].

2.1.3. Cancer classification

There are hundreds of different tumor types that originate from nearly every tissue and every organ. Tumors are subdivided in two major classes ''benign'' and ''malign''. Benign solid tumors are widely harmless and do not progress, invade or metastasise. They are usually not connected to the healthy surrounding tissue, but separated by a capsule of connective tissue. Malignancy or malignant tumor is another synonym for cancer. Malignant tumors have the tendency to become progressively dedifferentiated, and further invasion and metastasis into health tissues result in death of the whole organism. Malignant tumors have no well-defined capsule and the tumor cells grow in a much more disorganized form than benign tumors[10]. Cancers are classified in two different ways: by the type of tissue from which the cancer originates (histological type) at the primary site, or the location in the body where the cancer first developed. Cancers are generally classified as either non-adherent leukemias or solid tumors. Leukemias and lymphomas are neoplastic cells whose precursors are usually motile. Solid cancers originate from epithelial or mesenchymal cells that are usually immobile[5].

Examples of general cancer categories include:

1. Carcinomas – represent over 80% of diagnosed human cancers each year. They originate from epithelial cells in the skin or tissues that line or cover internal organs. Carcinomas include the common forms of breast, prostate, lung, and colon cancer.

2. Sarcomas – are malignant tumors derived from connective tissue or mesenchymal cells. Sarcomas include tumors of bone, cartilage, fat, muscle, vascular, or other connective or supportive tissues.

3. Leukemias – are a non-adherent cancer type which originate in the blood-forming tissues like bone marrow and are characterized by abnormal increase of blood cells that enter the blood stream. Leukemias can be further divided into acute leukemia (rapid increase of immature blood cells) and chronic leukemia (excessive increase of relatively mature, but still abnormal white blood cells).

4. Lymphomas – originate from cells of the immune system. It arises at lymph nodes or other lymphatic tissues and often manifests as painless enlargement of one or more lymph nodes. Lymphomas include tumors of B-, T-, and NK-cells.

5. Cancers of the central nervous system – originate in the tissues of the brain and spinal cord. They include gliomas, meningiomas, pituitary adenomas, vestibular schwannomas etc.[1,4-5].

2.2. Cancer therapies

Cancer is treated in several ways that depend on the medical condition of each person as well as type and location of the cancer. Cancer detected in early stages has a much better prognosis than metastatic malignancies. Several treatment methods can be used alone or in combination. Surgery is the oldest method and still offers the best chances for curative cancer tratment[4]. Other common treatment strategies involve: chemotherapy, targeted therapy, radiation therapy, immunotherapy or hormonal therapy.

2.2.1. Chemotherapy

Chemotherapy covers any therapeutic intervention that utilizes chemicals and pharmaceutical compounds to kill rapidly proliferating cells. Side effects of chemotherapeutic drugs are usually correlated with disruption of those tissues whose cells proliferate quickly. Somatic cells with a high proliferation ratio include hematopoietic cells in the bone marrow, mucosa of the digestive tract, and hair follicle cells[5]. Drug-induced damage of these tissues leads to diarrhea, hair loss, or immunosuppression. Chemotherapy is usually used in combination settings with the aim to increase anticancer activity, to decrease side effects, and to minimize the possibility for drug resistance. The majority of chemotherapeutic drugs interact directly

with cellular DNA or DNA-associated proteins resulting in the DNA synthesis inhibition. Additionally, they might affect microtubules and further disrupt chromosome organization during cell division. The bridge between the mode of action and the final activity (e.g. cell cycle arrest, necrosis, or apoptosis) for many chemotherapeutic drugs is not always fully understood[10].

2.2.2. Targeted therapy

Targeted therapy is a new generation type of medication that includes anticancer drugs, developed specifically to act against overexpressed molecules in cancer cells (see EGFR targeting, section 2.4.1). Targeted molecules are usually oncogenic products as mediators of cancer cell proliferation and survival. Targeted anticancer drugs are divided into two classes: antibodies and small molecule inhibitors. According to development stages of malignancies, different categories of targeted therapies can be defined: 1) Therapies directed against molecular targets directly involved in the initiation of neoplastic transformation. Generally, this treatment provides high response rates as single agent treatment (e.g. Imatinib for the treatment of chronic myeloid leukemia (CML)). 2) Therapies directed at molecular targets involved at a later stage of neoplastic transformation/progression, but do not correspond to the initial event. These treatments yield limited response rates as single agent but often improve progression free and/or overall survival in combination with other cytotoxic drugs (e.g. Trastuzumab in combination with paclitaxel for the treatment of HER2 positive breast adenocarcinoma or anti-angiogenic therapy)[60-61].

2.2.3. Radiation therapy

Radiation therapy is the application of ionizing radiation in cancer treatment. Common used forms of ionizing radiation are photon beams (X-rays and gamma rays) and electrons (β-particles). Those radiation forms induce massive DNA double-strand breaks and the formation of free radicals. Thus, double-strand DNA breaks are considered to be the significant molecular damage that correlates with death of cancer cells treated with radiation therapy[5]. Due to high proliferation rate and frequent loss of damage recognition mechanisms, cancer cells are especially sensitive to radiation (comparable to chemotherapeutics). Radiation therapy is commonly used in combination with surgery, chemotherapy or hormone therapy.

2.2.4. Immunotherapy

The goal in cancer immunotherapy in common sense is stimulation of patient's immune system to attack the malignant tumor cells. There are two basic strategies to enhance the antigen-specific immune response against tumor cells - vaccine therapy and adaptive therapy. Vaccine therapy is based on the repeated administration of an immune stimulator (viral and DNA vectors, protein antigens, dendritic cells, or whole tumor cells) to induce tumor specific response. Adaptive therapy involves the *ex vivo* isolation, manipulation, and expansion of immune effector cells followed by their adoptive transfer into the tumor-bearing host to enhance the antitumor response[5,62].

2.2.5. Hormone therapy

Over 100 years ago, it has been recognized that hormone manipulation can reduce tumor volume in patients with metastatic or locally advanced breast cancers. Today, hormone therapy is used for various types of cancers which derive from hormonally-responsive tissues like: breast, prostate, endometrium, and adrenal cortex. The aim of this therapy is to prevent steroid-mediated growth of tumor and/or metastases. This is achieved by removing gonadal steroid hormones from the patient and opposing their action using antagonists[5,10]. One of the best known examples for hormone therapy is tamoxifen, which is used as an antagonist of the estrogen receptor in breast cancer[63].

2.2.6. Therapy resistance

Therapy resistance is the main obstacle for successful cancer treatment. Nearly 50% of patients diagnosed with cancer are already resistant to chemotherapy before they are treated for the first time with drugs (intrinsic resistance), and a large proportion of the remaining 50%, develops resistance during treatment (acquired resistance)[64]. Host and tumor genetic alterations, epigenetic changes and tumor environment all contribute to the complex mechanisms of cancer drug resistance. Also cancer cells in culture can become resistant to a single drug after a long lasting exposure. After selection for resistance to a single drug, the cells are frequently resistant also to other structurally unrelated drugs. This cross-resistance phenomenon is also known as multidrug resistance (MDR) and might explain the failure of treatment regiments with multiple agents[65]. There are two major mechanisms of resistance: 1) Minimized delivery of anticancer drugs to tumor cells and 2) Acquired genetic and epigenetic alterations that affect tumor cell sensitivity against the drug[65]. Mechanisms that lead to

insufficient intracellular drug levels include poor accumulation of the administered drugs, increased drug metabolism, or increased excretion. ATP-driven efflux pumps play an important role in efflux-mediated drug resistance. Most prominent members of ATP-dependent pumps are members of the ABC-transporter family like: ABCB1 (P-glycoprotein), the 9-member ABCC family (multidrug resistance-associated related proteins - MRPs) and ABCG2 (BCRP)[66] (Table 1). All ABC transporters have been identified to be expressed in healthy tissues and play an important physiological role in protection of the organism against toxins[67-68]. Drugs that are affected by classical ABC-transporter-mediated multidrug resistance include: vinca alkaloids (vinblastine and vincristine), anthracyclines (doxorubicin and daunorubicin), RNA transcription inhibitor actinomycin-D and the microtubule-stabilizing drug paclitaxel[69]. Metaldrugs such as drugs containing platinum, arsenic and ruthenium have been also shown to be substrates of ABCC2 (MRP2) and ABCB1 (P-gp)[66,70-72] (see also metabolism of arsenic, section 2.3.3). ABCCs usually export their substrates as reduced glutathione (GSH) conjugates. Glutathione is a ubiquitous cysteine-containing tripeptide and a very important player in cell protection against oxidative stress. High intracellular concentrations of GSH have been also implicated in resistance to several chemotherapeutic agents. GSH reacts and forms GSH-conjugates with anticancer drugs like arsenic, platinum-containing compounds, alkylating agents such as melphalan, and anthracyclines etc. Those GSH-drug conjugates are potent efflux substrates for MRPs and especially MRP1[66,73-74].

Another protective mechanism against chemotherapy is enhanced DNA repair, especially in case of DNA damaging drugs. For example, the expression of cross-complementation group 1 (ERCC1) protein as an important player of nucleotide excision repair (NER) system correlates with resistance to platinum drugs. Additionally, loss of the mismatch repair pathway (MMR) was shown to be a sensitive mechanism against platinum drugs[75-76]. Moreover, genetic modulations of survival pathway proteins such as Bcl-2, p53, NFκB have been shown to be implicated in drug resistance[66].

Table 1

Tissue localization and possible functions of ABC transporters

Common Name	Systematic name	Tissue	Non-chemotherapy substrates	Chemotherapy substrates (known and suspected)	Defects in human disease
PGP/MDR1	ABCB1	Intestine, liver, kidney, placenta, blood-brain barrier	Neutral and cationic organic compounds, many commonly used drugs	Doxorubicin, daunorubicin, vincristine, vinblastine, actinomycin-D, paclitaxel, docetazel, etoposide, teniposide, bisantrene, homoharringtonine (STI-571)	None known; altered sensitivity to drugs
MDR2	ABCB4	Liver	Phosphatidylcholine, some hydrophobic drugs	Paclitaxel, vinblastine	Progressive familial intrahepatic cholestasis
MRP1	ABCC1	All tissues	Glutathione and other conjugates, organic anions, leukotriene C4	Doxorubicin, epirubicin, etoposide, vincristine, methotrexate	Non known
MRP2/ cMOAT	ABCC2	Liver, kidney, inetestine	Similar to MRP1, non-bile salt organic anions	Methotrexate, etoposide, doxorubicin, cisplatin, vincristine, mitoxantrone	Dubin-Johnson synrome
MRP3	ABCC3	Pancreas, kidney, intestine, liver, adrenal glands	Glucuronate and glutathione conjugates, bile acids	Etoposide, teniposide, methotrexate, cisplatin, vincristine, doxorubicin	None known
MRP4	ABCC4	Prostate, testis, ovary, intestine, pancreas, lung	Nucleotide analogues, organic anions	Methotrexate, thiopurines	None known
MRP5	ABCC5	Most tissues	Nucleotide analogues, cyclic nucleotides, organic anions	6-Mercaptopurine, 6-Thioguanine	None known
MRP6	ABCC6	Liver, kidney	Anionic cyclic pentapeptide	Unknown	Pseudoxanthoma elasticum (substrate unknown)
MXR/BCRP/ ABC-P	ABCG2	Placenta, intestine, breast, liver	Prazosin	Doxorubicin, daunorubicin, mitoxantrone, topotecan, SN38	None known
BSEP/SPGP	ABCB11	Liver	Bile salts	Paclitaxel	Progressive familial intrahepatic cholestasis
ABCA2	ABCA2	Brain, monocytes	Steroid derivatives, lipids	Estramustine	Intracellular steroid transport

Adapted from ref.[66]

2.3. Arsenic

Arsenic is a semimetal rarely present in its pure elemental state. It is commonly found in soil, water and air. On the periodic table, arsenic is a group 15 element with atomic number 33 and relative atomic mass 74.92. It is classified as metalloid with intermediate properties between those of typical metals and nonmetals. Greeks named it *arsenikon* which may have been derived from the persian word *az-zarnikh*, meaning yellow or gold[77].

Nitrogen and phosphorus are two major nutrient elements of living organisms next to carbon, hydrogen, oxygen and sulfur. In accordance, it was discovered recently that arsenic could be used instead of phosphorus by certain bacteria (GFAJ-1) to sustain its growth[78]. This is possible because of similarities between arsenic and phosphorus in atom radius as well as their identical electronegativity. However, the kinetic lability of the arsenic-oxygen bond makes it unlikely that arsenic can entirely replace the structure and function of phosphorus in nucleic acids, lipid membranes or ATP, although it might serve a transient kinetic role in the unusual metabolism[79]. Elemental arsenic has very few uses and nearly all applications are in form of salts. There are three inorganic forms of arsenic in nature: arsenic trisulfide (As_2S_3, yellow arsenic, referred to as arsenicon, aurum pigmentum, or orpiment), arsenic disulfide (As_2S_2, red arsenic, referred to as realgar or sandaraca) and arsenic trioxide (As_2O_3, ATO, white arsenic, referred to as arsenolite)[80](Figure 10).

Figure 10. ***Orpiment (yellow) and Realgar (red) minerals can occur together in nature***[81]

Sulfides of arsenic and some of their properties are known since ancient times. For example, the common relation of realgar and orpiment was noticed. The bright yellow color of orpiment and the scarlet-red color of realgar were used in ancient Egypt and Eurasia as pigments and cosmetics[82]. Arsenosulfide minerals usually appear in hydrothermal deposits, intrusive igneous rocks, volcanic emissions, hot springs, and microbial precipitates[83]. Arsenolite or ''white arsenic'' is supposed to be discovered by an Arabian alchemist Abu Musa Jabir, known as Geber in Latin around 760 AD by heating orpiment. He also recover elemental metalloid arsenic from ATO[84]. Arsenolite and other arsenic compounds were known for their toxic properties in medieval times. They have been

used in chemical warfare agents but also to commit suicide and murder[83]. Starting in the nineteenth century, continuing until present time, clinical researchers, environmentalists, and others became increasingly concerned about the potential impacts of arsenic on human health and the environment.

2.3.1. Arsenic as poison and carcinogen

Arsenic was a favorite agent to commit crime in the ancient times. The fatal dose of ATO for a human is 70-180 mg. A half teaspoon in a cup of water, wine or tea was usually used to kill[77]. Tasteless and uncharacteristic signs of poisoning made it attractive especially in the Middle Ages to dispose throne rivals. Therefore, arsenic was called "Poison of the Kings" and "King of Poisons"[70]. Its poisoning symptoms can be confused with a variety of other natural disorders, like hemorrhagic gastroenteritis, psychiatric disease and cardiac arrhythmias[85]. One of the earliest documented accounts is the assassination of Britannicus by Nero to secure the throne in the Roman Empire (AD 55)[77,83,86]. Many other famous people died by arsenic poisoning like emperor Leopold I of Austria[87], or the american arctic explorer Charles Francis Hall[83]. In 1961, the discovery of increased arsenic concentrations in one of Napoleon's hair samples excited the debate that poisoning with arsenic caused his death[88].

In terms of environmental pollutants, arsenic salts are as acutely poisonous as metal salts of mercury, copper, cadmium and many modern pesticides. Arsenic is a major pollutant because of its naturally elevation in the environment[77](Figure 11). The main human exposure routes with arsenic are food, air and water, whereas the last one is predominant.

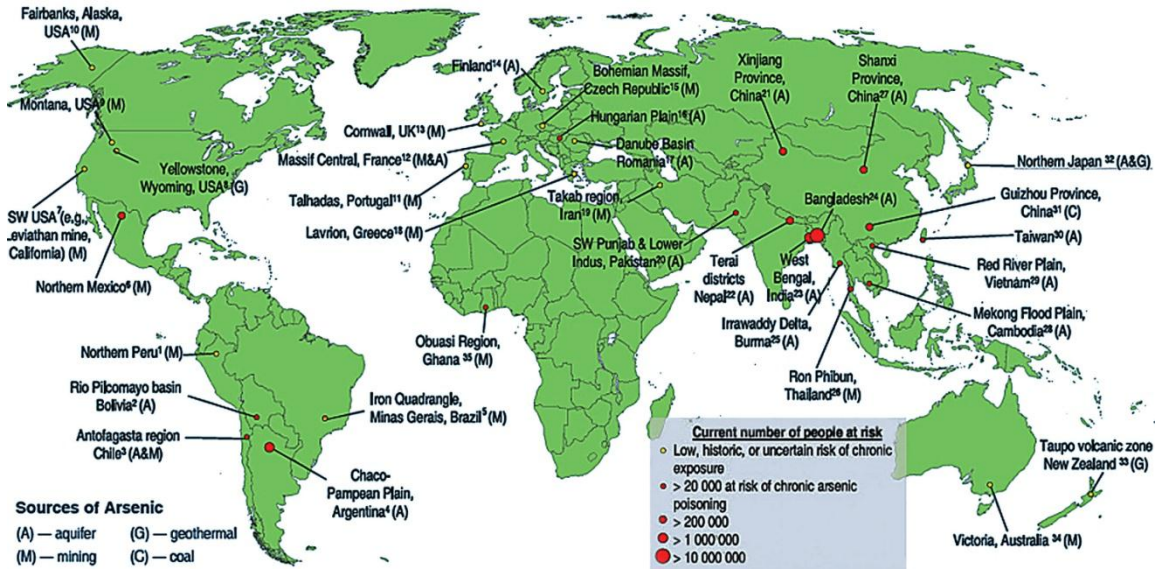

Figure 11. ***Distribution of arsenic contaminated regions worldwide, showing source of arsenic and numbers of people at risk of chronic exposure[81].***

The story of arsenicosis (long-term arsenic exposure) in Bangladesh is one of the tragic examples for environment poisoning. Bangladesh encompasses the world's largest delta, involving the convergent rivers of Ganges, Brahmaputra and Meghna. During monsoon season, around 70% of its land surface is routinely flooded and pollutes the drinking water. Consequently, pure drinking water was harvested by using tubewells, where iron tubes are bored into the underground aquifer. The earliest tubewell devices in Bangladesh date back to 1937 with slow rates of construction until 1970. In 1972 United Nations Children's Fund (UNICEF) installed 900,000 tubewells throughout Bangladesh and by the year 2000, 80% of the people were supplied with pure drinking water (Figure 12).

Figure 12. ***One of thousand tubewells installed in Bangladesh by UNICEF***[89]

As a direct result of tubewell water supply, mortality rate dropped from 151 per thousand in 1960 to 83 per thousand in 1996[77]. Unexpectedly, another disaster was released. At that time, tubewell water analysis did not contained tests for arsenic contamination. In 1984, the first concrete report of tubewell water contamination with arsenic was published by Dr. Saha, a dermatologist at the School of Tropical Medicine in Calcuta[90]. He observed symptoms of melanosis (hyperpigmentation - black drops and hypopigmenatation - white drops) on the limbs, chest and back of exposed inhabitants (Figure 13). Longer arsenic exposure caused keratosis (nodules on the hands and feet) in those persons consuming arsenic contaminated tubewell water.

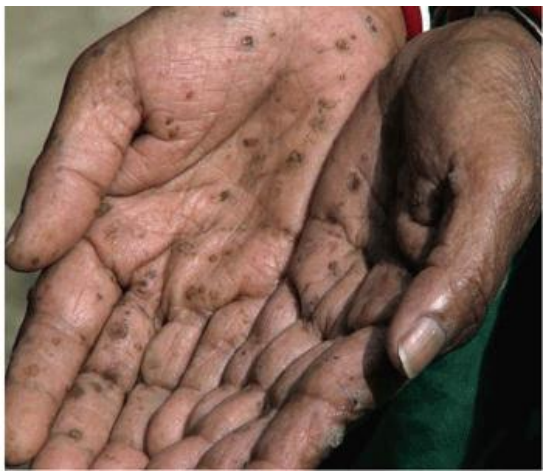

Figure 13. ***Brown calluses (black drops) as a hallmark symptom of arsenicosis***[91]**.**

In 1988, another Indian group of researches published that people who drank contaminated water (arsenic level, 0.2-2 mg/l) showed chronic arsenical dermatosis and hepatomegaly as compared to those using safe water (arsenic level <0.05 mg/l)[92]. Unfortunately, the poisoning problem was not taken that serious by the government until 1996. After an arsenic conference in Calcutta, United Nations World Health Organization (WHO) declared the

situation in Bangladesh a 'Major Public Situation Health Issue' with up to 77 million potentially affected people and called the disaster 'the largest mass poisoning of a population in history'[93]. In a WHO country situation report, arsenic test results were collected and revealed that about half of the measurement concentrations were above 50 µg/l, which is in excess of the maximum level of WHO recommended value (10 µg/l) and greater than the maximum permitted value in Bangladesh (50 µg/l). Bengal delta is not unique on the planet. Also, the deltas of Myanmar, Cambodia and Laos have also been reported to be contaminated. Arsenic contamination in drinking water was reported also from far inland, particularly Nepal, Thailand, Chile, USA, New Zealand, Mongolia and China[77].

The International Agency for Research on Cancer (IARC) has listed arsenic as a human carcinogen in 1980[94]. Chronic exposure with arsenic increases the risk of tumor development of the skin, bladder, lung or kidney[94-97]. One of the first reports in the association of arsenic with skin cancer and keratosis was published by doctor Jonathan Hutchinson in 1888[77]. Hyperpigmentation, hypopigmentation and keratosis are supposed to be the hallmarks of arsenic chronic exposure toxicity[98]. He observed patients who took Fowler's solution (1% solution of potassium arsenite) over years. Clinical signs of arsenic related skin lesions and cancer appear after a latency between 6 to 10 months or even more than 20 years[99-100]. In addition, studies in U.S. and Taiwan showed that smoking and high arsenic levels in drinking water, synergically increases cancer risk in bladder and lung[101-102]. There are also a numerous non-carcinogenic effects of chronic arsenic exposure like: neurobehavioral and memory funktions[103], neuropathic[104-105], reproductive effects[106], cardiovascular diseases[107], respiratory system deseases[98,108], type two diabetes-mellitus[109] etc.

2.3.2. Arsenic as therapy

The famous doctrine of Paracelsus ''The dose makes the poison" and that of William Withering ''Poisons in small doses are the best medicines, and the best medicines in too large doses are poisonous'', seems to be in paradigmatic agreement with arsenic. In the Far East, arsenic has been used as a therapeutic agent for more than 2400 years[70]. Around 430 BC in ancient Greece, Hippocrates was one of the first who suggested arsenic for medicinal purposes (Table 2).

Table 2

Medical use of arsenic in the past

Hippocrates used realgar (As_2S_2) and orpiment (As_2S_3) as remedies for ulcers.
Dioscorides used As_2S_3 as a depilatory.
Jean de Gorris used arsenic as a sudorific.
Angelus Salva used arsenic against the plague.
Lentilius and ***Friceius*** used arsenic as a treatment for malaria.
Many preparations of arsenic were applied therapeutically in the 18th century, and several (Aiken's Tonic Pills, Andrew's Tonic, Arsenauro, Gross' Neuralgia Pills, Cholor-Phosphide of Arsenic, Sulphur Compound Lozenges) were still in use at the end of the 19th century.
Arsenic was a mainstay of the 19th century materia medica.
Fowler's solution was praised for its success in treating asthma, chorea, eczema, Hodgkin's disease, pemphigus, pernicious anemia, and psoriasis.
Ehrlich discovered an organic arsenical (salvarsan) that cured syphilis and was used to treat trypanosomiasis.
Arsenic has been used in traditional Chinese medicine for hundreds of years, and derivatives are still used to devitalize the pulp of diseased teeth and in regimens for psoriasis, rheumatic diseases, and syphilis.

Adapted from ref.[80]

He developed a recipe for an ulcer lotion containing realgar, orpiment, dried beetle, juniper oil, copper flakes, lead, sulfur and hellebore[77]. Dioscordies (40-90 AD) noticed that ATO was a dangerous poison, but at low doses was effective in treating tuberculosis, emphysema and also cleared scabies, lice and many skin disorders[110]. Moreover, he used it as a depilatory[80]. In the early 2-nd century, Avicenna described the application of ATO to treat fevers[110]. Through his textbooks, the usage of arsenic was popularized in Muslim world and later in Europe. In 18th century, Fowler's solution was developed by Dr. Tomas Fowler and was used for the treatment of various diseases like asthma, cholera, eczema, pemphigus, psoriasis, anemia, Hodgkin's disease, and leukemia[80,111]. During his lifetime bacteriologist and founder of chemotherapy Nobel laureate Paul Ehrlich, synthesized 500 types of organic arsenic compounds that were in clinical use[80].

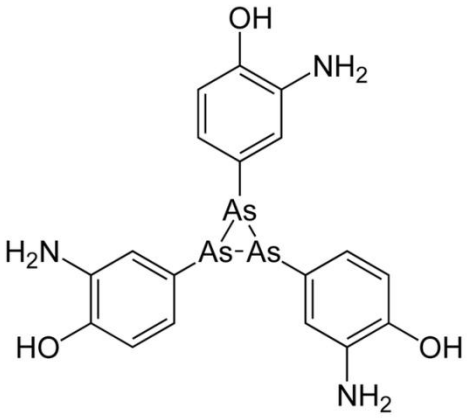

Figure 14. ***The organoarsenical salvarsan***

Ehrlich introduced *salvarsan* in 1910, an organic arsenical to cure syphilis and trypanosomiasis that raised its therapeutic reputation[85](Figure 14). Salvarsan was the standard therapy for syphilis for nearly 40 years before it was replaced by penicillin[112].

Antileukemic activity of ATO was first described in 1878, when the effect of Fowler's solution was reported on the reduction of white blood cell counts in two normal people and one patient with leucocythemia[111]. In the 1930s, ATO efficacy was announced in patients with chronic myelogenous leukemia (CML)[113]. Introduction of chemotherapy and radiation therapy in the early 20th century, replaced arsenic treatment for nearly 40 years. In the 1970s, reports from a Chinese group described the anticancer effect of AILING-1 (Crude mixture of arsenic and herbal extracts) in APL (acute promyelocytic leukemia) patients[114]. In 1994, pure ATO was introduced to treat APL patients, and subsequently combination with retinoic acid (RA) improved the therapy response to a revolution in the prognosis of this disease[110,115]. Results of observational studies have been confirmed in randomized clinical trials in the U.S.[116-117]. Finally, in September 2000, ATO (Trisenox™) was approved for the treatment of relapsed or refractory APL by the U.S. Food and Drug Administration (FDA) (Figure 15).

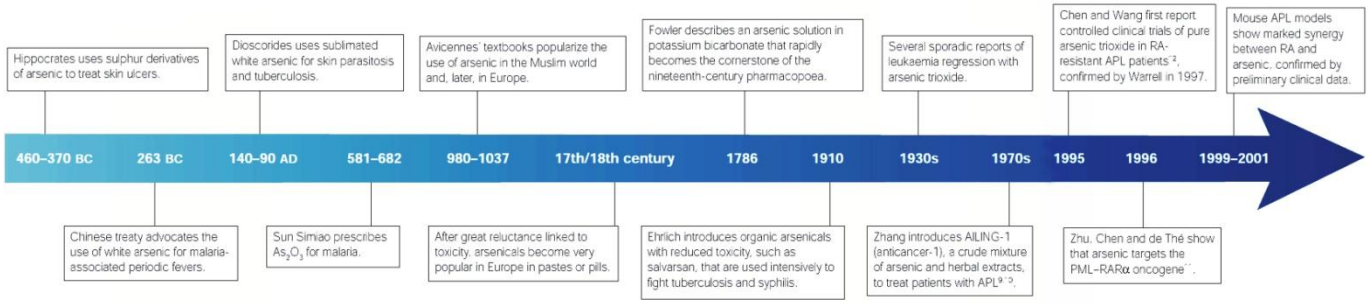

Figure 15. ***Milestones of arsenic as a drug[110]***

2.3.3. Metabolism of arsenic

Arsenic has two biological important oxidation states (As^{III} and As^{V}) that can interconvert and can be metabolized. In general, As^{III} compounds have a higher reactivity than the As^{V} forms. However, metabolically formed trivalent arsenicals (methylarsonic acid) $MMAs^{III}$ and (dimethylarsinic acid) $DMAs^{III}$, have higher cytotoxicity than inorganic arsenic (iAs)[83]. Liver is

the major organ for iAs metabolism. There are two basic metabolites of iAs^{III} and two of iAs^{V} in humans: methyl-arsenic (MAs^{III} and MAs^{V}) and dimethyl-arsenic ($DMAs^{III}$ and $DMAs^{V}$) metabolites. AS3MT (Arsenic (+3 oxidation state) methyl transferase) is the only enzyme responsible for methylated metabolites of iAs, that is shown to catalyze all critical steps involved in the conversion of iAs^{III} to tri- and pentavalent methylated arsenicals[118]. The activity of AS3MT in hepatocytes can be modulated by direct interactions of dithiol-containing reductants (e.g. GSH), thioredoxin (TR) and thioredoxin reductase (TRx) but also factors that can affect availability of the substrates[119](Figure 16).

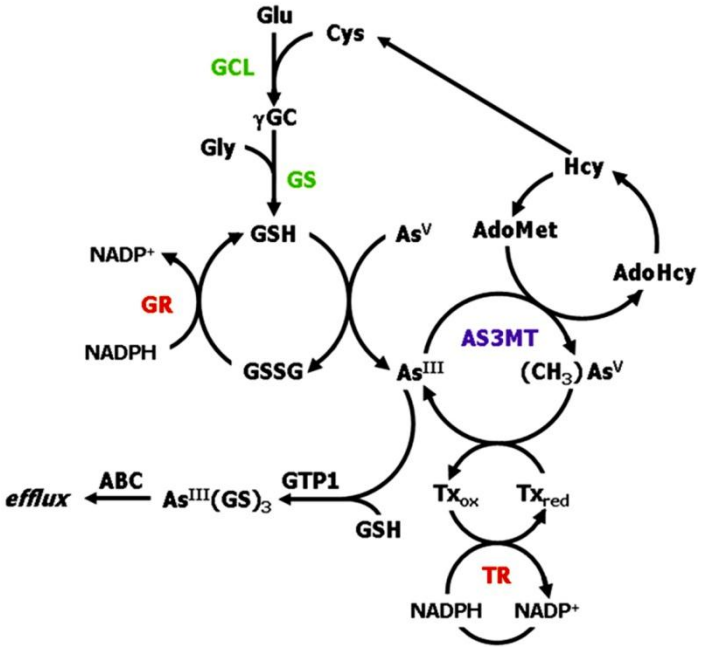

Figure 16. ***Interconnections in the metabolism of arsenic (As)***[120]

Inorganic As^{III} (iAs^{III}) and their trivalent arsenicals preferentially react with sulfhydryl groups of proteins, such as thiols in cysteine residues. Thiol groups play the critical catalytic activity of many enzymes and binding of As^{III} to these catalytic sites may inactivate the enzyme activity. This enzymatic loss of function is believed to be a common mechanism of action of arsenic[121]. There are several membrane transporters responsible for uptake und efflux of iAs and its metabolites. IAs can be transported alone or in form of GSH complexes. Enzymes of GSH transferase (GST) family may provide the formation of the GSH complexes with iAs^{III}, MAs^{III} or $DMAs^{III}$ [121-122].

Multidrug resistance-associated protein 2 (MRP2 or ABCC2) and P-glycoprotein (P-gp or ABCB1) are members of the superfamily of ATP-binding cassette (ABC) transporters[122]. MRP2 as well as P-gp are involved in the efflux of arsenic metabolites into the bile (Figure 17).

Trivalent arsenicals form complexes with GSH which are substrates for the MRP2 and, possibly, P-gp[119]. Permeases, GLUT2 (Glucose transporter 2) and AQP9 (aquaglyceroporin-9) can transport iAs^{III} and MAs^{III} in both directions (uptake and efflux) among the concentration gradient. However, none of those permeases can transport $DMAs^{III}$. Liver specific organic anion transport protein (OATP-C) is also a bidirectional basolateral transporter that may be involved in the efflux of both iAs^{III} and iAs^{V} metabolites into the blood[119]. Additionally, ABC transporter MRP1 (multidrug resistance-associated protein 1 or ABCC1) is reported to be involved in arsenic resistance in various malignacies[123-125].

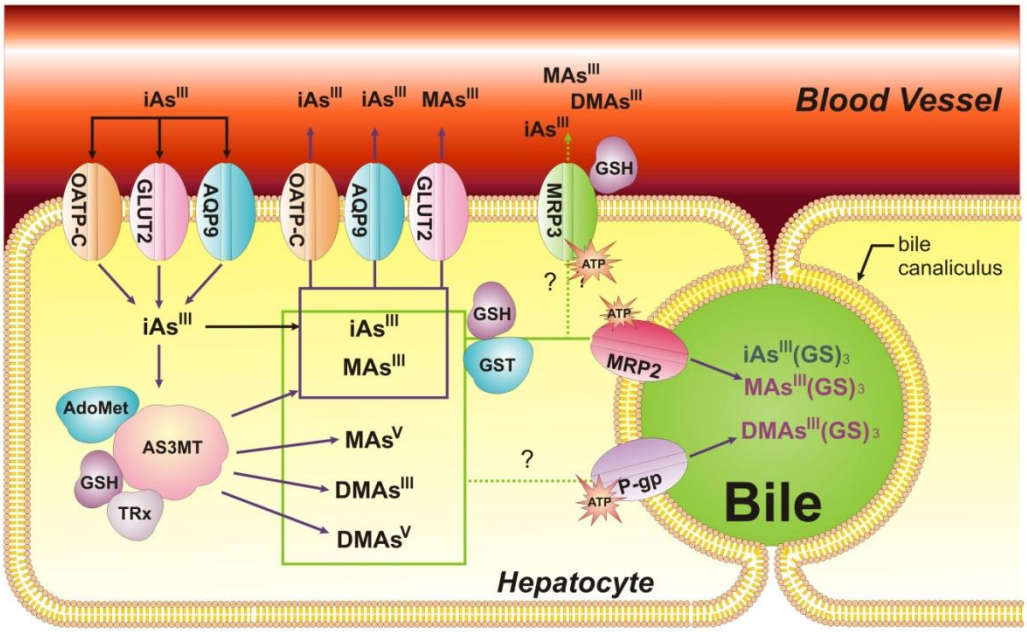

Figure 17. ***A hypothetical scheme of arsenite (iAs^{III}) metabolism in the liver:*** *molecular components involved in the uptake and methylation of iAs^{III} in hepatocytes and in the efflux of iAs^{III} and its methylated metabolites to the blood and bile (Adapted from ref. [119])*[7]

Conclusively, therapy resistance can be related to interaction of drugs with various cellular transporters. ATO, its metabolites, and many other substances used as therapies are substrates of those transporters and lose their activity because they are pumped out of the target cells.

2.3.4. ATO induces differentiation and apoptosis in APL

The best known application of arsenic in cancer therapy is its successful use for the treatment of APL[126-128]. This rare disease has considerable importance as one of the best understood malignancies and one of the few that has been cured by targeted therapies. The current treatment of APL patients is combination of retinoic acid (RA) and chemotherapy. More than 90% of the treated patients were disease-free and still off-treatment after 5 years in several

recent clinical trials[115]. Retinoic acid receptor-α gene (RARα), was shown to be the only constant genetic disruption in APL patients with specific translocation t(15,17) fused to promelocytic leukemia (PML) gene. Fusion oncogenic protein encoded from PML-RARα blocks the normal myeloid differentiation program of granulocytes in a specific stage of promyelocytes and might induce both hematopoietic lineage switching and self-renewal of the affected cells[129]. This is also a multifaceted fusion protein that modulates several key pathways (e.g. apoptosis resistance, cell differentiation and stemness) that cooperate to enforce leukemic transformation[115].

Moreover, PML-RARα protein binds to transcriptional corepressors and histone deacetylases (HDAC) with higher affinity compare to wild-type RARα. This explains also PML-RARα enhanced repressor activity[110]. Both RA and ATO, which are chemically unrelated, have been shown to degrade PML–RARα and to trigger differentiation of APL cells into granulocytes[130-132]. RA dislocates corepressors from PML–RARα fusion protein changing from a repressor into a transcriptional activator of target genes[133-134] (Figure 18).

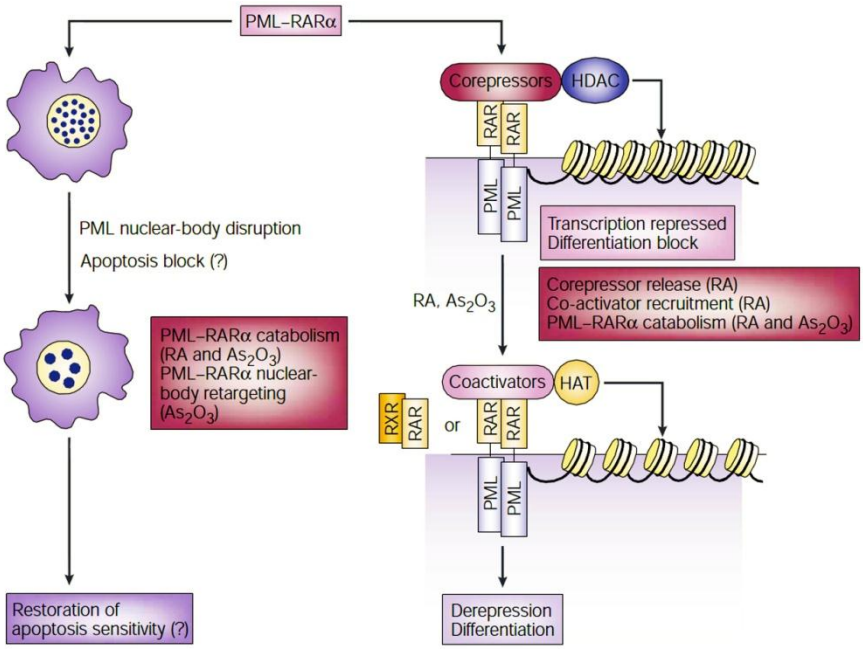

Figure 18. ***Two effects of retinoic acid and ATO on PML-RARα funktion[110]***

Furthermore, differentiation of APL cells induced by RA, activates proteases that cleave RARα, the half part of PML–RARα[135-136]. In contrast, ATO targets the PML part of PML–RARα fusion protein[137-138]. Transfer of nucleoplasmic PML is rapidly induced by arsenic to the nuclear matrix, resulting in swelling of the nuclear bodies, PML sumoylation and, finally, PML degradation. Nuclear body formation was originally proposed to result from intermolecular

interactions between SUMO-conjugated PML and a SUMO-binding domain of PML[139-140]. There are two mechanisms of ATO leading to PML sumoylation. Firstly, ATO induces ROS (reactive oxygen species), that triggers the formation of PML intermolecular disulphide crosslinks. ROS-induced PML multimeres are targeted to nuclear bodies and allow PML sumoylation by ubiquitin-conjugating enzyme 9 (UBC9). Secondly, ATO can also react directly with PML cysteines which recruits UBC9 to the PML RING finger and enhances PML sumoylation. Sequence analysis of the PML gene has indicated the presence of a cystein-rich region that may be a principal candidate for interaction with arsenic[141]. RING finger protein 4 (RNF4) is a SUMO-dependent ubiquitin ligase that polyubiquitylates SUMO-PML onto nuclear bodies. Ubiquitylated PML is finally targeted to the proteasome for degradation[115](Figure 19).

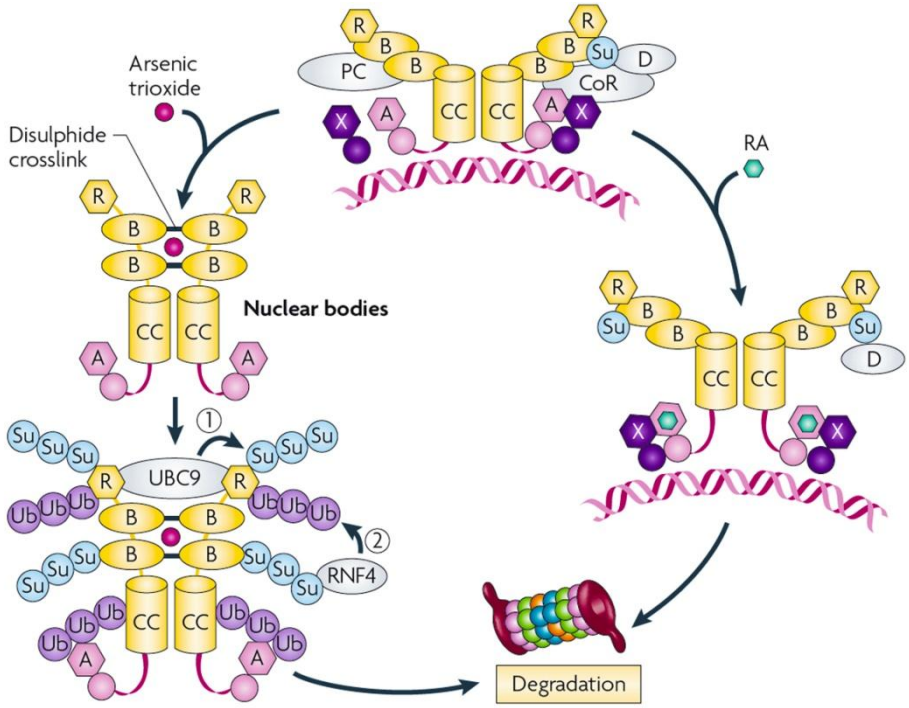

Figure 19. ***Schematic representation of PML–RARα degradation induced by RA and ATO****. RING (R), B boxes (B) and coiled-coil (CC) domains of the PML-moiety of the fusion are indicated. A (pink) represents RARα, X (purple) depicts retinoid X receptor-α (RXRα), PC refers to the polycomb group repressive complex 2 (PRC2), CoR is the nuclear receptor co-repressor (NCOR) and D is death domain-associated protein (Daxx). RA (green hexagon) binding to PML–RARα induces a conformational change that recruits the proteasome. Crosslinking of the PML moiety of PML–RARα through direct ATO binding (red) and formation of disulphide bonds, triggers nuclear body reformation. This, together with ATO binding to the RING domain (not shown), enhances ubiquitin-conjugating enzyme 9 (UBC9; also known as UBE2I) association, resulting in enhanced sumoylation (arrow 1). PML-RARα dimerization and sumoylation recruits RING finger protein 4 (RNF4), which ubiquitylates PML–RARα (arrow 2) and thereby targets it for proteasome-mediated degradation. Conjugation by SUMO (Su) and ubiquitin (Ub) are indicated*[115].

It was reported that PML co-localizes with p53 in the PML nuclear body and physically interacts with p53 both *in vitro* and *in vivo*[142]. Degradation of PML induced by arsenic in non-APL cells decreases p53 activity and protects cells with genetic abnormalities from apoptosis.

Although, arsenic ability to stimulate other proapoptotic pathways may counterbalance the effects of PML degradation[141].

The relation between the well-documented tumor suppressor gene p53 and ATO was a goal of many studies in different malignant cell lines[143-145]. Contradictory results have been reported suggesting induction, disruption or no effect of arsenic on p53 expression or phosphorylation[146-149]. Arsenic has been shown to induce apoptosis that was both p53-depended and p53-independent. Moreover, observation of exposure to arsenic *in vivo*, showed both increased and decreased expression of the p53 protein[96]. Overall, the relationship of p53 and arsenic in carcinogenesis or in cancer therapy seems uncertain but probably is cell- and tissue-specific.

2.3.5. ROS-mediated apoptosis of ATO

Oxidative stress is a result of disturbed balance between ROS and the antioxidant defense ability of a cell. ROS can result in the damage of proteins, lipids, RNA and DNA which in turn can lead to cell death[150]. Redox metabolism is known to be altered in cancer cells compared to healthy tissues. Cancer cells usually have enhanced levels of ROS as a consequence of the specific milieu of solid tumors often characterized with high metabolic activity, hypoxia and reductive conditions[121]. Oxidant stress plays a major role in the toxicity of ATO as well as of many other chemotherapy agents. ATO and many other metal complexes can increase cellular levels of ROS by inhibiting ROS detoxification apparatus and finally lead to apoptosis (Figure 20).

The protective systems against ROS include: glutathione (GSH), thioredoxin, superoxide dismutase, catalase, and glutathione peroxidase[151]. A decreased level of intracellular GSH as an important antioxidant is also known as sensitizing factor against ATO. Intracellular GSH is an important resistance factor against arsenic who potentially titrates it or its

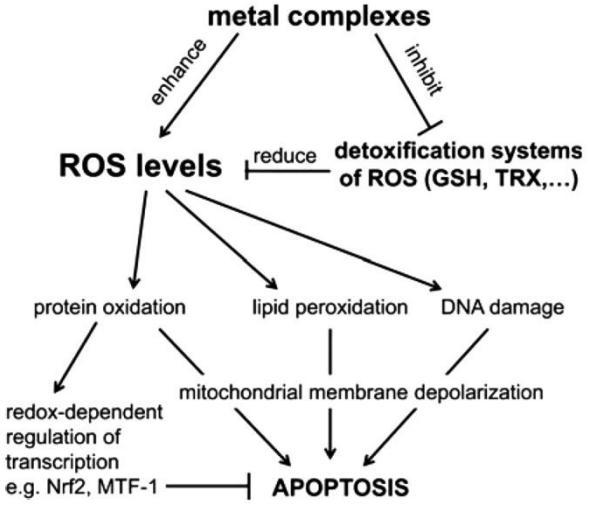

Figure 20. ***General overview on the role of ROS in the activity of anticancer metal drugs[121]***

metabolites by forming $As(GS)_3$ complexes which are then pumped outside the cells[151] (Figure 21). Additionally, ATO inhibits glutathione peroxidase and thioredoxin by targeting their active thiol groups required for preventing ROS detoxification[83,151]. Nicotinamide adenine dinucleotide phosphate (NADPH) oxidase is an enzyme complex needed for the normal antibacterial function of white blood cells. Stimulation of this enzyme is also reported to be associated with ATO induced ROS generation[152].

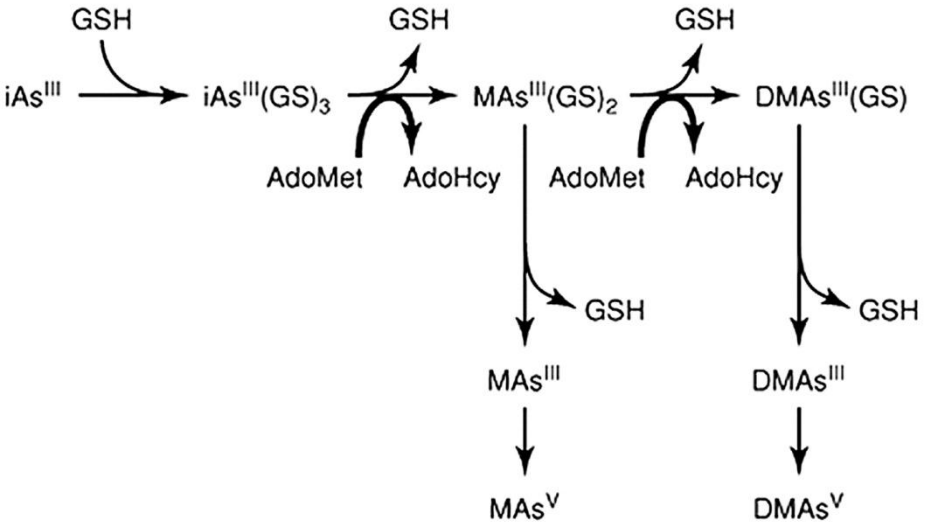

Figure 21. ***GSH interacts with inorganic arsenic and its metabolites[153]***

2.3.6. ATO induces apoptosis via the mitochondrial pathway.

There is some evidence that arsenic can induce apoptosis by disturbance of the mitochondrial membrane potential[154-155]. Mitochondria are the suppliers of the chemical energy in eukaryotic cells and are involved in a range of other processes, such as cell signaling, cell differentiation, apoptosis, as well as control of the cell cycle and cell growth[156]. Mitochondria are also known to be the major intracellular generators of ROS[121]. ATO can induce mitochondrial-mediated apoptosis in different ways. ATO can inhibit ROS detoxification apparatus or it can directly bind and oxidize thiol groups, which are part of the mitochondrial permeability transition pore complex (PTPC). Opening of PTPC leads to the decrease of the mitochondrial membrane potential ($\Delta\Psi m$), mitochondrial collapse and, finally, apoptosis. ATO downregulates the expression of the tumor suppressor gene Bcl-2, which is another mitochondria-related apoptosis inducer[150,157] (Figure 22). Bcl-2 downregulation has been associated with ATO-mediated growth inhibition and apoptosis in several cell types[158-159].

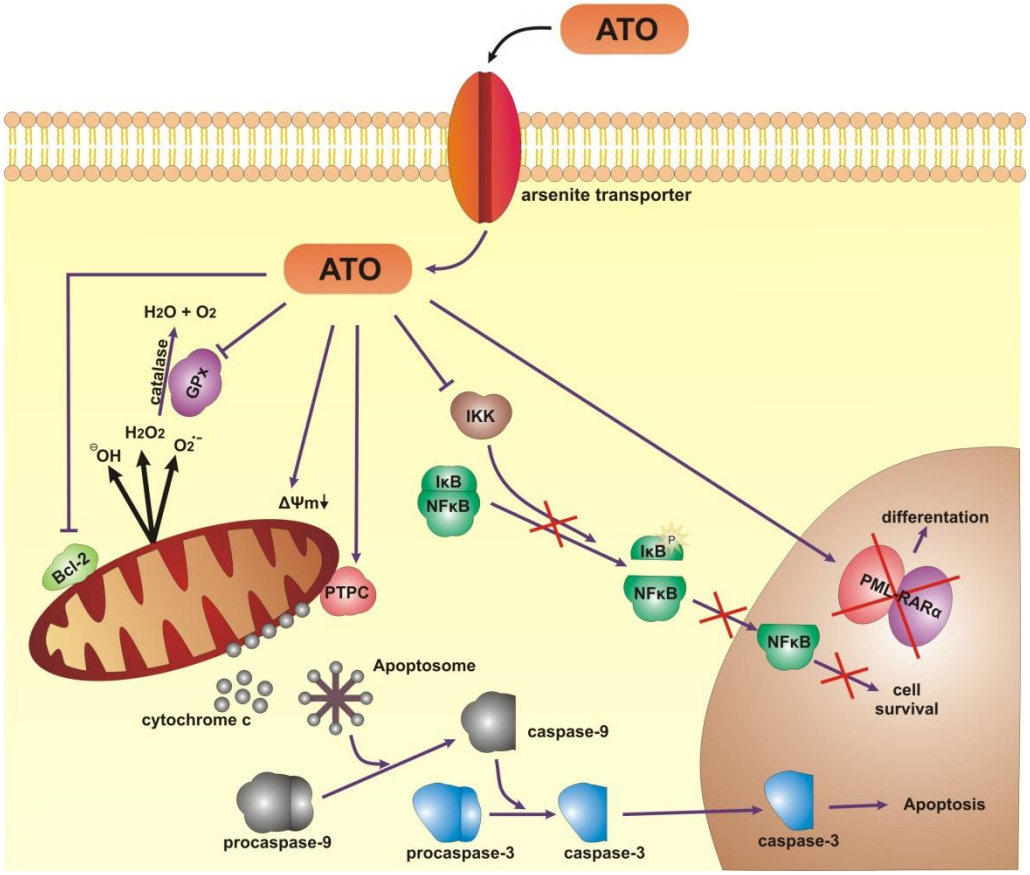

Figure 22. ***ATO: modes of action*** *(Adapted from ref.*[155]*)*[7]

2.3.7. ATO and NFκB

Nuclear factor-kappa B (NFκB) is a transcription factor that promotes cell survival and has an important role in many malignant diseases. Its target genes encode stress response enzymes, cell-adhesion molecules, inflammatory cytokines, and several anti-apoptotic proteins. The mechanism of NFκB regulation is well understood[96]. In its normal state, NFκB is an inactive multimere in the cytoplasm. The inactive state is maintained by inhibitor κB-proteins (IκBα) (Figure 22). Stimuli of various kind, like growth factor tumor necrosis factor alpha (TNFα), bacterial lipopolysaccharides, viruses, ROS or ionizing radiation can activate NFκB-mediated transcription[160]. Moreover, extracellular stimuli through cell-surface receptors trigger IκB phosphorylation by multisubunit IκB kinase (IKK) complex. Phosphorylated IκB is targeted by ubiquitinilation for degradation after release from NFκB. Free NFκB can translocate into the nucleus and bind to distinct DNA sequences which regulate the transcription of specific genes. ATO inhibits IKK by binding to the cysteine residue (Cys-179) in the activation loop of IKK catalytic subunit[150]. Activation of NFκB generally results in suppression of apoptosis, whereas its inhibition can promote apoptosis[161-162]. Studies have shown that arsenic has different effects on NFκB activity. NFκB can be activated, inhibited or be unaffected by

arsenic[19]. Low concentrations (≤ 5μM) of arsenic seem to activate TNFα-mediated NFκB that is associated with cell proliferation, whereas higher concentrations may result in an activation of NFκB that is associated with apoptosis[96,163-164]. The potential role of NFκB as an inhibitor or promoter of apoptosis, may be an important key in determining whether arsenic acts as a carcinogenic agent or as effective therapeutic drug. Generally, impact of arsenic on NFκB is cell-specific.

2.3.8. ATO and AP-1

Activator protein 1 (AP-1) is a transcription factor composed of homodimers or heterodimers of the *jun* and *fos* gene familly products. It mediates gene regulation of different stimuli, including cytokines, growth factors, stress signals, bacterial and viral infections, as well as oncogenic stimuli[165]. AP-1 plays a role in cell differentiation, cell proliferation and apoptosis[166]. Furthemore, AP-1 is involved in tumor progression and metastasis[167-168]. Similar to NFκB, AP-1 is also considered as stress response transcription factor, which regulates the expression of a gene variety that are known to be involved with cellular anti-oxidant defense mechanisms[96]. In contrast to NFκB, heterodimers of AP-1 are basically localized inside the nucleus and AP-1 transactivation is achived by phosphorylation[169]. Extracellular-signal-regulated kinases (ERKs) and c-Jun N-terminal kinase (JNK) are two major mitogen activation kinases (MAPK) who activate AP-1 by phosphorylation in its transcriptional activation domain. Different studies have shown that arsenic induces AP-1[169-171]. Increased arsenic activity is accomplished by induction of c-Fos and c-Jun proteins, upregulating of *c-fos* and *c-jun* gene expression, induced transactivation and DNA binding activity of AP-1[96]. DNA binding activity and gene regulation of AP-1 and NFκB was investigated after acute (24 h) and chronic (10-20 weeks) exposure with arsenic in human fibroblasts[169]. In this study it was shown that up regulation and induction of transcription factor binding activity after short-term arsenic exposure appears to be a defense response. In contrast, down regulation and decreased transcription factor binding activity induced by arsenic after long-term exposure may be a factor in arsenic induced carcinogenesis[169].

2.3.9. Other targets of arsenic

Gli family zinc fingers (GLI) are central transcription factors downstream in the hedgehog (HH) signaling pathway. This signaling is important in embryonic development and hematopoetic stem cell proliferation[172-173]. Tumorigenesis can be another result of a

disrupted HH signaling pathway[174-176]. Recent studies have shown that arsenic targets Gli proteins, inhibits their activity and their gene expression. Data from those studies indicate that arsenic binds direct to Gli protein, blocking the activity but not its DNA binding affinity[177-179].

Another target of arsenic is the inhibition of GTP-induced polymerization of cytoskeletal tubulin. Tubulin, a sulphydlil-rich cytosceletal protein, is an important compound of cellular microtubules. It has been shown that arsenic blocks its binding site for guanosine triphosphate (GTP) and, thus, induces vicinal cysteine cross-links. This disruption of microtubule assembly and spindle formation consequently leads to mitosis abnormalities and apoptosis after ATO treatment[180].

Angiogenesis is the physiological process of growing new blood vessels and already a vital process for the growth and survival of solid tumors. Many tumor types show increased vascular density and vascular endothelial growth factor (VEGF). It has been shown that arsenic can also inhibit VEGF production that is important in angiogenesis[181].

2.4. EGFR

The epidermal growth factor receptor (EGFR, HER or ErbB) belongs to the receptor tyrosine kinase (RTK) super family. There are four known members: EGFR or HER1/ErbB1, HER2/ErbB2, HER3/ErbB3, and HER4/ErbB4. EGFR has become a prototype of classical RTKs as the most intensively studied receptor of the four family members[182]. Abnormal activation of the EGFR pathways can support five of the six major hallmarks of cancer with the exception of limitless replicative potential[183](Figure 23).

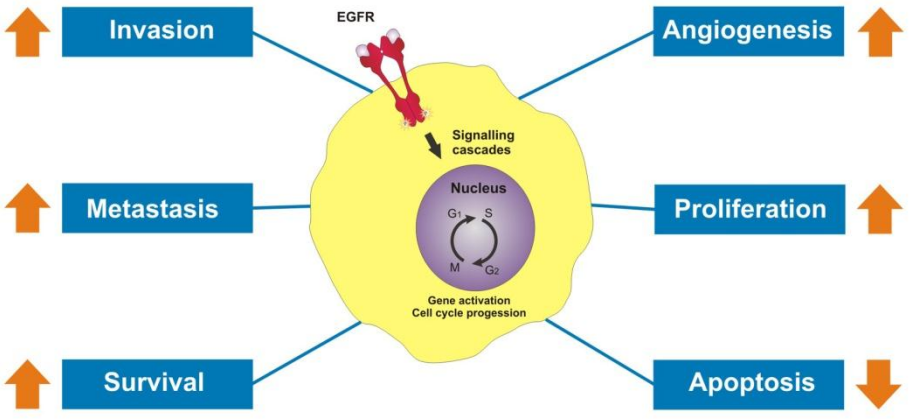

Figure 23. ***Cellular effects resulting from activation of the EGFR pathway.*** *EGFR signaling mediates the activation of a variety of cellular processes associated with carcinogenesis. All of the hallmarks of cancer are activated with the exception of limitless replicative potential (Adapted from ref.[183])*[7]

Thus, aberrant activation of the EGFR pathway has been associated with carcinogenesis. There are several mechanisms which lead to stimulation of this pathway: 1. enhanced production of ligands by cancer cells, 2. Increased, amplification, expression, and accumulation of EGFR in the plasma membrane and 3. activating mutations of the *EGFR* gene[183]. Epidermal growth factor (EGF), transforming growth factor-α (TGF-α) and heparin-binding EGF (HB-EGF) are some of the ligands expressed from cancer cells (autocrine stimulation) or cancer microenvironment (induced by cancer cells) to activate EGFR. Those ligands bind to the extracellular domain of the receptor and induce the formation of receptor homo- and heterodimers (Figure 24). Overexpression of EGFR receptors increases the possibility of dimerisation and signal transduction that is often the case in lung- and colon cancer. Furthermore, a higher efficiency in growth and proliferation signaling is achieved if both receptor and its respective ligand are overexpressed[9]. ErbB2 overexpression is often associated with breast cancer and accounts for 20 to 25% of the cases[184]. Monomers of this receptor do not need any ligand to form heterodimers and activate other receptors of the EGFR family. Moreover, its overexpression may facilitate spontaneous homodimerization and activation[10]. Receptor dimerisation results in phosphorylation of specific tyrosine residues within the cytoplasmic tail and activation of the kinase domain[185].

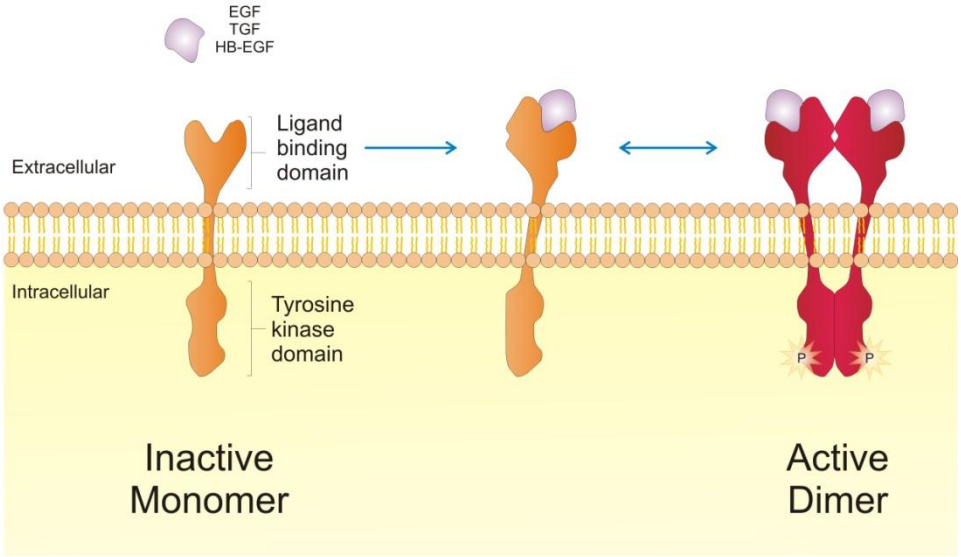

Figure 24. ***Binding of ligands to extracellular domain of the receptor and receptor dimerisation*** *(Adapted from ref.[10])*[7]

Five major autophosphorylation sites of EGFR have been reported (tyrosines 992, 1068, 1086, 1148, and 1173)[10]. Additional sites have been shown to be phosphorylated by other proteins like Src (Y891, Y920)[186]. These tyrosine sites act as docking sites for a variety of signaling

molecules. Recruited proteins include adaptor proteins (Grb2, Shc, Crk, Nck, and Dok-R), as well as non-RTKs with enzymatic activity (Src and Abl), tyrosine phosphatases (PTB-1B and SHP-1), phospholipase C-γ (PLCγ) or GTPase activating proteins for Ras and p120 RasGAP[10](Figure 25).

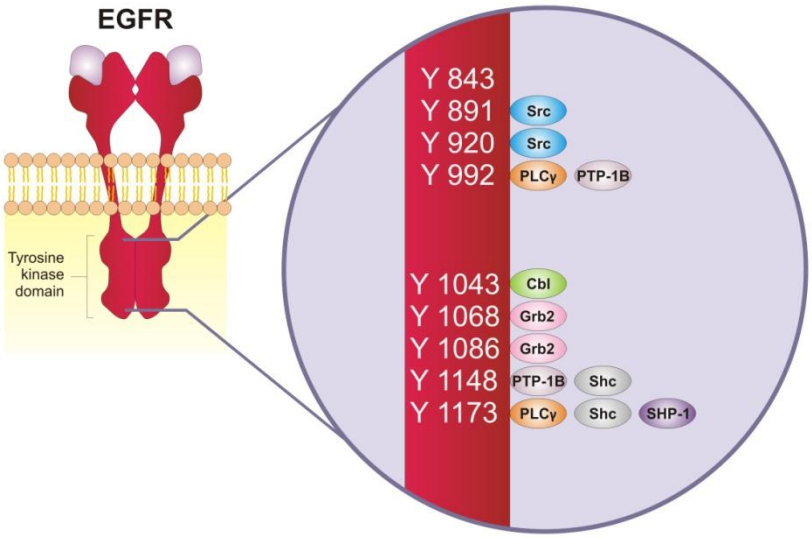

Figure 25. ***Adaptor proteins bind to specific phosphorylation sites*** *(Adapted from ref.[10])*[7]

Some of the bounded proteins (e.g. PLCγ) can be autophosphorylated and increase their enzymatic activity or the phosphorylation of bounded protein creates additional docking sites for other proteins (e.g. phosphorylation of Shc creates a docking site for Grb2)[187]. Downstream signaling depends on the catalyzed proteins on phosphorylation sites of EGFR. Dimerised EGFR activate two main intracellular signaling pathways: On the one hand, Ras-Raf-MEK-ERK1/2 mitogen-activated protein kinase (MAPK) pathway, which is involved mainly in controlling cell proliferation and differentiation, and on the other hand, phosphoinositine 3-kinase (PI3K)-Akt-mTOR signaling cascade, which acts as a pro-survival and anti-apoptotic pathway[183]. Another target of EGFR is also the Janus kinase/signal transducers and activators of transcription (STAT) pathway. STATs are involved in cell survival and oncogenesis and can be activated directly by interaction with EGFR or indirectly through Src family kinases[188-189]. Additionally, knowledge about new cellular processes influenced by EGFR signaling is growing. The complete biochemical network associated with EGFR is still not fully understood.

2.4.1. MAPK signaling

Downstream MAP kinase pathways regulated by EGFR include extracellular-signal regulated kinases (ERK), c-Jun N-terminal kinases (JNK) and p38 kinases. ERKs are mainly involved in growth factor-induced cell differentiation, proliferation and transformation signaling, whereas JNK and p38 mediate cytokine and numerous stess-induced cell responses, cell growth, cell arrest and apoptosis[96]. ERKs play a role in signal transduction initiated by tumor promoters such as TPA and growth factors like EGF and platelet derived growth factor (PDGF). The pathway starts with binding of Grb2 or Shc to the activated EGFR and recruitment of nucleotide exchange factor SOS which places EGFR in a close proximity to Ras (guanosine triphosphate (GTP) binding protein)[10] (Figure 26).

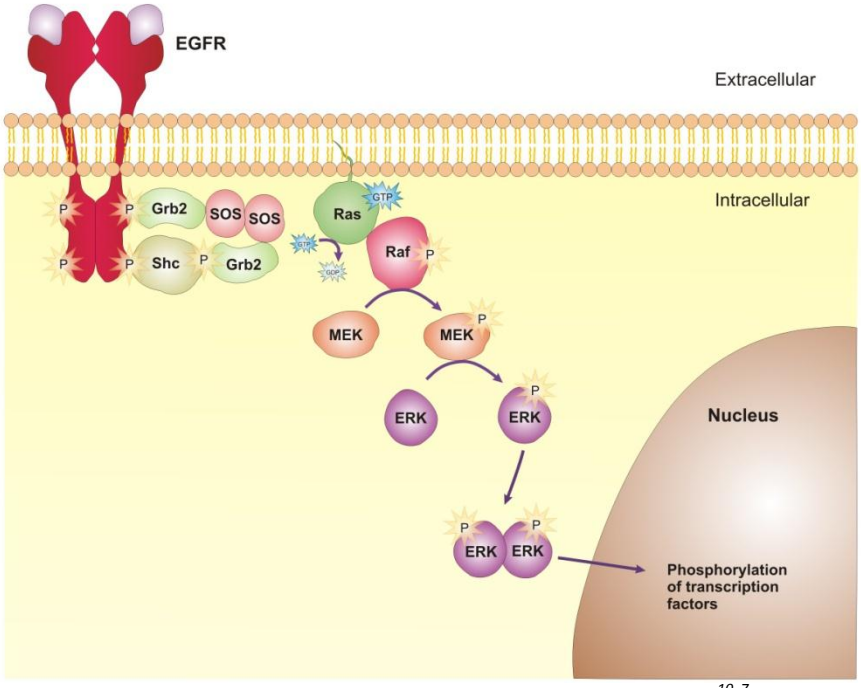

Figure 26. ***Ras-Raf-MAP kinase pathway*** *(Adapted from ref.[10])*[7]

Ras protein exists in tree isoforms (K-Ras, N-Ras, and H-Ras) which are encoded by KRAS, NRAS, and HRAS oncogenes. Those oncogenes are often mutated in cancer cells[190]. SOS enables inactive Ras to catalyze the exchange of GTP for GDP and converting Ras into its GTP-bound active form. Active Ras leads to the direct activation of serine-threonine kinase B-Raf. Activated Raf kinase phosphorylates MEK1 and MEK2 kinases which in turn activate the extracellular-signal regulated kinases (ERK1 and ERK2). ERK kinases translocate to the nucleus and increase gene transcription by phosphorylation of various nuclear transcription factors like AP1, Sp1, E2F, Myc, and Elk-1[10].

2.4.2. PI3K/Akt signaling

Phosphoinositide 3-kinases (PI3Ks) have been implicated in the regulation of cell growth, proliferation, survival, differentiation and cytoskeletal changes[191] (Figure 27).

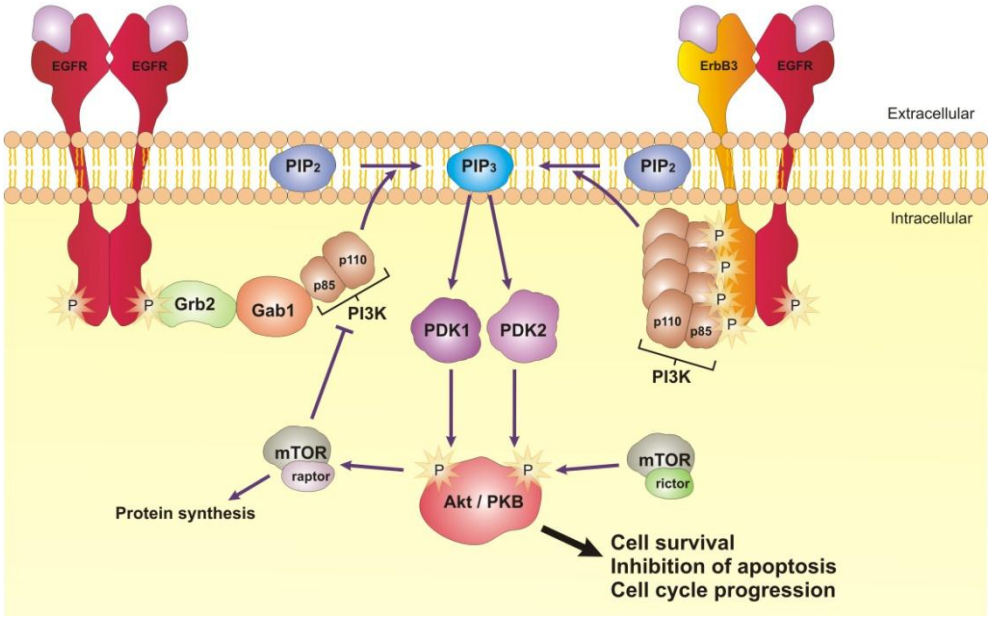

Figure 27. ***PI3K/Akt signaling activated by EGFR*** *(Adapted from ref.[10])*[7]

PI3K is indirectly recruited to EGFR via the adaptor protein Gab1 which interacts with Grb2. Grb2 binds to phosphorylated tyrosine residues Y1068 or Y1086 of EGFR. The p85 subunit of PI3K can also directly bind to the phosphorylation of heterodimers between EGFR and ErbB3. The catalytic part of PI3K, subunit p110, catalyses the conversion of phosphatidylinositol-4,5-bisphosphate (PIP_2) to phosphatidylinositol-3,4,5-trisphosphate (PIP_3) in the plasma membrane[10]. PIP_3 can phosphorylate PDK1 and PDK2 kinases which carry the phosphorylation further to Akt or protein kinase B (PKB) as one of the best characterized downstream mediators of PI3K pathway[191]. Akt is involved in promoting cell survival by inhibition of proapoptosis proteins such as BAD, glycogen synthase kinase 3 and the forkhead transcription factor FKHR-L1. Another effect of Akt is promotion of cell-cycle progression and proliferation maintained by downregulation of the CDK4 inhibitor p27[10]. The mammalian target of rapamycin (mTOR) is an atypical serine/threonine kinase that is also an important player in PI3K-Akt signaling. It is present in two distinct complexes: mTOR-raptor complex (mTORC1) and mTOR-rictor complex (mTORC2). Protein complex mTORC1, is modulated by Akt and serves as a negative feedback loop for PI3K. Active mTORC1 has a number of downstream biological effects including translation of mRNA, suppression of

autophagy, ribosome biogenesis, and activation of transcription. In addition, mTORC2 protein complex was shown to induce Akt phosphorylation and thus promote cell survival. Aberrant mTOR signaling is involved in induction of cancer, cardiovascular disease, and metabolic disorders. Rapamycin is an immunosuppressant that is used to inhibit mTORC1 specifically[192-193].

2.4.3. Arsenic and EGFR pathway

There are several reports on the activation of EGFR-pathway by arsenic. Such, chronic arsenic exposure showed a stimulation of EGFR ligand expression like TNFα and HB-EGF in animal models and humans[195-196]. Additionally, phosphorylation and upregulation of EGFR was also observed in bladder cell lines exposed to arsenic[194-195]. However, the mechanisms underlying this activation are not completely understood. Several studies reported an interaction of arsenic at diverse nodal points of the EGFR pathway. On the one hand, arsenic might directly interact with EGFR molecules to induce conformational changes or dimerise EGFR for activation[196]. On the other hand, the non-receptor tyrosine kinase Src might be involved in arsenic-induced EGFR expression, as Src has been shown to be activated by arsenic in several cell lines[195]. MAP kinases ERK1/2, JNK and p38 were also reported to be activated by phosphorylation in cells exposed to arsenic[196]. The regulation of those kinases seems to vary in time- and dose- dependent manner. Moreover, arsenic activation of the ERK pathway appears to be associated with proliferative responses, whereas activation of JNKs and p38 by arsenic have been linked to apoptosis and inhibition of proliferation[196](Figure 28).

A study on a mesothelioma cell line (NCI-H2052) revealed the involvement of JNK- and ERK-dependent pathways in ATO-induced apoptosis. The authors reported that ATO induces apoptosis through activation of JNK1/2 followed by induction of the caspase cascade. When JNK1/2 was inactivated, ATO induced apoptosis through activated ERK1/2 in a caspase-independent way[197]. Additionally, ROS generation by ATO can be another factor for activation of p38 and JNK MAP kinases that consequently leads to apoptosis[150]. As already mentioned, the PI3K/Akt pathway maintains cell survival by inhibition of proapoptotic proteins. Upregulation of this pathway is reported to promote resistance against ATO. However, ATO inhibits PI3K/Akt pathway by modulation of E3 ubiquitin ligase Cbl-b protein, as a negative regulator of PI3K activation[198].

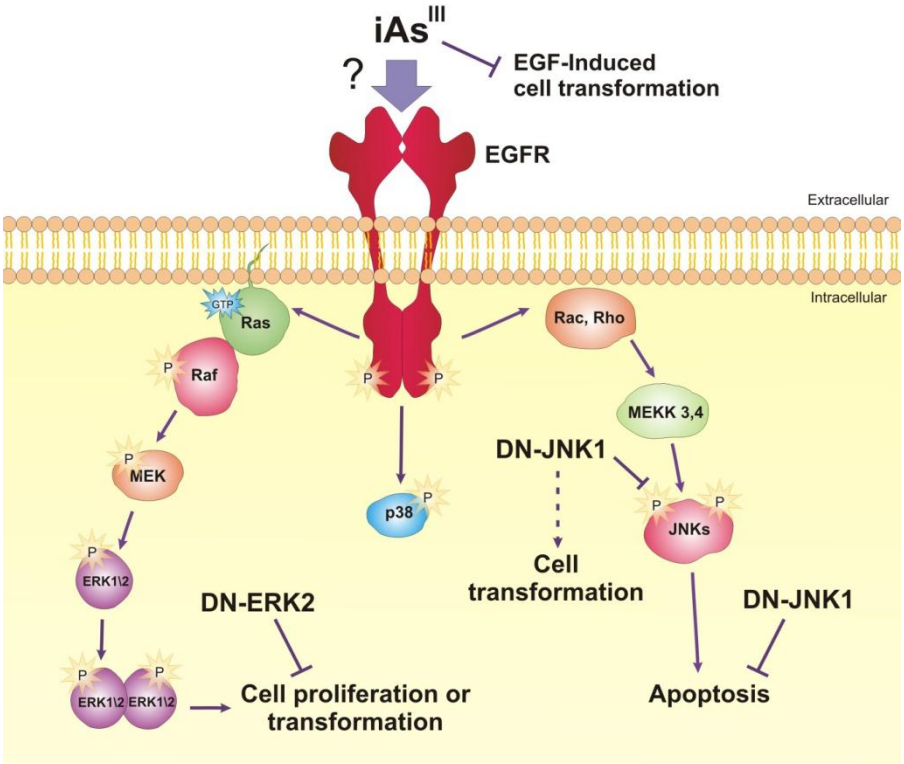

Figure 28. ***Arsenic induction of MAP kinase pathways leading to apoptosis or cell transformation*** *(Adapted from ref.[96])*[7].

2.4.4. Targeting EGFR

Considering the deregulation in growth factor signals in tumor cells, there has been increasing interest in the development of novel therapeutic agents against those pathways. In particular, agents targeting EGFR have shown promising therapeutic efficacy[199].

Table 3

EGFR Expression in various tumor types

Tumor type	Percentage of tumors expressing EGFR
Head and neck	80-100
Renal	50-90
Lung	40-80
Breast	14-91
Colon	25-77
Ovarian	35-70
Prostate	39-47
Glioma	40-63
Pancreas	30-50
Bladder	31-48

Adapted from ref.[199]

Increased gene expression levels of EGFR are observed in cancers of the head and neck, lung, colon ovary, cervix, bladder, oesophagus, stomach, brain, breast etc. (Table 3). EGFR gene expression in some of those cancers is correlated with a poor prognosis[200]. Inhibition strategies of EGFR are based either on monoclonal antibody-mediated blockade of the extracellular ligand-binding domain or by small molecular inhibitors of the intracellular tyrosine kinase domain (Table 4).

Table 4

Agents targeting EGFR

Agent	Tumor target	Status
Monoclonal Antibodies		
Cetuximab (C225)	Colorectal, SCCHN, NSCLC, pancreatic, breast, cervical, endometrial, gastric, hepatocellular, ovarian, renal cell	Approved for colorectal and SCCHN: phase II/III for other indications
Panitumumab (ABX-EGF)	Colorectal, RCC, NSCLC	Phase II/III
Matuzumab (EMD-7200)	Head and neck, colorectal, gastroesophageal, ovarial, cervical	Phase I/II
Nimotuzumab (h-R3)	Glioma, NSCLC	Phase I/II
MDX-447	Head and neck	Phase I/II
mAb806	Glioma, epithelial carcinoma	Preclinical
Tyrosine kinase inhibitors		
Gefitinib (ZD1839)	NSCLC, colorectal, head and neck, breast, prostate, bladder, esophageal	Approval for the use of gefitinib in previously treated NSCLC has been withdrawn after results of the ISEL trial; phase II/III for other indications
Erlotinib (OSI-774)	NSCLC, pancreatic, head and neck, breast, ovarian, prostate, colorectal, glioblastoma multiforme	Approved for NSCLC and pancreatic; phase I/III for other indications
Lapatinib (GW572016)	NSCLC, esophageal, breast, ovarian, head and neck, prostate, glioblastoma multiforme	Phase II/III
Canertinib (CI-1033)	Skin, squamous cell carcinoma, NSCLC	Phase I/II
EKB-569	Colorectal	Phase I/II
PKI-166	Kidney, prostate	Phase I
PD153035	Breast, glioma, head and neck	Preclinical

ISEL= Iressa (gefitinib) survival evaluation in lung cancer. Adapted from ref.[199]

The monoclonar antibody trastuzumab (Herceptin) was among the first targeted drugs to be approved by FDA for the treatment of HER-2 (ErbB-2)-positive breast cancer[199]. Trastucumab binds to the extracellular domain of HER-2 and disrupts its activity by induced receptor internalization and degradation, inhibition of active heterodimers, and induced formation of non-active receptor tetramers. The two most studied small-molecule tyrosine kinase inhibitors (TKI) that inhibit the tyrosine kinase domain of EGFR are erlotinib (Tarceva) and gefitinib (Iressa). These TKIs were initially FDA approved (Gefitinib in 2003; Erlotinib in 2004) for NSCLC patients who had failed to respond to conventional chemotherapy. Moreover, FDA approval for gefitinib was withdrawn after its failure to demonstrate a survival benefit in three

phase III trials[201-203]. According to data from two pivotal phase III studies (IPASS and INTEREST), gefitinib has received european approval for the treatment of adult patients with locally advanced or metastatic NSCLC with activating mutations of the EGFR-TK[204-206]. Currently, erlotinib is indicated as monotherapy in treatment-refractory advanced or metastatic NSCLC and in combination with gemcitabine for the first-line treatment of pancreatic cancer[199]. Erlotinib reversibly competes with ATP to bind to the catalytic kinase domain of the receptor and, thus, inhibits its activity, whereas the EGFR internalization or its degradation is unaffected[207](Figure 29).

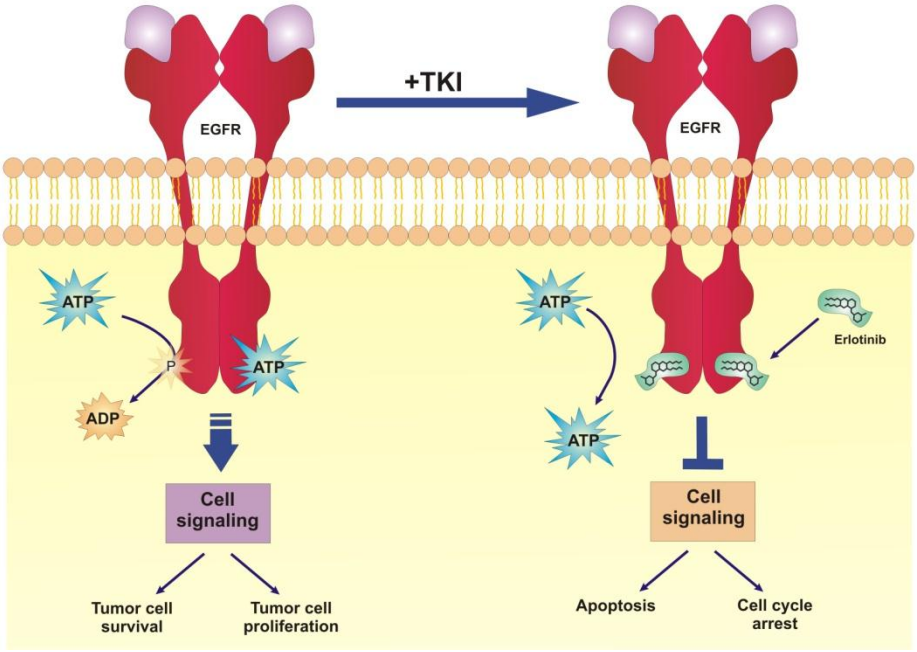

Figure 29. *Tyrosine kinase inhibitors* - *Erlotinib: mode of action*[7].

Inhibition of EGFR by irreversible EGFR-TKIs is the next step in the development of targeted therapies and has brought novel drugs in clinical trials. Furthermore, development of multi kinase inhibitors or combination of different drugs that inhibit multiple targets important for oncogenic phenotypes could improve antitumor activity.

2.4.5. Resistance to EGFR TKIs

Resistance is an important consideration for EGFR TKIs as well as other therapies (see therapy resistance, section 2.2.6). Multiple cases of therapy relapse were observed even in those patients who initially responded to erlotinib[207]. The sensitivity to gefitinib and erlotinib strongly correlates with a class of somatic activating mutations in the EGFR kinase domain of NSCLC patients (Figure 30).

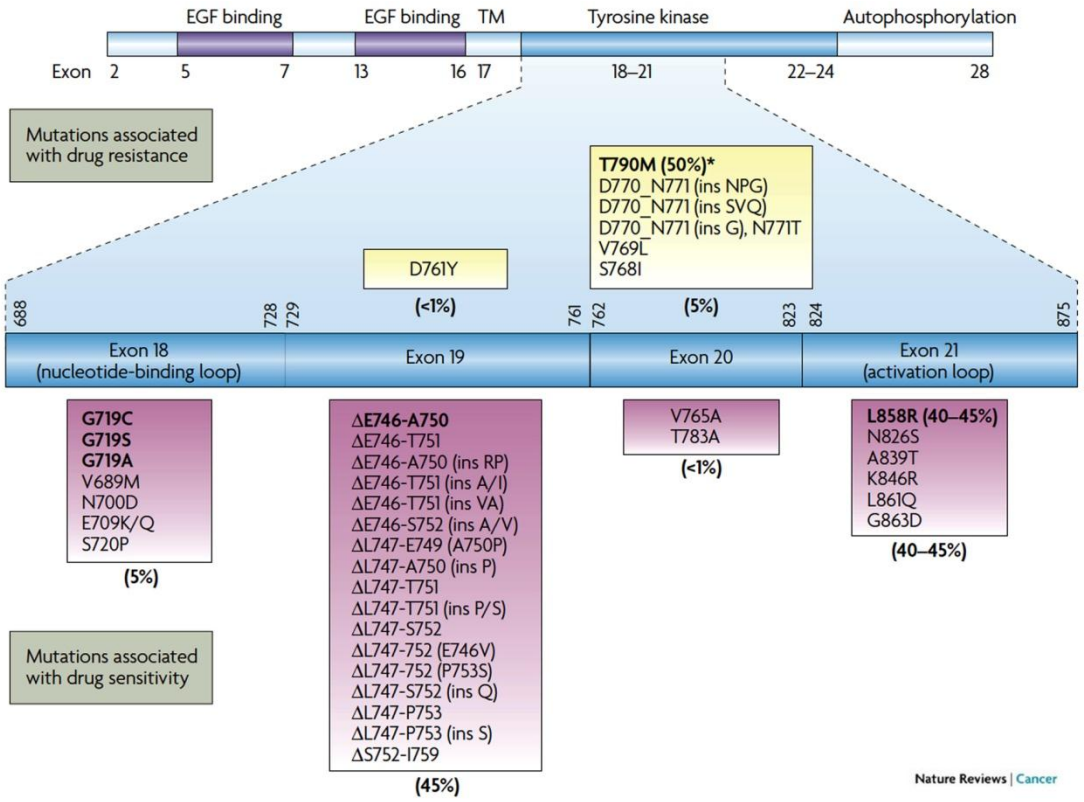

Figure 30. ***Gefitinib- and erlotinib-sensitizing mutations of EGFR in NSCLC***[200].

In general, NSCLCs that harbor exon 19 deletion mutations (e.g. ΔE746-A750), seem to respond better to gefitinib and erlotinib than tumors with point mutations in exon 21 (e.g. L858R) and may predict treatment benefit[200]. Gefitinib- and erlotinib-sensitizing mutations constantly hyperactivate EGFR signaling and promote anti-apoptotic and pro-survival signals. On the other hand, insertion mutations in exon 20 (e.g. T790M - substitution of threonine by methionine at position 790) have been reported in nearly 50% of EGFR-TKI-resistant tumors. In the most cases, T790M mutation is associated with acquired resistance. The threonine residue at position 790 of the EGFR kinase domain is located in the hydrophobic ATP-binding pocket of the catalytic region[208]. This threonine residue has been shown to form a critical hydrogen bond with both erlotinib and gefitinib. Therefore, substitution of threonine by methionine probably results in steric clash with the aromatic moieties on these two drugs[209-210]. Notably, it was reported that T790M mutation alone does not abolish the catalytic activity of wild-type EGFR. Thus, when T790M mutation occurs in combination with drug sensitizing mutations like L858R or ΔE746-A750, it results in a dramatic enhancement of EGFR activity[211]. Moreover, activating mutations that correlate with resistance to EGFR-TKIs can occur also in other oncogenes who encode downstream kinases in the EGFR signaling pathway. Thus, activating mutations in codons 12 and 13 of the KRAS gene found in 15–30% of NSCLCs,

have been proposed as a mechanism of primary resistance to gefitinib and erlotinib[212] (Figure 31)

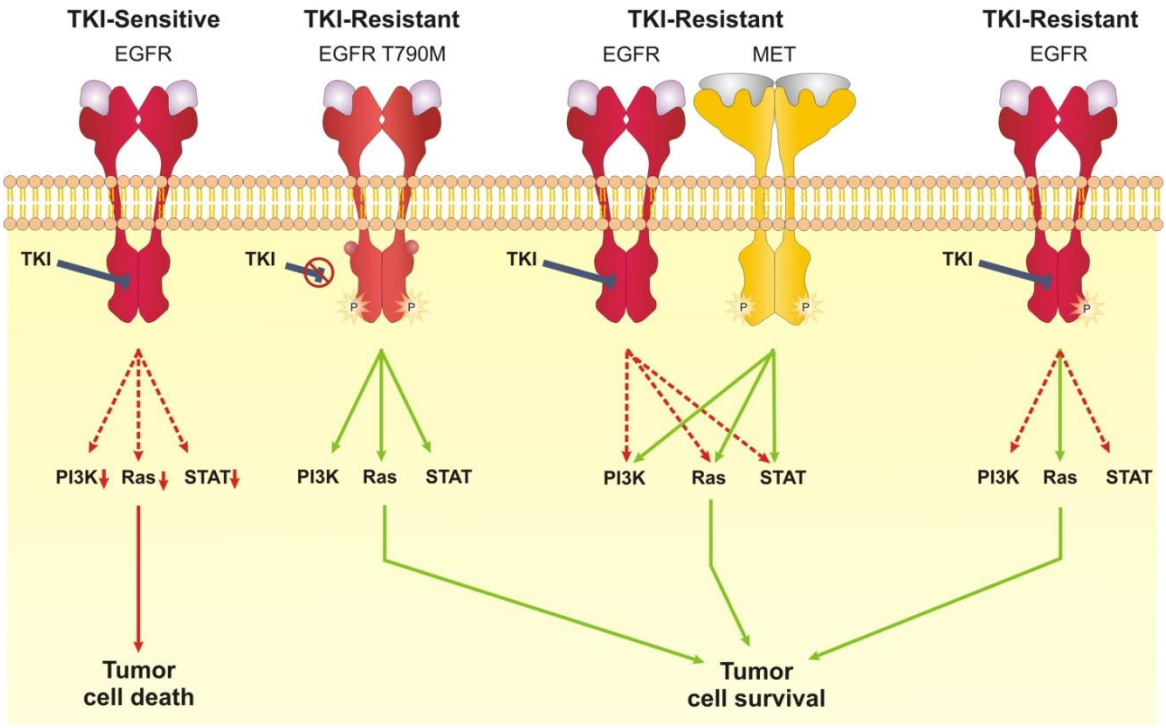

Figure 31. ***Mechanisms of EGFR resistance to TKIs in NSCLCs*** *(Adapted from ref.[183])*[7]

Finally, resistance can also occur through changes in other RTK that share downstream effectors with EGFR. Especially, amplification of *MET* proto-oncogene has been observed in approximately 20% of patients resistant to EGFR TKIs[183]. Activated MET tyrosine kinase was found to be a marker of primary resistance to gefitinib in lung cancer patients. It is believed that resistance by activated MET kinase is based on the immediately use of the MET pathway by the tumor cells, when EGFR survival signaling is blocked[213-214].

3 Aim of the study

Arsenic has been considered as a toxic metal for centuries. One the one hand, there is evidence indicating that exposure of humans to arsenic via contaminated air and drinking water causes cancer. On the other hand, arsenic represents one of the oldest remedies used in history to treat several diseases, including malignancies. The effects of arsenic in form of ATO have been extensively studied in APL. Two different activities have been explored, differentiation and apoptosis induction in leukemic cells depending on length and dose of ATO treatment. Regarding PML-RARα fusion kinase in APL, ATO influences distinct signaling pathways involved in mediating proliferation or apoptosis[150]. Consequently, a better understanding of molecular targets of ATO will promote a rational application in cancer types other than APL. Several reports suggest that arsenic may be combined with other agents to induce a synergistic effect that may reduce the toxicity of arsenic and enhance its anticancer effect[96]. Thus, clinical trials are underway with the aim of possible use of ATO in combination with vitamin c, retinoid acid, and growth factors against different leukemias[96,141,215]. Furthermore, synergistic activities were observed combining ATO with targeted therapeutics like imatinib or bortezomib against myelomas[91,216].

The aim of the here presented study was:

1) To investigate the anticancer activity of ATO in co-treatment with erlotinib and other TKIs against cell lines derived from various solid (non-hematological) tumors with a special focus on multidrug-resistant and cisplatin-resistant cells.
2) To analyze the effects of this drug combination with regard to apoptosis induction, impact on cell cycle distribution and on DNA synthesis rate.
3) To gain more insights into the role of EGFR pathway in cells treated with ATO/erlotinib. Thereby, cells expressing mutated or dominant-negative EGFR were analyzed in comparison to wild-type cells. Also cell models which do not express EGFR or which are resistant to EGFR inhibition based on Met overexpression or secondary EGFR mutations were tested.
4) To evaluate the impact of erlotinib on the intracellular ATO accumulation levels and the role of MDR proteins.
5) To investigate the impact of the synergistic combination of ATO with erlotinib in A549 xenografts in SCID mice.

Materials and methods

4

4.1. Drugs

All drugs that have been used in this study are shown in Table 5. For the *in vitro* experiments, ATO was dissolved in 1 M NaOH at a 50 mM concentration and was frozen in aliquots at -20°C. Cisplatin was dissolved in PMF at 20 mM.

Table 5

Drugs used for *in vitro* and *in vivo* experiments

Drug/Reagents	Specification	Structure	Solvent	Source
ATO (Arsenic trioxide)	Arsenic drug		1 M NaOH	Sigma-Aldrich
Cisplatin	Platin drug		PMF	Sigma-Aldrich
Erlotinib (Tarceva)	EGFR Inhibitor	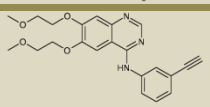	DMSO	LC Laboratories
Gefitinib (Iressa)	EGFR Inhibitor	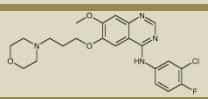	DMSO	LC Laboratories
Lapatinib (Tykerb)	EGFR and HER2 Inhibitor	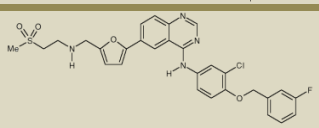	DMSO	LC Laboratories
Sorafenib (Nexavar)	Raf-1,BRAF, VEGFR-2, PDGFR-β, c-KIT, Flt-3	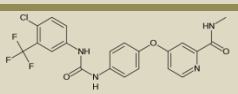	DMSO	LC Laboratories
Sunitinib (Sutent)	VEGFR 1-3; PDGFR-a and β, FMS-like Tyr. Kin., c-KIT; RET	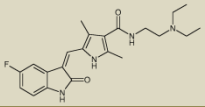	DMSO	LC Laboratories
MK-2206	Akt Inhibitor	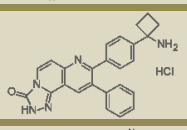	DMSO	Selleck
SB203580	p38 Inhibitor	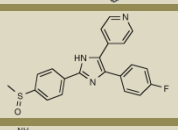	DMSO	LC Laboratories
U0126	MEK1/2 Inhibitor	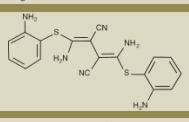	DMSO	LC Laboratories
PF-2341066	c-Met Inhibitor	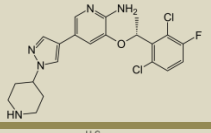	DMSO	Selleck
Cyclosporin A (CSA)	Immunosuppressant, MDR inhibitor	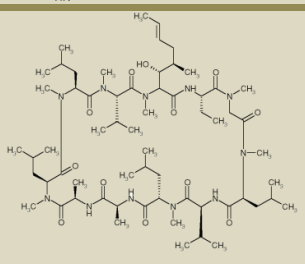	DMSO	Sigma-Aldrich

Buthionine sulfoximine (BSO) and N-acetylcysteine (NAC) were dissolved in 0.9% NaCl and sterile filtered directly before use. All other drugs were dissolved in dimethyl sulfoxide (DMSO). For all experiments, final DMSO concentrations were always below 1%. For *in vivo* experiments, ATO was dissolved in 1M NaOH and further diluted in phosphate buffered saline (PBS). Before intraperitoneal administration, pH of the solution was further adjusted to 7 - 7.6. Erlotinib was diluted in DMSO and further dissolved in Cremophor and 96% EtOH. For oral application, this solution was further diluted 1:10 in sterile water.

4.2. Cell culture

The panel of human cell lines used in this study and some of their genetic characteristics are summarized in Table 6. All cells were grown in their respective media supplemented with 10% fetal bovine serum (FCS) in a humidified atmosphere containing 5% CO_2 at 37°C (Table 6).

Table 6

List of used cell lines

Cell line	Histology	Specification	Growth medium	Source
A2780	Ovarian carcinoma	p53 wt	RPMI 1640	Sigma-Aldrich
A2780/cis	Ovarian carcinoma	p53 wt, cisplatin resistant	RPMI 1640	Sigma-Aldrich
A427	NSCLC, Adenocarcinoma	Ras (mut +/-), p53 wt, EGFR wt	MEME	ATCC
A549	NSCLC, Adenocarcinoma	p53 wt, Ras mutated (hom)	RPMI 1640	ATCC
H1650	NSCLC, Adenocarcinoma	EGFR mutated (delE746-A750 and PTEN loss)	RPMI 1640	ATCC
H1975	NSCLC, Adenocarcinoma	EGFR mutated (L858R and T790M)	RPMI 1640	ATCC
HCC827	NSCLC, Adenocarcinoma	EGFR mutated (delE746-A750)	RPMI 1640	ATCC
H2073	NSCLC, Adenocarcinoma	c-Met	RPMI 1640	ATCC
H1993	NSCLC, Adenocarcinoma	c-Met overexpression	RPMI 1640	ATCC
HCT116	Colorectal carcinoma	p53 wt, MMR KO, k-Ras mut (codon13), EGFR wt	McCoy	B. Vogelstein, John Hopkins University, Baltimore
HepG2	HCC	p53 wt, P-gp expression, N-ras mut (Codon-61), c-myc wt, K/H-ras wt, EGFR-, ERB2+, ERB3++, ERB4-	MEME	ATCC
P31	Mesothelioma	mTOR	MEME	K. Grankvist Umeå University
P31/cis	Mesothelioma	mTOR, cisplatin-resistant	MEME	K. Grankvist Umeå University
SW1573	NSCLC, Adenocarcinoma	-	DMEM	ATCC
$SW1573_{2R160}$	NSCLC, Adenocarcinoma	P-gp, MRP1	DMEM	ATCC
SW480	Colorectal carcinoma	p53 mut, Pgp, myc wt, k-ras mut, h-ras mut, N-ras (nd), EGFR wt	MEME	ATCC
SW579	squamous cell carcinoma	-	RPMI 1640	ATCC
SW1736	Thyroid carcinoma	-	RPMI 1640	ATCC
SW620	HCC	No EGFR expression	RPMI 1640	ATCC
VM-1	Melanoma	b-Raf mut (-/+?), N-ras wt	RPMI 1640	ICR
VMC 6	Mesothelioma	-	RPMI 1640	ICR
VMC 12	Mesothelioma	-	RPMI 1640	ICR
VMC 14	Mesothelioma	-	RPMI 1640	ICR
VMC 23	Mesothelioma	-	RPMI 1640	ICR

MEME - MEME + 0.2% Na-pyruvate + 1% non essential amino acids; DMEM - Dulbecco's Modified Eagle's Medium; HCC – Hepatocellular carcinoma; NSCLC – Non-Small-Cell Lung Carcinoma; ATCC – American Type Culture Collection;ICR – Institute for Cancer Research, Vienna

4.3. Cell proliferation and cell vitality assays

4.3.1 Cytotoxicity assay (MTT)

Background:

MTT assay is a colorimetric method commonly used for determination of cytotoxic or cytostatic activity of different anticancer drugs as single agents or in combination in cell culture experiments. This assay is based on the enzymatic reduction of 3-(4,5-dimethylthiazol-2-yl)-2,5-diphenyl-tetrazolium bromide (MTT) to formazan that is visible as a purple color. The color intensity is then measured at a wavelength of 450 nm by a spectrophotometer (620 nm is commonly used as reference). Reduction of MTT to formazan is catalyzed by an active and functional mitochondrial reductase enzyme that is usually produced in living cells with intact mitochondria (Figure 32). The color intensity directly correlates with the number of viable cells. Thus, MTT assay allows the evaluation of the impact of new compound on cell proliferation and viability by comparison of the color in untreated controls with samples after drug treatment. In this study, cell vitality was measured with the MTT based EZ4U kit (Biomedics, Vienna, Austria).

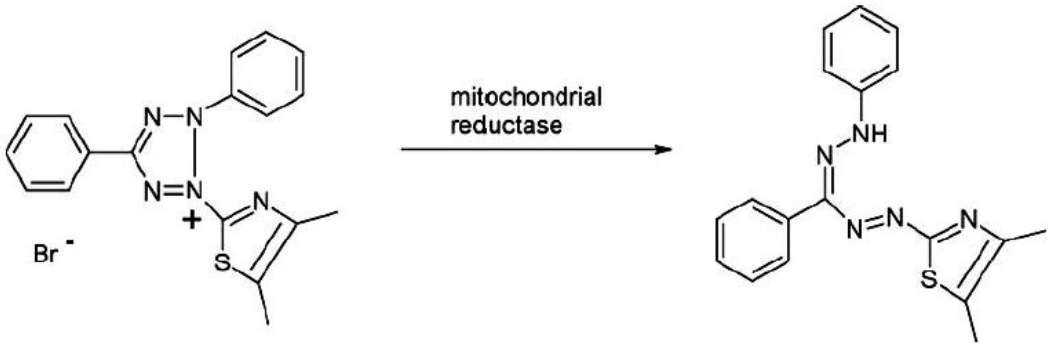

Figure 32. ***The reduction of 3-(4,5-dimethylthiazol-2-yl)-2,5-diphenyltetrazolium bromide (MTT) by mitochondrial reductase to formazan.***

Preparation:

Cancer cells were seeded in 96-well microtiter plates at a density of 2-4 x 10^4 cells in 100 µl culture medium per well. After a recovery period overnight, drugs (diluted in respective cell culture media with 10% FBS) were added to the cells in different concentration ranges (2 fold concentrated stock). In single drug treatment tests, 100 µl of dissolved drug were added to a final volume of 200 µl per well, whereas in combination tests with two drugs, 50 µl for each drug solution (4 fold concentration stock) was added to final volume of 200 µl pro well. After the incubation time, the proportion of viable cells was determined by MTT assay following the manufacturer's procedure (EZ4U, Biomedica, Vienna, Austria). To achieve an intensive

medium coloration, cells were incubated for 1-5 hours (depending on the metabolic capacity of the different cell lines). Plates were gently shaken before measurement at absorbance wavelength of 450 nm or 620 nm as reference. Cytotoxicity was expressed as IC_{50} values (half maximal inhibitory concentration) and was calculated by GraphPad Prism 5.0 software from dose-response curves.

Modifications:

A) *Time-dependence*: The drug incubation time was varied from 24 to 72 hours.

B) *Drug-pulsing-experiments*: After 6, 14, and 24 hours incubation time, drug-containing medium was replaced with fresh medium without drugs. Afterwards, cells were further incubated. After total incubation time of 72 hours, cell viability was determined.

4.3.2 Hoechst 33258-PI staining

Background:

Hoechst 33258, a blue-fluorescence DNA intercalating dye (excitation ~465 nm, when bound to DNA), stains the condensed chromatin of apoptotic bodies or condensed chromosomes during mitosis brighter than chromatin in normal cells (Figure 33).

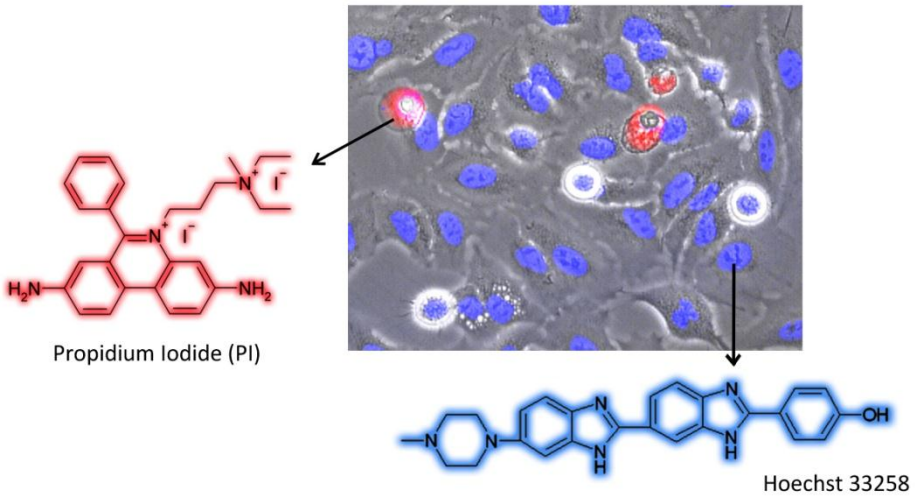

Figure 33. ***Dual staining with Hoechst 33258 and propidium iodide***

This dye is able to pass through intact membranes of both living and fixed cells. In contrast, propidium iodide (PI) is a red-fluorescence, DNA intercalating dye (excitation ~488 nm, when bound to DNA) that cannot pass the intact membrane of living cells and, thus, stains only dead cells (necrotic and late apoptotic cells). Using these dyes simultaneously, it is possible to distinguish normal, apoptotic, and dead cell populations by fluorescence microscopy.

Preparation:

Cells were plated in 24-well plates at a density of 2 x 10^4 cells in 500 µl growth medium per well. After recovery for 24 hours, cells were treated with drugs in different concentration ranges. Dissolved drugs were diluted in culture medium (RPMI with 10% FBS) and the cells were exposed for 24, 48 and 72 h. After treatment, 2 µl/ml HöPI mix (Höcht33258 (1 mg/ml) and PI (2.5 mg/ml)) was added direct to the wells. After 1 h incubation at 37°C live photos of the culture plates were made using a fluorescent microscope (Nikon Eclipse Ti inverted microscope system). Triplicate photos for each treatment were taken with DAPI-, CY3-filters, and in phase contrast. Morphological features of more than 300 cells for each treatment were counted.

4.3.3. ^{3}H-thymidine incorporation assays

Background:

This method is based on the incorporation of tritium-labeled deoxythymidine (dT), into new synthetized DNA strands. Thymidine is a 2'-deoxynucleosid composed of pyrimidine nucleobase, thymine, and the pentose D-deoxyribose (Figure 34).

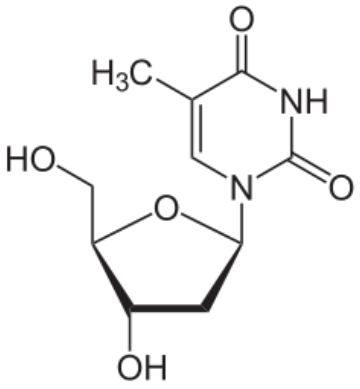

Figure 34. ***Chemical formula of Deoxythymidine***

The phosphorylated form of thymidine, pairs with deoxyadenosine to form A-T base pairs in the double helix. Unlike other deoxynucleosides which arise as building blocks of both RNA and DNA, thymidine is found only in DNA. The quantification of radioactive labeled thymidine represents a very sensitive method for the evaluation of the DNA synthesis ratio. Proliferating cell populations show enhanced thymidine incorporation as a result of increased ratio in DNA synthesis (during S-phase). On the other hand, dying or cell cycle-arrested cells show decreased DNA synthesis and, thus, reduced thymidine incorporation. Radioactivity of ^{3}H-thymidine can be measured after total cell lysis using scintillator solution via a liquid scintillator counter. This measurement is based on the detection of fluorescence of a transparent crystal (usually phosphor or organic liquid) which fluoresces after encountering radioactive radiation.

Preparation:

Cells were seeded in 96-well microtiter plates at a density of 5 x 10^4 cells in 100 µl culture medium per well. After recovery overnight, cells were incubated for 24 h with drug solutions which then were replaced with 100 µl of a 2 nM solution of ^{3}H-thymidine (specific activity: 25 ci/mM; GE Healthcare). Cells were incubated for 1 h at 37°C with ^{3}H-thymidine solution, and then washed twice with ice-cold PBS, lysed in 100 µl lysis-buffer, and transferred into scintillator tubes. The wells were washed again with 100 µl PBS that was also transferred to the corresponding cell lysates in the scintillator tubes. After addition of 2 ml liquid scintillator (KFORO Laboratories), the samples were mixed by turning upside down. Finally, the radioactivity of the samples was measured using a liquid scintillation analyzer (Tri-Carb 1900TR, Packard). In parallel, a normal cell viability MTT assay was performed to check and compare whether the same concentrations of tested drugs had an impact on cell viability.

Solutions:

10x PBS:

95 g Na_2HPO_4 x $2H_2O$

32 g NaH_2PO_4 x H_2O

44 g NaCl

Σ 1 L ddH_2O

Lysis buffer:

10 mM Tris-HCl, pH= 7.8

1% SDS

Σ 1 L ddH_2O

4.4. Flow cytometry

Flow cytometry (FCM) is a technology that is used to count and analyze cell properties at rates of up to 10,000 cells per second. Tested cells pass a focused laser beam where cell size, fluorescent dye distribution, internal structure, membrane potential, and nuclear diameter can be determined (Figure 35). Laser beams at specific wavelengths, excites fluorochromes that emit different wavelengths of light which can be detected by photomultiplier tubes (PMTs)

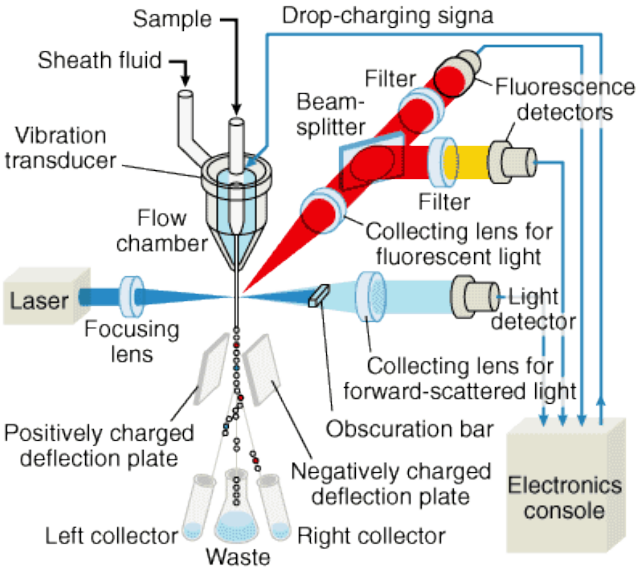

Figure 35. ***A functional illustration of a typical flow cytometer***

in the flow cytometer. This method is routinely used in diagnostics of health disorders, especially blood cancers as well as for many other applications in scientific research. Flow cytometry allows the detection of every single cell from cell suspension that pass the laser beam of the detector. In this study, flow cytometry was used to observe changes in cell cycle distributions or mitochondrial membrane potential of cancer cells after treatment with drugs.

4.4.1. Analysis of cell cycle distribution with PI

Background:

In order to test whether the drug combination investigated in this study induced changes in cell cycle distribution and to gain a deeper insight into their mode of action, PI staining was performed. Cell cycle is a tightly controlled set of events, resulting in cell growth and division into new daughter cells (compare mechanisms of cancer development). Diploid cells run through four stages of the cell cycle G1-S-G2-M, which are characteristic by varying amounts of DNA. Additionally, some nonproliferative cells enter a quiescent state called G0 and contain a constant chromosomal DNA amount (2n). These are mainly terminally differentiated cells like neurons or heart muscle cells. In contrast, cancer cells proliferate permanently and, thus, continuously undergo all phases of the cell cycle. The fluorescent dye PI is often used to quantify cell cycle distribution by flow cytometry. As already mentioned, PI cannot pass intact cell membranes and stains only DNA of permeabilized cells. Consequently, before staining, cells have to be chemically permeabilized to make the PI intercalation possible. The intensity of PI fluorescence (excitation at 488 nm) correlates with DNA amount of stained cells and gives insights to the effects on cell cycle distribution induced by different treatments (Figure 36).

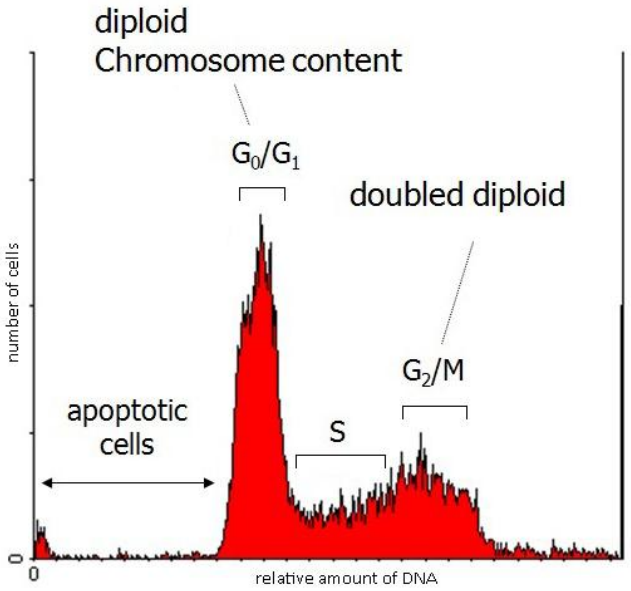

Figure 36. ***DNA histogram of a cell population using PI staining***

Preparation:

Cells were seeded in 6-well plates (2-4 x 10^5 cells in 2 ml growth medium per well) and left to recover for 24 hours. After drug incubation for 24 or 48 h, cells were trypsinised and washed once with FACS-PBS. Cell pellets were resuspended in 100 µl 0.9% NaCl and dropped slowly into 70% ice-cold ethanol. Ice-cold ethanol is used here for cell fixation and to render the membranes permeable for PI diffusion and DNA intercalation. After at least 1 h incubation at -20°C, cells were centrifuged for 1 min at 8000 rpm and then resuspended in 1 ml FACS-PBS. PI intercalates not only DNA, but also RNA. To prevent false-positive staining, RNAse A (0.79 Kunitz units/ml) was added to the samples followed by 30 min at 37°C. Cells were filtrated into FACS tubes and then stained with 1 mg/ml PI for another 30 min incubation at 4°C. Finally, fluorescence was measured by flow cytometry (FACS Calibur - Becton Dickinson, Palo Alto, CA) using Cell Quest Pro software.

Recipes:

FACS-PBS:
11.5 g (78.1 mM) Na_2PO_4 x 2 H_2O
2 g (14.7 mM) KH_2PO_4
2 g (26.8 mM) KCl
80 g (1.37 M) NaCl
Σ 1 L ddH_2O

4.4.2. Apoptosis analysis by JC-1 staining

JC-1 (5,5´,6,6´-tetrachloro-1,1´,3,3´-tetraethylbenzimidazol-carbocyanine iodide) is a lipophilic fluorescent dye that incorporates into the mitochondrial membrane, where it forms polymeres (known as J-aggregates) based on the physiological potential of mitochondria membranes (ΔΨm) (Figure 37). Polymerization of JC-1 shifts the fluorescence properties from green to red inside the mitochondria. Intact cells stained with JC-1 have red fluorescent mitochondria, whereas in cells with disturbed ΔΨm, the fluorescence switches from red to green (monomeric form of JC-1). Based on this chemical reaction, loss of ΔΨm can be detected. The mitochondrial intensity is an important stain parameter for cellular health and disruption of the mitochondrial membrane potential as an early event during apoptosis. Thus, JC-1 can be used as an indicator of apoptotic cell death induction (via the mitochondrial pathway). Flow cytometry can be applied to detect this fluorescence shift (from 527 nm to 590 nm) and, thus, easily distinguish apoptotic from non-apoptotic cells (Figure 38).

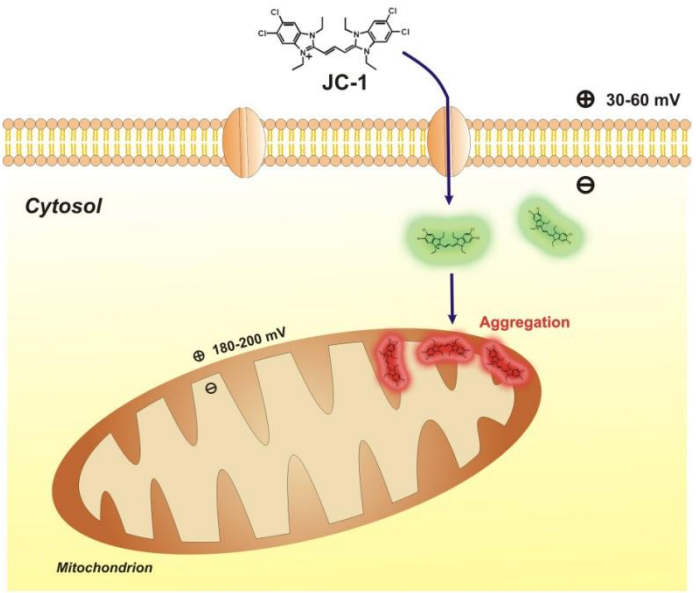

Figure 37. ***JC-1 staining of ΔΨm:*** *In healthy mitochondria the fluorescence of JC-1 shifts from 527 nm to 590 nm upon aggregation. This ratio of "green" to "red" fluorescence excited at 488 nm is used to detect ΔΨm changes*[7].

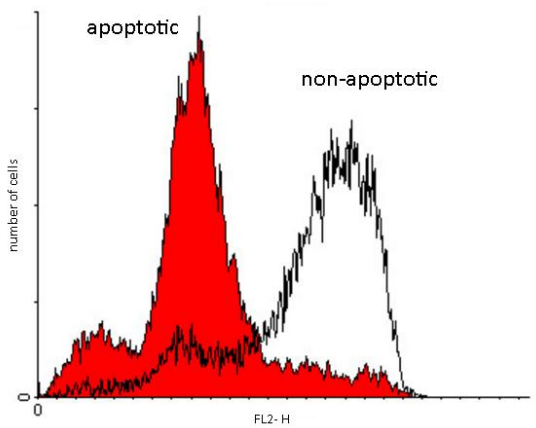

Figure 38. ***A histogram showing non-apoptotic and apoptotic cells stained with JC-1***

Preparation:

Cells were seeded in T25 cm^2 culture flasks (5 x 10^5 cells in 5 ml growth medium) and treated with the tested drugs after 24 hours recovery. After drug exposure, cells were collected by trypsinisation, washed once with ice-cold FACS-PBS and then resuspended in 1 ml JC-1 solution (10 µg/ml in DMSO). After 10 minutes incubation at 37°C, cells were centrifuged (5 minutes, 1200 rpm) and washed with 1 ml FACS-PBS following filtration of the cell suspension into FACS tubes. Fluorescence of the samples was analyzed by flow cytometry (FACS Calibur - Becton Dickinson, Palo Alto, CA).

4.5. Inductively-coupled plasma mass spectrometry (ICP-MS)

Inductively-coupled plasma mass spectrometry (ICP-MS) is a highly sensitive analytical technique used for determination of a range of metals and several non-metals. It can be used for the measurement of element concentrations down to the sub nanogram-per-liter (ng/l) or part-per trillion levels (ppt). This technique is based on the ionization of metals in argon plasma at approximately 10000 Kelvin (ICP) coupled with separation and detection by a mass spectrometer (MS) (Figure 39).

The analytic ions are then focused by a series of ion lenses into a quadrupole mass analyzer, which separates the ions based on their mass-to charge ratio. Finally, a detector receives the separated ions by an electron multiplier, proportional to ion concentration. The ICP-MS is widely used for the determination of trace level elements in many industries and research laboratories.

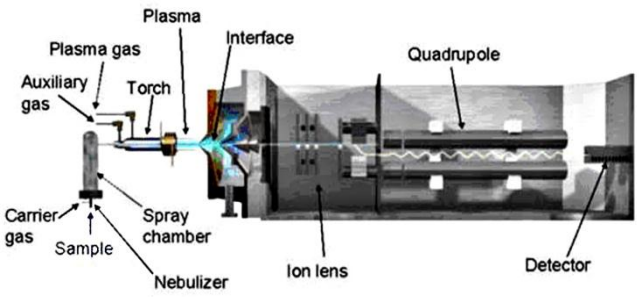

Figure 39. ***Agilent ICP-MS Block Diagram***

4.5.1. Accumulation of arsenic in cytosol

Preparation:

Cells were seeded in 6-well plates (1 x 10^5 cells in 2 ml growth medium per well), allowed to recover overnight and then treated with drugs (arsenic single treatment and in combination with erlotinib) for 3 hours. After drug exposure, cells were washed with ice-cold PBS and lysed with 400 µl tetramethylamonium hydroxide (TMAH). Wells were washed twice with 1 ml ddH_2O and together with collected cell lysates were transferred to 50 ml Falcon tubes.

Additionally, 1.6 ml 0.6 N HNO_3 was added to the samples and finally filled up with ddH_2O to 25 ml total volume. Two wells containing only growth medium and drugs without cells were prepared as negative control to determine whether arsenic unspecifically binds to plastic culture flasks, but also the amount of arsenic in water that was used to prepare the culture media. Another well was used to determine the overall cell number before lysis with TMAH. Arsenic concentrations were measured by ICP-MS using Elan 6100 (Perkin-Elmer/Sciex Corporation).

4.6. Protein analysis

4.6.1. Protein extraction

Cells were seeded in 6-well plates (3 x 10^5 cells/well in 2 ml culture medium) 24 hours prior to drug treatment. After 24 h and 48 h exposure time, cells were collected by scratching into the medium and transferred to Falcon tubes. Cell suspensions were centrifuged at 1200 rpm for 5 min, washed with PBS and then lysed on ice with 30-50 µl lysis buffer for 10 min. For further destruction of cell membranes, the samples were treated 3 min with sonicator and centrifuged for 15 min at 14000 rpm at 4°C. Supernatants containing protein lysates were collected and stored in aliquots at -80°C. Concentration of protein lysates was determined by using Micro BCATM Protein Assay Reagent Kit (Pierce Biotechnology, Rockford, USA).

Recipes:

Lysis buffer:

500 µl lysis buffer: 50 mM Tris
300 mM NaCl
0.5% Triton X-100

5 µl phenylmethanesulphonylfluoride (PMSF) – serine protease inhibitor, Roche

12.5 µl Complete (protease inhibitor cocktail tablets, Roche)

25 µl PhosSTOP (phosphatase inhibitor cocktail tablets, Roche)

4.6.2. Western blot analysis

Background:

Information about the activity of cellular proteins plays an important role in cell biology. One of the methods used to analyze proteins is Western blotting (also known as protein immunoblot). This is a commonly used immunochemical technique, that allows visualization of targeted proteins from prepared cell or tissue extracts via specific antibodies. It also allows

the determination of the molecular weight of a protein but also relative amounts of proteins present in different samples. Western blotting was used here to observe protein expression levels as well as protein phosphorylation status in treated cell lines with different drugs. The whole method includes three main steps: 1) separation of proteins from a protein extract according to their size, 2) transfer of proteins to nitrocellulose or PVDV membranes, and 3) detection of targeted proteins with specific antibodies.

Sodium dodecyl sulfate polyacrylamide gel electrophoresis – SDS-PAGE

SDS-PAGE uses a highly cross-linked gel of polyacrylamide as inert matrix through which the proteins migrate. It consists of two different gels, a stacking and a separating gel that are prepared by polymerization of acrylamide monomers (Figure 40-A). The protein samples are loaded into the collecting gel where components become stacked into a very thin, sharp band prior to enter the separating gel in which the proteins are fractionated by size (Figure 40-C).

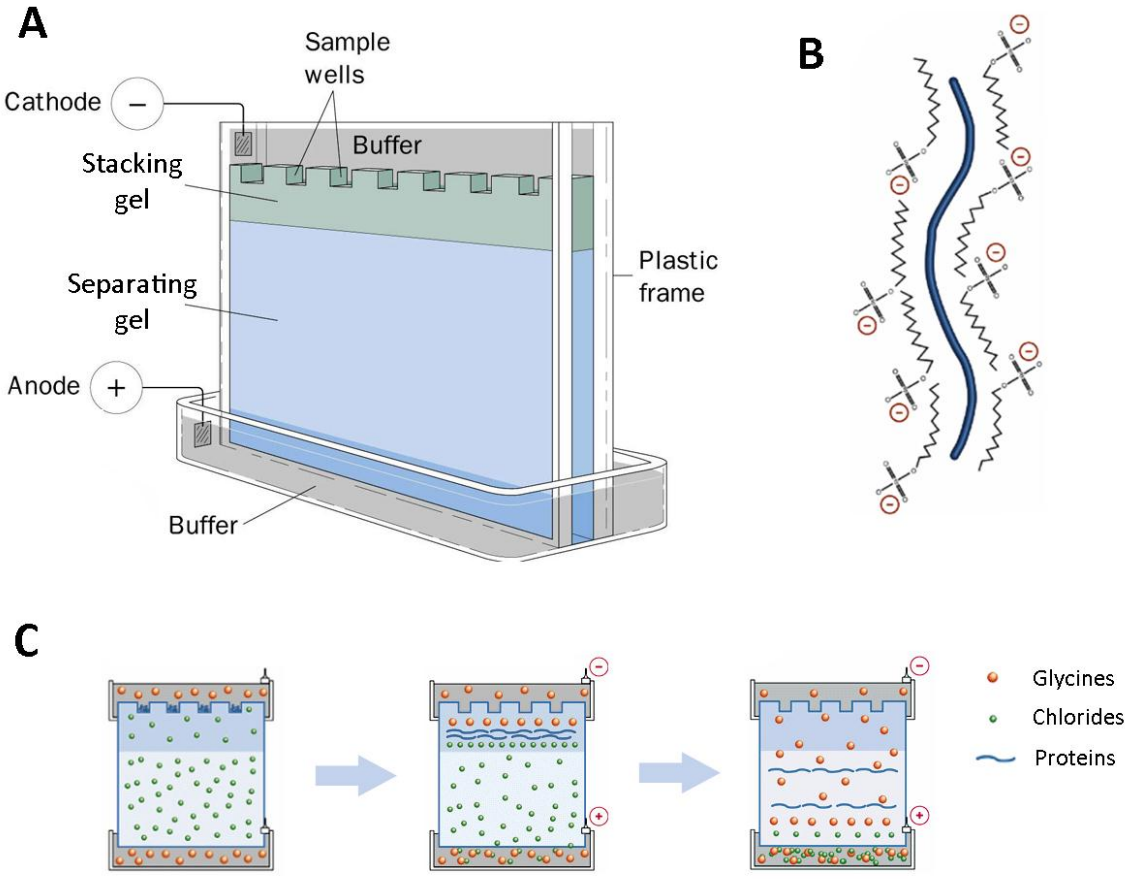

Figure 40. ***SDS PAGE protein electrophoresis.*** ***A*** *- Discontinuous gel showing stacking gel where the samples are loaded followed by separating gel where the proteins are separated.* ***B*** *- Treatment of proteins with SDS creates a uniform charge to mass ratio between different proteins.* ***C*** *- SDS-PAGE protein electrophoresis in process: Proteins are loaded onto a chloride containing gel (green dots) which is situated in a tank with electrode-buffer that contains zwitterionic glycine. Due to resulting electric current, proteins are stacked into a thin layer between the leading chloride ions and the trailing glycine molecules. Finally, proteins become fractionated in the separating gel.*

The size of pores of the gel can be adjusted to retard the migration of protein molecules of interest depending on the amount of acrylamide. Polymerization chain process starts using the radical ammonium persulfate (APS) and catalyzed by tetramethylethylendiamine (TEMED). Before starting the separation process, protein samples have to be unfolded. Therefore, the protein extracts are mixed with a strong negatively charged detergent, sodium dodecyl sulfate (SDS) that binds to hydrophobic regions causing denaturation of proteins into extended polypeptide chains (Figure 40-B). SDS is also added to polyacrylamide gels, to ensure the protein denaturation during protein electrophoresis. Additionally, negatively charged SDS masks the native charge of proteins in a constant ratio (1.4 g SDS/g protein) and allows samples to be separated only due to their molecular weight. Additionally, a reducing agent, such as β-mercaptoethanol was used to break the S-S bonds of two and three dimensional multisubunit polypeptides. Thus, the subunits containing only the primary structure can be analyzed separately. The separating gel and the electrode buffer have an alkaline composition (pH 8.8), whereas the stacking gel contains a neutral composition (pH 6.8). As electrophoresis is started, glycine ions supplied by the electrode buffer move slowly through stacking gel because of the zwitterionic form of the molecules at pH 6.8. In contrast, the chloride ions from the gel have a much higher mobility and migrate in front. The mobility of proteins is intermediate between glycine and chloride ions which compress the proteins into very thin layers in order to their electrophoretic mobility at the top of the separating gel. The alkaline pH 8.8 in separating gel increases the movement of glycine ions that are now negatively charged. The negative ion front moves and separates the proteins according to their size through the pores of polyacrylamide gel which act as molecular sieve.

Semi-dry blotting

The separated proteins were transferred from polyacrylamide gel to a solid polyvinylidene fluoride transfer membrane (PVDF) to make them accessible for antibody detection (Figure 41).

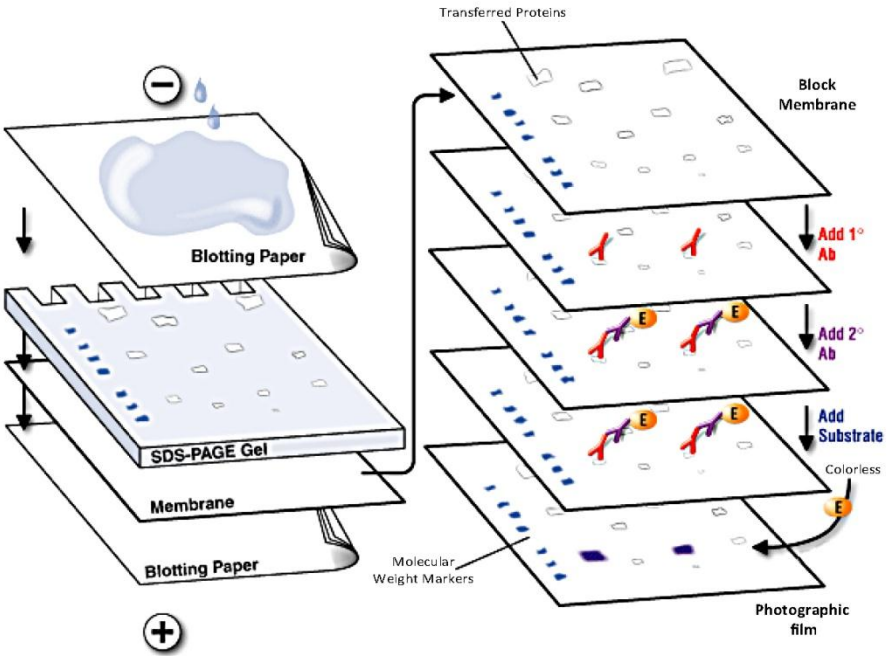

Figure 41. *Western blotting* - *Illustrated steps during semi dry blotting and protein detection*

Semi-dry blotting is an electrophoretic method that uses electric field which forces the negatively charged proteins to migrate from the gel to the membrane where they are bound mainly due to hydrophobic interactions. Gel and membrane are sandwiched between to stacks of filter paper soaked with a cathode buffer at the top and an anode buffer below the membrane. These buffers act as ion-reservoirs and support the electrical potential between the poles. By adding methanol to the anode buffer, SDS is removed from protein-detergent-complex and, thus, provides a greater binding of the proteins to the membrane.

After blotting, a blocking process followed prior to protein detection to eliminate nonspecific interactions between the membrane and the antibodies. This is achieved by incubation of membrane in a solution containing 0.5% bovine serum albumin (BSA) and 1% non-fat dry milk. The proteins from this solution attach to all remaining polypeptide-free areas on the membrane. After blocking and washing with tris-buffered saline with Tween (TBST), the membrane is ready for the detection process.

Detection of a target protein

The blocked membrane was incubated to a solution containing a primary antibody which binds specifically monoclonal or several polyclonal epitopes of the target protein. After incubation, the membrane was washed 3 times with TBST to remove unbound antibodies. After this washing step, the secondary antibody was added that binds the species-specific

region of the first antibody. The secondary antibody is labeled with a reporter horse radish peroxidase enzyme that produces a luminescence in the presence of a chemiluminescent agent. For the final detection, a sensitive photographic film was placed on the membrane, where the luminescence signal blackens the film at the specific protein bands (Figure 41).

Preparation:

Isolated protein extracts (15 µg proteins per sample) were diluted with lysis buffer and mixed with 4x loading buffer. SDS-PAGE was performed using 7.5% or 10% separating gel and 4.5% collecting gel. Contents of separating and stacking gel are shown in Table 7.

Table 7

Polyacrylamide gels

Separating gel			Stacking gel	
Contents	**10%**	**7.5%**	**Contents**	**4.5%**
H_2O	3.65 ml	4.1 ml	H_2O	1.56 ml
Acrylamide	1.875 ml	1.4 ml	Acrylamide	0.281 ml
TrisHCl; 1.5M, pH 8.8	1.875 ml	1.875 ml	TrisHCl; 0.5M, pH 6.8	0.625 ml
20% SDS	75 µl	75 µl	20% SDS	25 µl
10% APS	25 µl	25 µl	10% APS	12.5 µl
TEMED	5 µl	5 µl	TEMED	2.5 µl

Gel contents were mixed in a loading station for polymerization (Bio Rad), and then were putted in the electrophoresis chamber (Bio Rad) which was filled with 1x Lämmli-Electrophoresis buffer. Then, the protein samples were filled into the gel slots. Additionally, Precision Plus Protein marker was used (Bio Rad) as molecular weight marker loaded in one of the slots. Electrophoresis was conducted with 90 V until protein bands reached the end of the Western blot chamber. Proteins from the gel were blotted using Trans-Blot SD (Bio Rad) onto a PVDF membrane. The filter sandwich was made as follows (from the bottom started): 1) Filter papers (pre-wetted in Bjerrum-Blotting Buffer with SDS), 2) PVDF membrane (pre-activated in Bjerrum-blotting buffer with SDS), 3) SDS-PAGE (pre-wetted in Bjerrum-blotting buffer with methanol) and 4) Filter papers (pre-wetted in Bjerrum-blotting buffer with methanol). Blotting was performed using 0.08 mA (one sandwich) for 45 minutes. After blotting, the membrane was stained with Ponceau solution to prove the successful protein transfer and then washed with TBST. PVDF membranes were blocked with milk solution (0.5% BSA, 1% milk powder) for at least 1 hour. Afterwards, membrane was incubated at 4°C overnight with the primary antibodies (1:1000 dilution with 3% BSA) against EGFR, $pEGFR_{tyr922}$,

MRP1, MRP2, and ß-actin (Cell Signaling; Santa Cruz; Sigma). Membranes were washed three times with TBST and incubated for 1 hour using the respective secondary antibodies (1:10000 dilution with 1% BSA). After another three times washing with TBST, proteins were detected using SuperSignal West Pico Chemiluminescent Substrate (Pierce)-kit following the instruction of the manufacturer.

Receipts:

Tris-HCl 1.5 M, pH= 8.8:
18.2 g (150 mM) Tris
Σ 100 ml ddH_2O, pH= 8.8

Tris-HCL 0.5 M, pH= 6.8
3 g (25 mM)Tris
Σ 50 ml ddH_2O, pH= 6.8

Lysis buffer:
50 mM Tris-HCl, pH= 7.6
300 mM NaCl
0.5% Triton X-100
Σ 500 ml ddH_2O

4x Sample loading buffer:
4 ml 10% Glycine
2 ml 2-Mercaptoethanol
0.92 g SDS
2.5 ml 1 M Tris-HCl (pH= 6.8)
∑ 10 ml ddH_2O

Blocking solution
TBST
+1% powdered milk (fet free)
+0.5% Bovine Serum Albumine (BSA)

1x TBST:
100 mM Tris
0.9M NaCl
1% Tween (polyoxyethylene sorbitan monolaurate, Bio Rad)

10x Laemmli-Electrophoresis buffer:
30 g (250 mM) Tris
144 g (1.92 M) Glycine
10 g (35 mM) SDS
Σ 1 l ddH_2O

Bjerrumbuffer with SDS:
5.82 g (48 mM) Tris
2.93 g (39 mM) Glycine
0.375 g (1.3 mM) SDS
Σ 1 l ddH_2O

Bjerrumbuffer with Methanol:
5.82 g (48 mM) Tris
2.93 g (39 mM) Glycine
200 ml (12.3 mM) Methanol
Σ 1 l ddH_2O

Ponceau solution (0.25 mg/ml)
10x TBST
100 mM Tris
0.9 M NaCl
1% Tween (polyoxyethylene sorbitan monolaurate, Bio Rad)

4.7. Gene transfer via adenovirus infection

Background

Adenoviruses are a family of non-enveloped DNA viruses associated mainly with upper respiratory tract syndromes, infant diarrhea, conjunctivitis, common cold etc. They possess a linear dsDNA genome and are able to replicate in the nucleus of mammalian cells using the host's replication machinery. Adenoviruses can be engineered and used in gene therapy and cancer research as vectors to introduce genes of interest into a human cell (Figure 42). After a successful infection, the gene of interest will make a functional protein. Notably, adenoviruses can infect both dividing and non-dividing cells regarding the fact that only a proportion of cells undergo cell division at any given moment. In general, adenoviral dsDNA does not integrate into host cell chromosomes but remains episomal within the nucleus. Adenoviral vectors are replication-defective and unable to form new viral particles. Consequently, they are continuously diluted when cells undergo repeated rounds of mitosis[10].

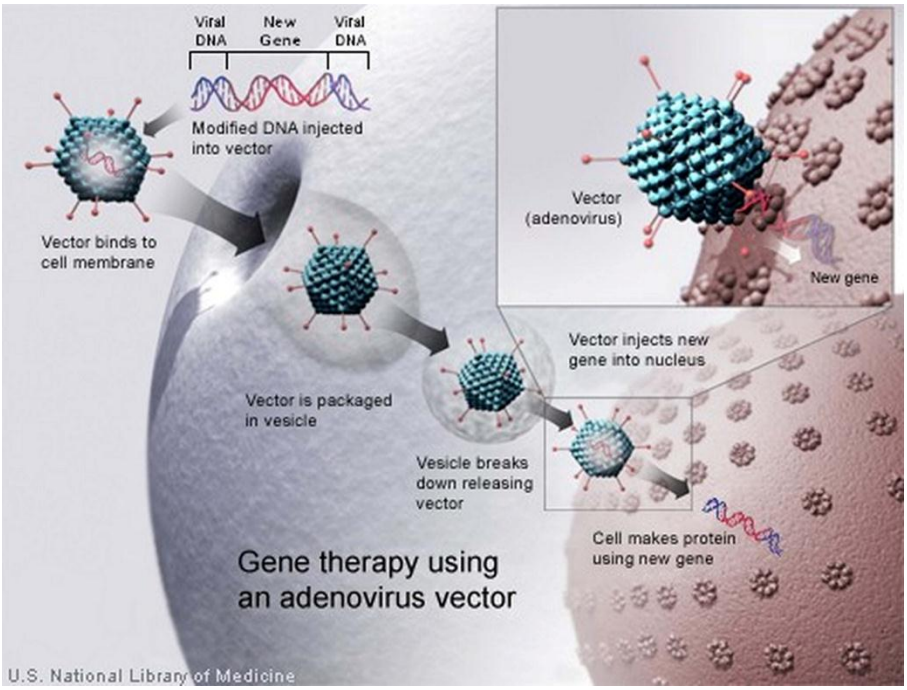

Figure 42. ***Adenovirus infecting the host cell***[81]

Adenoviruses used in this study were engineered as previously published (ref[217]): 1) one containing dominant negative EGFR fused with a GFP gene (dnEGFR-GFP) and 2) one containing only the GFP gene. Virus containing dnEGFR-GFP expressed a non-functional EGFR with GFP part instead of its tyrosine kinase. dnEGFR was used to observe its impact in A549 cells treated with ATO. Both viruses were detected by fluorescence microscopy.

Preparation

A549 were seeded in 6-well plates (2 x 10^5 cells in 2 ml growth medium per well). After a recovery period overnight, they were incubated with adenoviruses (MOI 1, 5, and 25) for 24 hours. GFP and dnEGFR-GFP expression were detected using a fluorescent microscope (Nikon Eclipse Ti). Infected cells were trypsinised and seeded in 96-well plates (2 x 10^3 cells/well). After another 24 h recovery period, cells were treated with ATO for 72 h. Cell viability was determined by MTT assays (see above).

4.8. *In vivo* xenograft experiments

Background:

Generally, xenotransplantation is known as the transplantation of living cells, tissues or organs from one species to another. In cancer research, human cancer cells are usually used to investigate the anticancer effects of various drugs.

In this study, A549 cells were injected into SCID (Severe combined immunodeficiency) mice to analyze the *in vivo* antitumor effects of ATO in combination with erlotinib (Figure 43).

SCID mice are characterized with a specific recessive mutation in chromosome 16 that encodes an enzyme subunit (DNA-PK or DNA-dependent protein kinase) which is required for the non-homologous end joining (NHEJ) of DNA. DNA-PK is also required for V(D)J recombination (Variable, Diverse, and Joining), a process that utilizes NHEJ to promote immune system diversity. The absence of V(D)J recombination as an important process in producing antibodies, leads to maturation failure of humoral and cellular immune system of SCID mice. In addition, SCID mice are also deficient in production of cells from the adaptive immune system such as B or T lymphocytes as well as in the activation of some components of the complement system. The absence of a functional immune system to fight infections or reject tumor cell transplants makes SCID mice an ideal model organism for *in vivo* cancer research.

Figure 43. ***SCID mouse***

Preparation:

The experimental design was approved by the Ethic Review Board and the experiments were performed following FELASA guidelines. A549 cells ($1x10^6$ in 50 µl serum free RPMI medium) were injected subcutaneously (s.c.) into the flanks of female CB-17/SCID mice. After cell inoculation, mice were assigned into four treatment groups, each consisting of 4 or 5 mice: 1) treated with solvent (intraperitoneal - i.p. and oral - p.o.); 2) treated i.p. with ATO (5 mg/kg) every day for two weeks; 3) treated p.o. with erlotinib (25 mg/kg) every day for two weeks; 4) combined treatment with ATO and erlotinib as mentioned above. Tumor growth ((length x $width^2$)/2) and body weight was measured every second day using a micro-caliper.

4.9. Statistical analysis

The data are expressed as the mean values ± standard deviation (SD) of three separate experiments. Statistical significance of differences between control and treatment group in different time points and drug concentrations was determined (as indicated) by t-test or two-way ANOVA using GraphPad Prism 5. Statistical significance was considered as: *$p < 0.05$; **$p < 0.01$; ***$p < 0.001$.

Results

5

5.1. ATO and erlotinib as single agents against various cancer cell lines

MTT viability assays (72 h drug exposure time) were performed to determine the antiproliferative effects of ATO and erlotinib as single agents in cancer cell lines of various origin. ATO single treatment showed an anticancer activity against the tested cells in the low μM range (Figure 44). The most resistant cell line was A549 with an IC_{50} value of 17.56 μM followed by the mesotheliomas VMC23, VMC6, and VMC12 with IC_{50} values of 12.36 μM, 11.82 μM, and 11.3 μM, respectively (Table 8). The highest sensitivity against ATO exhibited SW579 and A2780 cells with IC_{50} below 2 μM. The rest of the tested cell lines displayed intermediate IC_{50} values (5.8-9.5 μM). With regard to erlotinib, the majority of tested cell lines were non-responsive to erlotinib even in the highest concentrations (with the exception of VMC23 which had an IC_{50} of 17μM). Overall, ATO was found to be more cytotoxic than erlotinib in all tested cell lines.

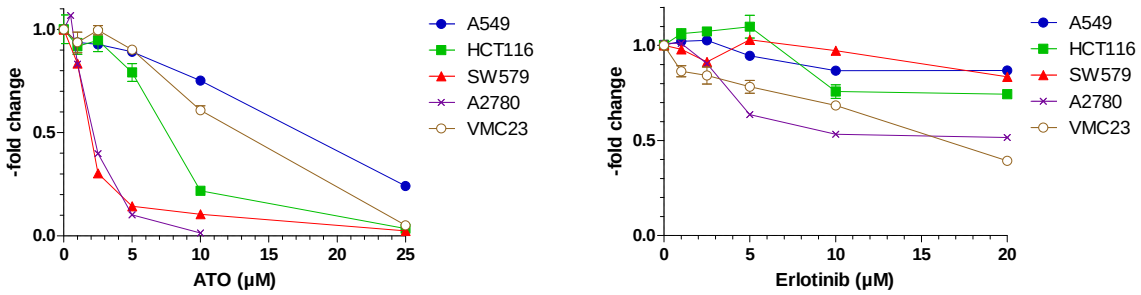

Figure 44. ***Viability of several cancer cell lines measured with MTT assay after 72 h treatment with ATO or erlotinib***

Table 8

IC_{50} values of different cell lines treated with ATO or erlotinib

Cell line	Histology	ATO (μM) IC_{50}	Erlo (μM) IC_{50}
A549	NSCLC	17.65	>20
HCT116	Colorectal carcinoma	9.46	>20
SW579	Thyroid carcinoma	1.94	>20
A2780	Ovarian carcinoma	1.83	>20
Hep3B	HCC	5.85	>20
A427	NSCLC	5.8	>20
VMC6	Mesothelioma	11.82	>20
VMC12	Mesothelioma	11.3	>20
VMC14	Mesothelioma	8.56	>20
VMC23	Mesothelioma	12.36	17
SW480	Colon carcinoma	8.67	>20
SW1736	Thyroid carcinoma	8.54	>20
VM-1	Melanoma	8.46	>20

5.2. Combination analysis with ATO and erlotinib

Combination tests with ATO and erlotinib were performed against various cell models, most of them resistant to both single agents (Figure 45). In all investigated cell models, predominantly synergistic activities were observed. Drug combination effects were validated by the calculation of combination indices (CI) using CalcuSyn software. Values smaller than 0.8 indicate synergism, CI values between 0.8 - 1.2 additive activity (marked with dotted lines, right panel), and values higher than 1.2 indicate antagonism. The highest synergistic activity was observed in A549, HCT116 and HepG2 cell lines (Figure 45 A-C). In these cell lines, ATO in co-treatment with low erlotinib concentrations (1 - 2.5 µM) showed synergistic values CI < 0.6, whereas ATO in co-treatment with higher erlotinib concentrations (5 - 20 µM) induced strong synergism CI ≤ 0.3 (see respective isobolograms Figure 45 A-C). Such, combination tests with 2.5 µM erlotinib decreased ATO IC_{50} values up to 11-fold, whereas, combination of ATO with 10 µM erlotinib decreased ATO IC_{50} values up to 16.8-fold (Table 9). Combination of ATO and erlotinib showed distinct synergistic anticancer activity also in several mesothelioma (VMC6, VMC12, VMC14, and VMC23), thyroid cancers (SW579, SW1736), melanoma (VM-1) and colon cancer (SW480) cell lines (Figure 45 D and Figure 46 A-D). The weakest synergism was observed in case of the lung cancer cell model A427, where only weak synergistic to additive activities (CI 0.3 - 1.0) were derived (Figure 46 D). Such, ATO co-treatment with 2.5 µM and 10 µM erlotinib decreased the IC_{50} value of ATO only up to 1.5-fold and 1.2-fold, respectively (Table 9). Notably, there were no antagonistic effects found in any of the tested cell lines. These data indicate that ATO in co-treatment with erlotinib increases synergically their antiproliferative activity in various cell models.

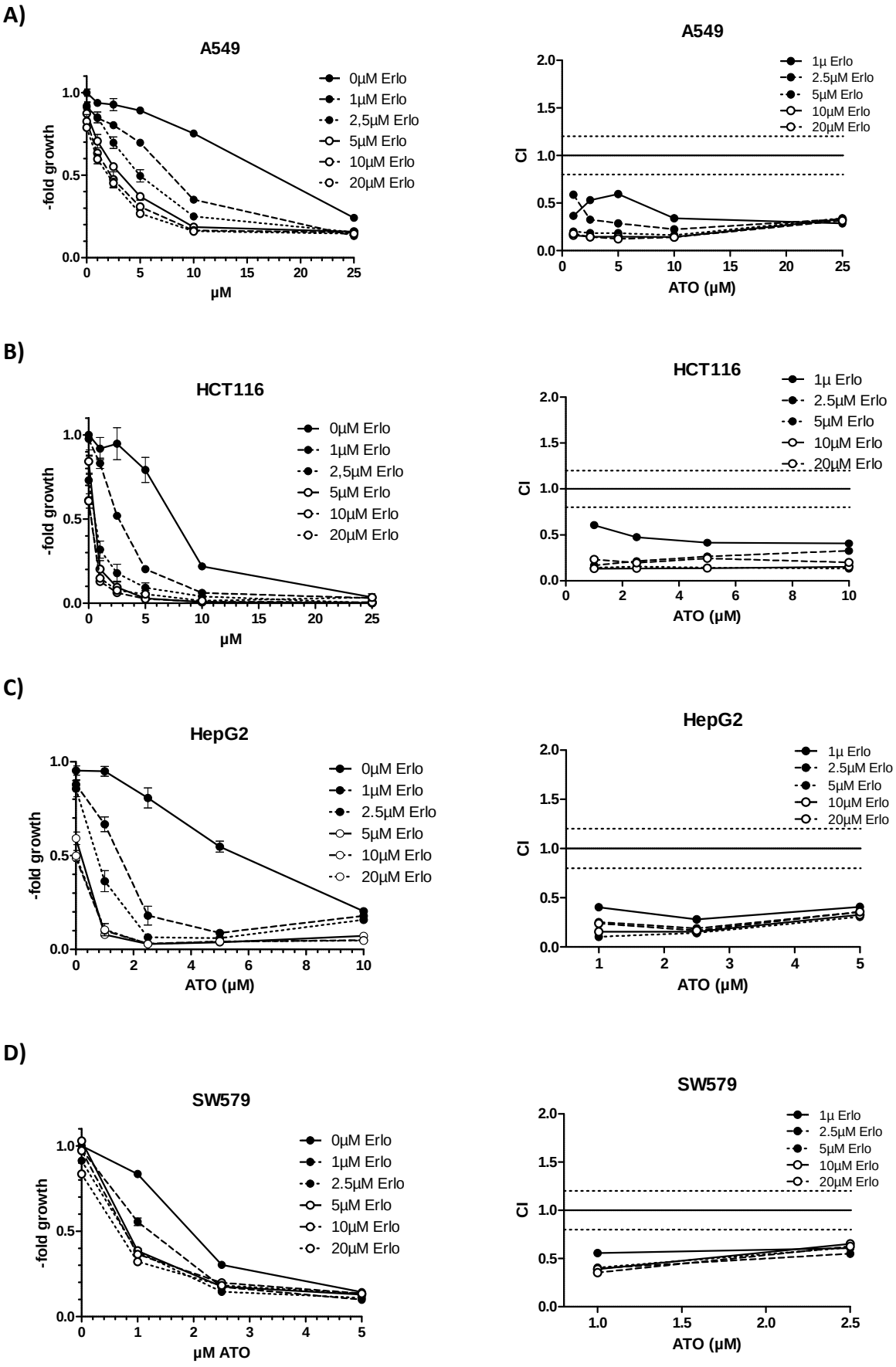

Figure 45 A-D. ***Activity of ATO co-treatment with erlotinib after 72 h exposure of different cell lines.*** *Diagrams on the left show viability changes measured by MTT assay. Respective isobolograms on the right show combination indices (CI) calculated following the method of Chou and Talaly by using CalcuSyn Software.*

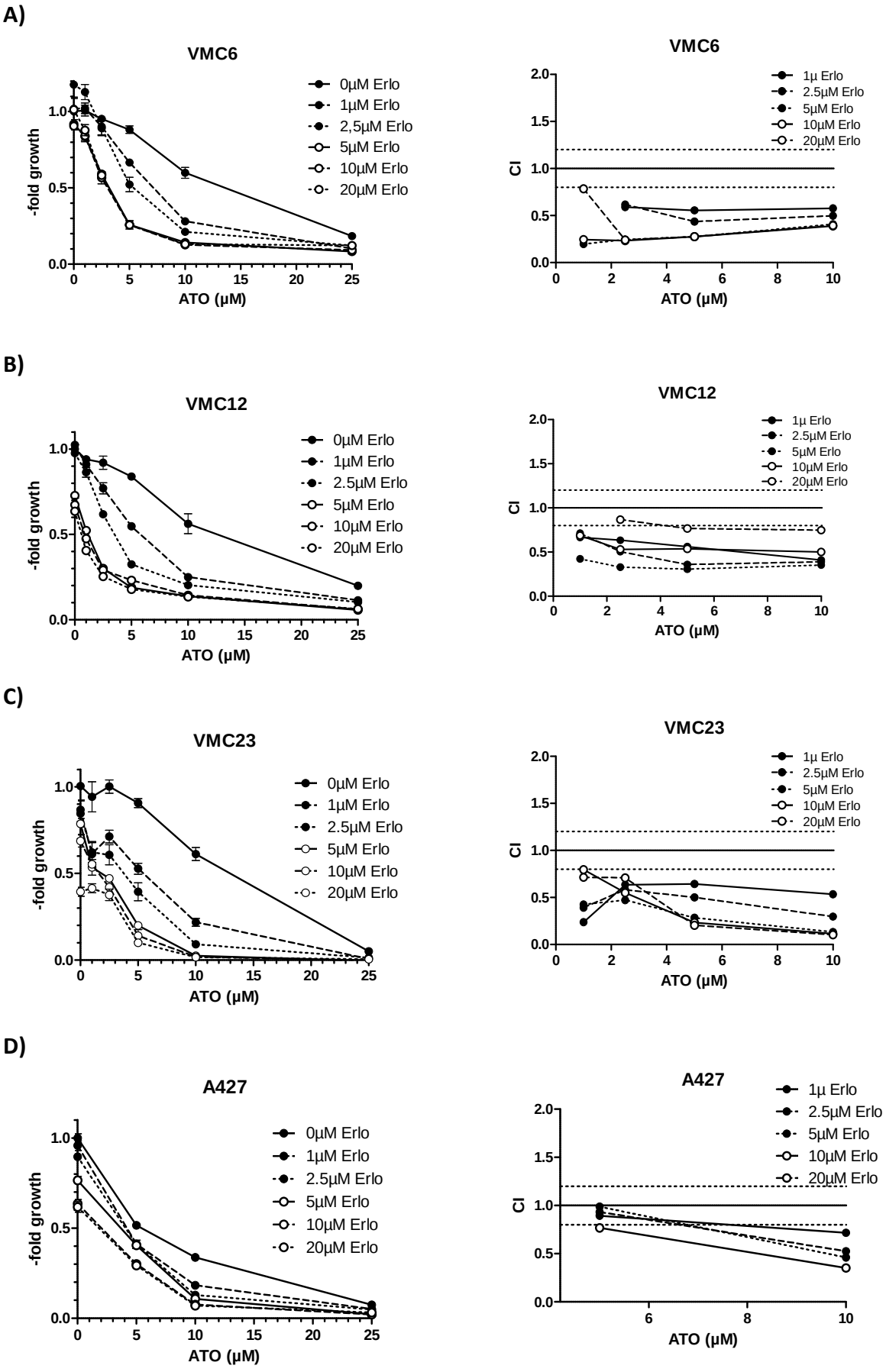

Figure 46 A-D. ***Activity of ATO co-treatment with erlotinib after 72 h exposure of different cell lines.*** *Diagrams on the left show viability changes measured by MTT assay. Respective isobolograms on the right show combination indices (CI) calculated following the method of Chou and Talaly by using CalcuSyn Software*.

Table 9

IC_{50} values of different cells treated with ATO, erlotinib or their combination

Cell line	Histology	ATO (µM) IC_{50}	Erlo (µM) IC_{50}	ATO with 2.5µM Erlo IC_{50}	Fold decrease	ATO with 10µM Erlo IC_{50}	Fold decrease
A549	NSCLC	17.65	>20	5.65	3.12	3.33	5.3
HCT 116	Colorectal carcinoma	9.46	>20	0.87	10.9	0.563	16.8
HepG2	HCC	5.85	>20	0.85	6.9	0.57	10.26
SW579	Thyroid carcinoma	1.94	>20	0.81	2.4	0.75	2.6
A427	NSCLC	5.8	>20	5.5	1.05	4.8	1.21
VMC6	Mesothelioma	11.82	>20	4.47	2.64	3.17	3.73
VMC12	Mesothelioma	11.3	>20	3.42	3.3	2.04	5.54
VMC14	Mesothelioma	8.56	>20	2.85	3	2.18	3.9
VMC23	Mesothelioma	12.36	17	4.76	2.6	3.21	3.85
SW480	Colon carcinoma	8.67	>20	2.74	3.16	2.36	3.67
SW1736	Thyroid carcinoma	8.54	>20	4.8	1.78	-	-
VM-1	Melanoma	8.46	>20	6.72	1.26	5	1.7

5.2.1. Antiproliferative effects of ATO/erlotinib combination in cisplatin-resistant cell models.

Resistance to the metal drug cisplatin is an important drawback in its use as a cytostatic in cancer chemotherapy. The aim of this experiment was to investigate whether ATO in co-treatment with erlotinib is able to overcome *in vitro* cisplatin-resistance in cancer cell models. Two cell sublines (from an ovarian cancer $A2780_{cis}$ and a mesothelioma $P31_{cis}$ cell line) that were previously selected for resistance against cisplatin were used to investigate the effects of ATO or erlotinib (Figure 47). As expected, both cell models were less sensitive against cisplatin in comparison to their parental cells (A2780 and P31). Thus, $A2780_{cis}$ and $P31_{cis}$ displayed a 6.2-fold and 5.2-fold resistance, respectively. Similarly, both cisplatin-resistant cell models were more resistant against ATO compared to their parental cells. Consequently, $A2780_{cis}$ was 2.3-fold more resistant against ATO than A2780 (ANOVA $p < 0.001$), whereas $P31_{cis}$ was 1.5-fold resistant to ATO in comparison to P31 (ANOVA $p = 0.01 – 0.001$) (Table 10). With respect to cisplatin and ATO, erlotinib was less active to all four cell lines. Interestingly, despite the weak antiproliferative impact of erlotinib to all cells, cisplatin-resistance cell models were slightly hypersensitive to erlotinib as compared to their parental cell lines.

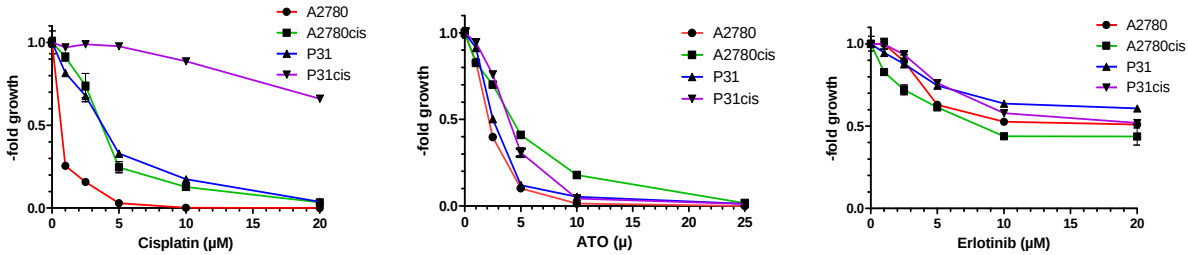

Figure 47. ***Cell viability of cisplatin-resistant cell models and their parental cell lines treated with cisplatin, ATO, and erlotinib measured by MTT assay after 72 h drug exposure.***

Table 10

IC_{50} values of cisplatin-resistant cell models and their parental cells treated with cisplatin, ATO, erlotinib, and ATO/erlotinib combination

Cell line	Cisplatin (µM) IC_{50}	ATO (µM) IC_{50}	Erlo (µM) IC_{50}	ATO with 2.5µM Erlo IC_{50}	Fold decrease
A2780	0.6	1.83	>20	1.5	1.22
$A2780_{cis}$	3.72	4.25	7.9	1.86	2.28
P31	3.82	2.53	>20	0.58	4.36
$P31_{cis}$	>20	3.9	>20	1.58	2.46

ATO co-treatment with erlotinib resulted in synergistic anticancer activity to both cisplatin-resistant cell models in all concentrations used (Figure 48). Synergistic effects were observed in both P31 and $P31_{cis}$. Notably, P31 showed a higher synergistic activity (CI = 0.13 - 0.47) than $P31_{cis}$ (CI = 0.3 - 0.7). ATO cytotoxicity in P31 combined with 2.5 µM erlotinib was increased up to 4.3-fold compared to 2.4-fold decrease of ATO IC_{50} in $P31_{cis}$. In contrast to the mesothelioma cell model, drug combination was synergistic only in ovarian cisplatin resistant-subclone $A2780_{cis}$ (CI < 0.8), whereas in parental A2780 it exhibited additive up to weak antagonistic activity (CI 0.7 - 1.9). Additive activities were measured in A2780 after treatment with low erlotinib concentrations combined with ATO, and only 20 µM erlotinib showed antagonistic effects. Synergistic effects were reflected in decrease of cell viability in $A2780_{cis}$. For example, treatment of ATO combined with 2.5 µM erlotinib decreased ATO-IC_{50} up to 2.3-fold (Table 10). In summary, it can be concluded that the ATO/erlotinib combination shows a synergistic antiproliferative activity also against cisplatin-resistant cell lines and can be used as a potential therapy to overcome this resistance.

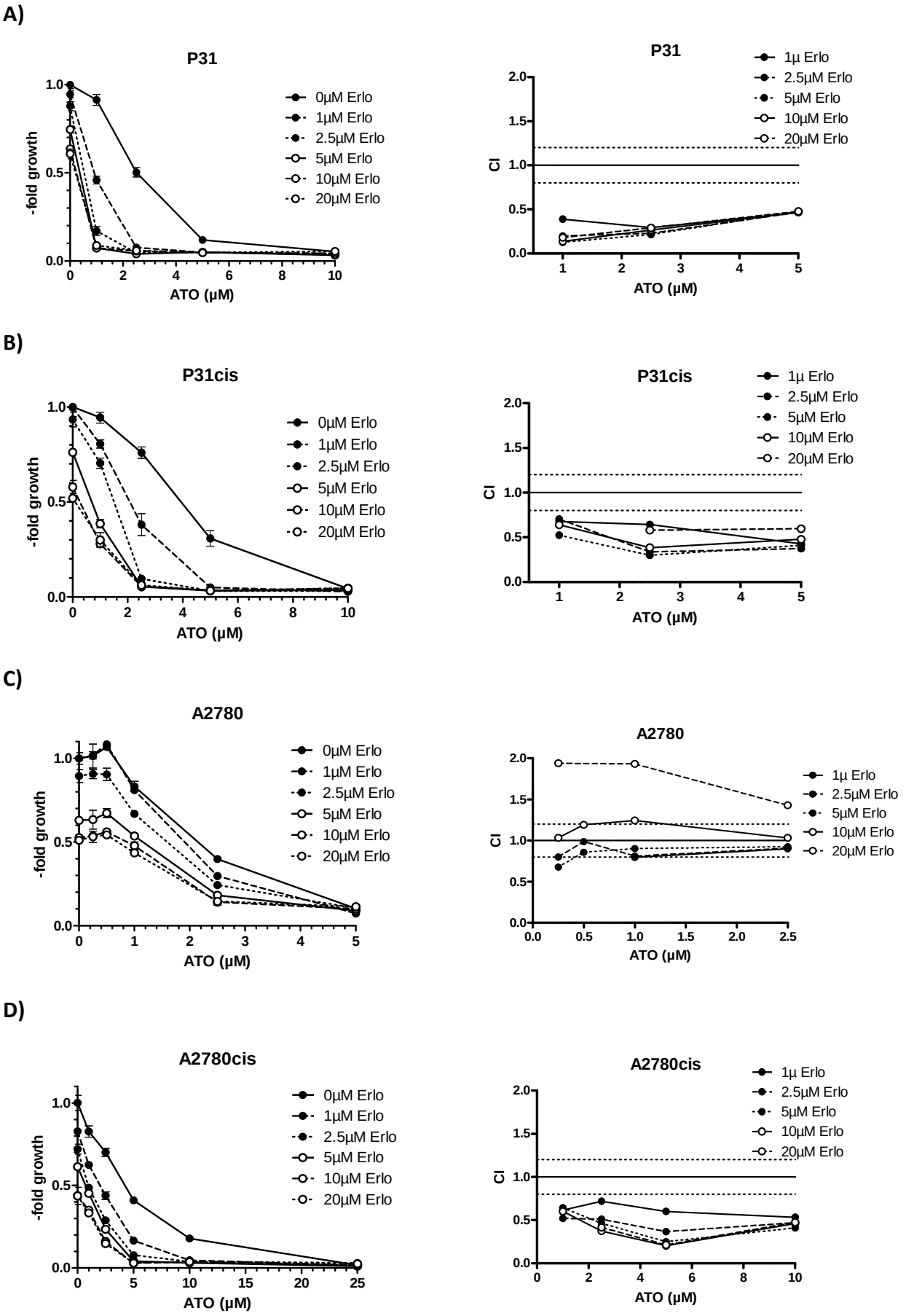

Figure 48. ***Anticancer activity of ATO/erlotinib combination in cisplatin-resistant and their parental cell lines.*** *Cell viability was measured by MTT assay after 72 h drug exposure. Respective CI values (Isobolograms) are shown on the right.*

5.2.2. Kinetic of the ATO/erlotinib combination in A549 cells

In previous viability tests, MTT assays were performed after 72 h drug exposure. To gain more insights into the time course of the investigated synergism of ATO with erlotinib, as a next step vitality of the treated cells was evaluated after 24 h and 48 h drug exposure. Figure 49-A shows that after 24 h treatment no significant effects on cell viability were observable. After 48 h exposure, strong synergistic antiproliferative activities were induced (CI 0.55 – 0.23) (Figure 49-B) which were comparable to activities observed after 72 h drug exposure (CI 0.6 - 0.12) (Figure 45-A).

To determine the triggering point for the synergistic anticancer effect, shorter drug exposure time experiments (''pulsing experiments'') were performed. In this case, test medium was replaced with fresh culture media after short-time treatment for 6, 14, and 24 h. Subsequently, MTT assays were performed after 72 h (Figure 50). Already 6 h of common cell contact was found to be significant for some synergistic activity (CI up to 0.17) (data not shown). For full synergistic activity, 24 h drug pulsing was necessary. This data indicate that at least 6 h drug contact is needed to incorporate enough drugs inside the cells to induce a significant synergistic activity. However, effects on cell viability can be seen only after 48 h.

A)

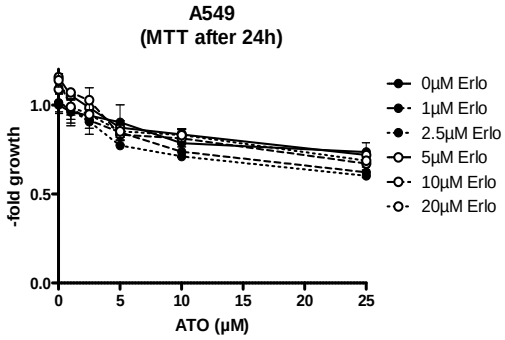

B)

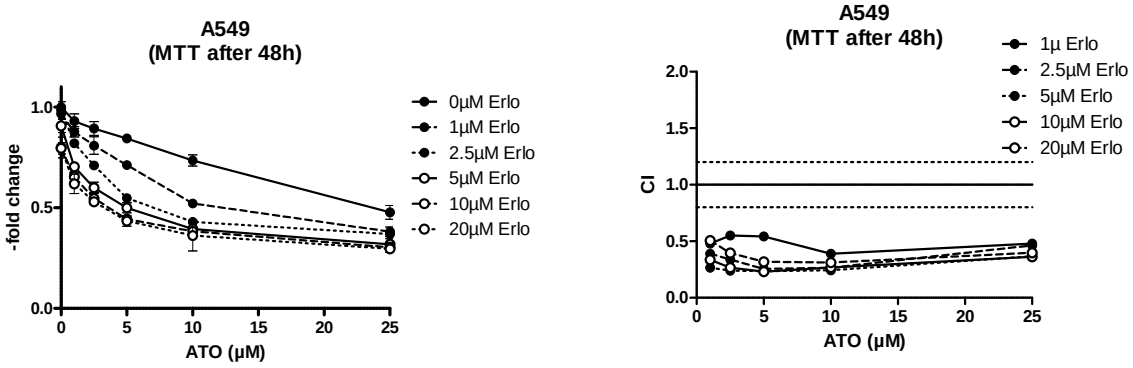

Figure 49. ***Activity of ATO combined with erlotinib against A549 after 24 and 48 h exposure measured by MTT assay*** *- Drug activities are given as CI values.*

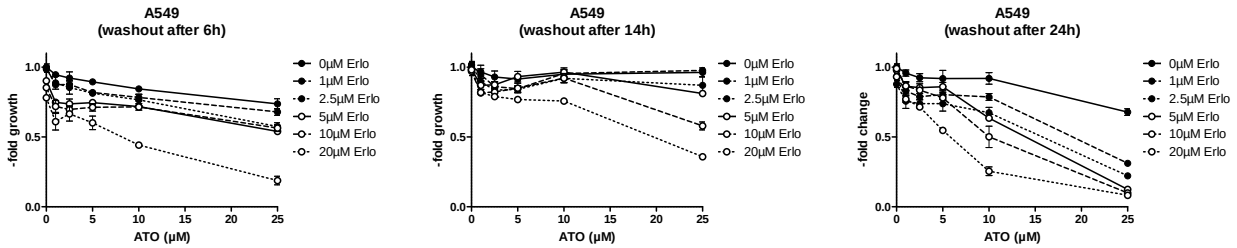

Figure 50. ***Changes in viability of A549 after 6, 14, and 24 h drug exposure measured by MTT assay after 72 h incubation time***

5.2.3. Impact on DNA synthesis

[^{3}H]-thymidine incorporation assays were performed to investigate whether ATO in combination with erlotinib influences DNA synthesis in A549 cells. After 24 h drug exposure, cells were incubated for 60 min with radioactively labeled thymidine. Then, thymidine incorporation was measured (as described in materials and methods) and compared to cell viability (measured with MTT assay). Figure 51-A shows thymidine incorporation in comparison to cell viability at indicated drug concentrations. As already mentioned, ATO in co-treatment with erlotinib had no influence on cell viability after 24 h (section 5.2.2.). On the other hand, after 24 h drug exposure a significant decrease of thymidine incorporation was detected in all treated samples. ATO mono-treatment had a minor effect in DNA synthesis in both concentrations used. Interestingly, mono-treatment with erlotinib induced a considerable reduction in DNA synthesis after 24 h, compared to its ineffectiveness on cell viability even after 72 h. Additionally, ATO in co-treatment with erlotinib induced a synergistic decrease of thymidine incorporation and, consequently, DNA synthesis in all four concentration combinations used (CI < 0.5)(Figure 51-B).

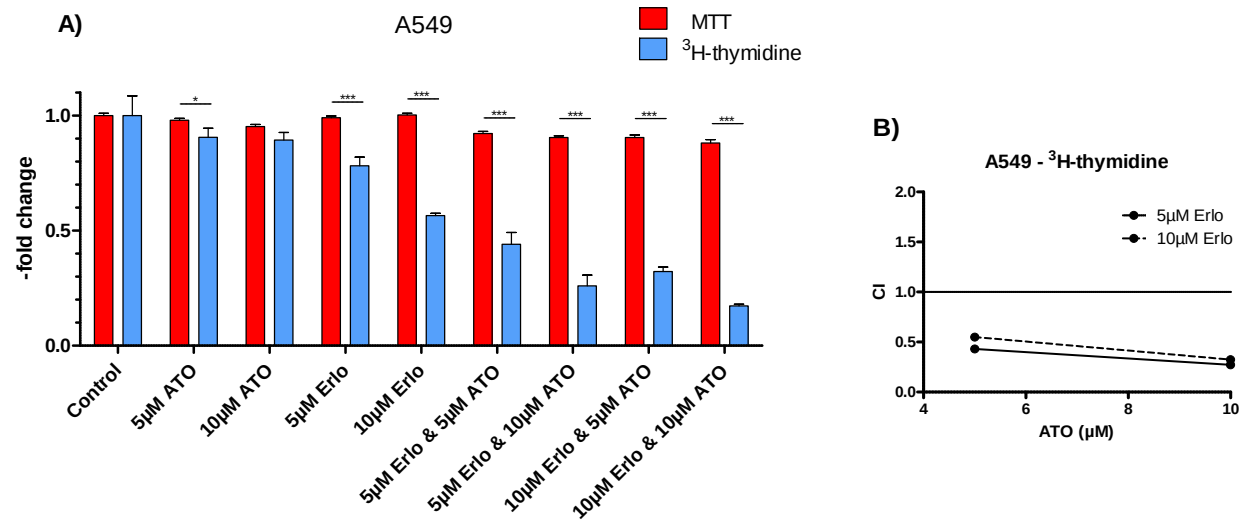

Figure 51. ***Impact of ATO and erlotinib on DNA synthesis at the indicated concentrations.*** *A - Cell viability (MTT) vs. ^{3}H-thymidine incorporation after 24 h incubation with drugs. B - CI calculated from radioactivity values of incorporated ^{3}H-thymidine in cells treated with ATO/erlotinib combination.*

5.3. Apoptosis induction potential

In order to investigate the role of apoptosis in the synergism of ATO and erlotinib, Hoechst-propidium iodide stainings were performed. The proportion of normal and apoptotic cells (cells with condensed chromatin and PI-positive cells) were counted using a fluorescent microscope. After 24 h drug exposure, there was no significant increase of apoptotic A549 cells treated with ATO, erlotinib or their combination (data not shown). Figure 52 - A shows that also after 48 h mono-treatment with ATO or erlotinib there was no increase of apoptotic cells observable. A slight increase of apoptotic cells was detected combining 2.5 µM ATO with 10 µM erlotinib (from 3% and 1% to 10%). There was a considerable apoptosis induction after co-treatment of 5 µM and 10 µM erlotinib with 10 µM ATO which induced 16% and 22% apoptosis, respectively. After 72 h mono-treatment with both used ATO concentrations, a slight increase of apoptotic cells (from 2% to 9% and 11%) was induced (Figure 52 - B). In contrast, a considerable increase of apoptotic cells (up to 21%) was counted after mono-treatment with erlotinib. With regard to the combination, up to 27% of the counted cells were apoptotic after co-treatment of erlotinib with 2.5 µM ATO. Moreover a strong apoptosis induction was observed after combining 10 µM ATO with 5 and 10 µM erlotinib which increased apoptosis to 60% and 90% of the counted cells, respectively (Figure 52 - B and 53 - B). An early step in apoptosis induction (disruption of mitochondrial membrane potential) was also measured after 48 h drug exposure using JC-1 staining (Figure 53 - A). Therefore, this data indicate that apoptosis induction by the drug combination in A549 is one of the effects causing decreased cell viability.

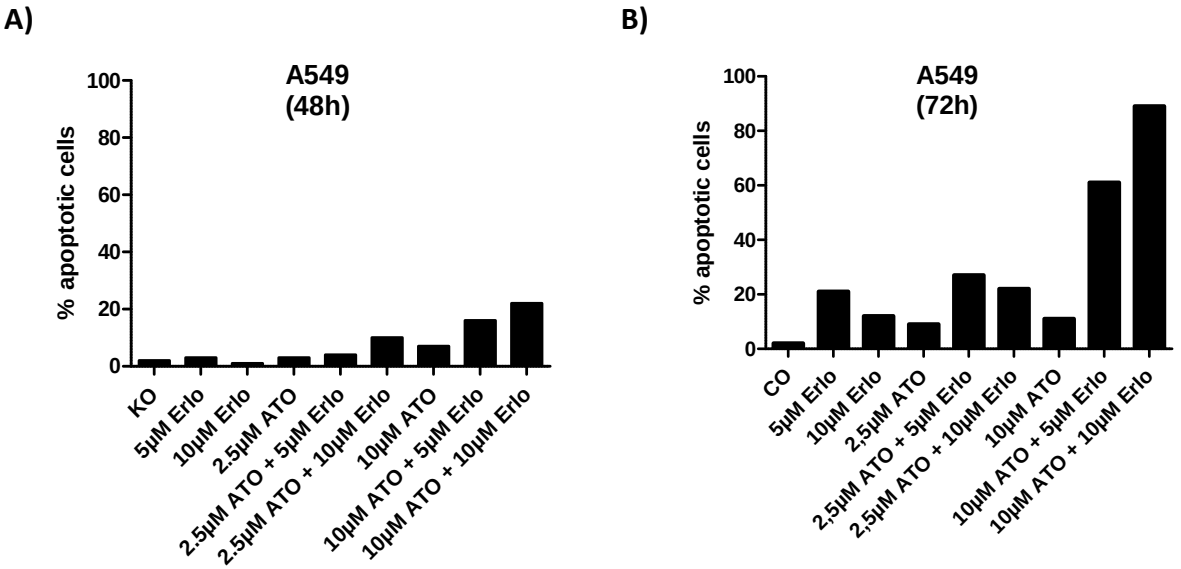

Figure 52. ***Apoptotic A549 cells counted after ATO/erlotinib exposure for 48 h (A) and 72 h (B) stained with HöPI***

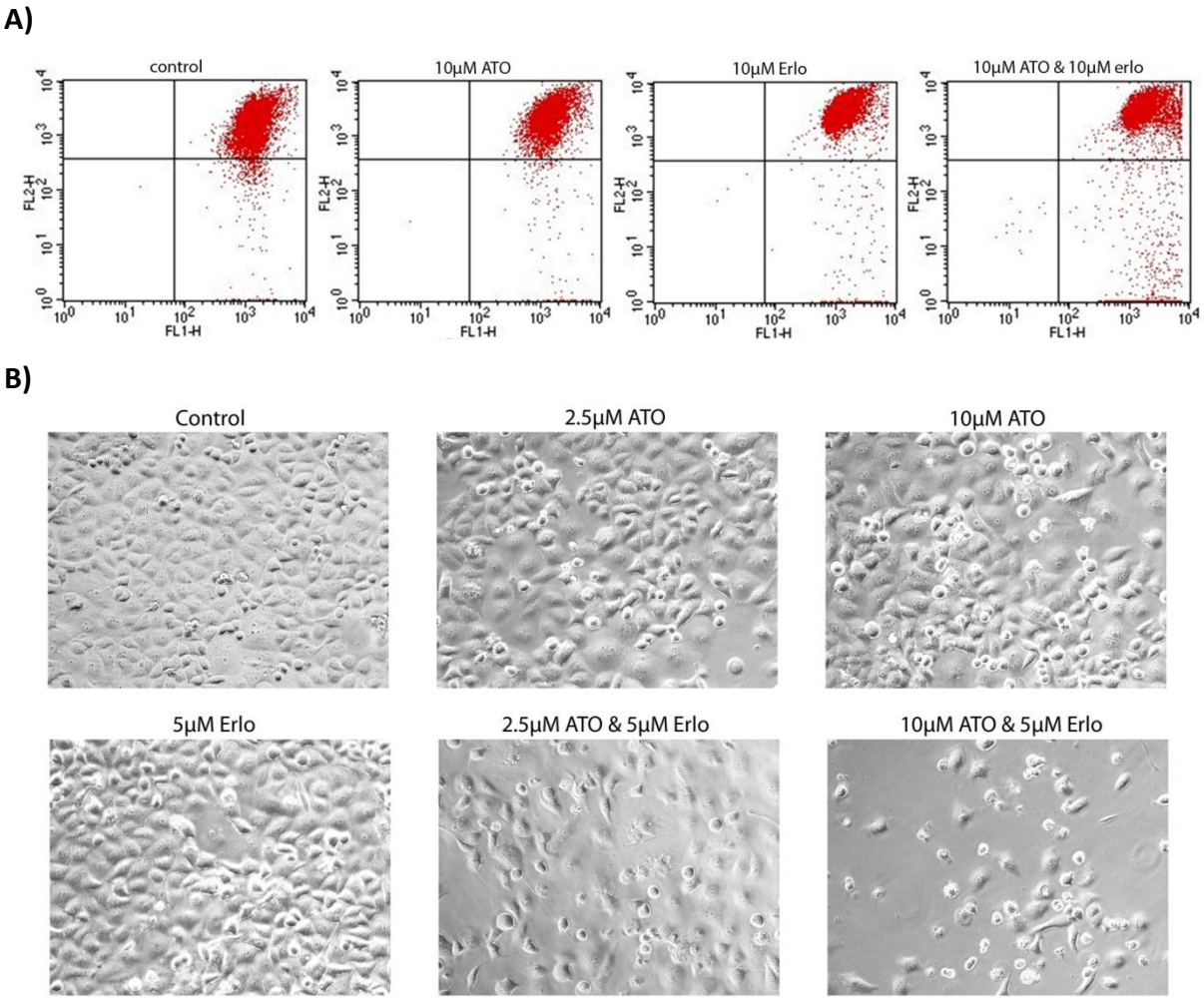

Figure 53. ***Apoptosis induction potential. A*** *– FACS cytograms of A549 cells stained with JC-1 showing normal cells in upper right quadrants and cells with depolarized mitochondria in lower right quadrants regions after 48 h treatment at indicated concentrations.* ***B*** *– Phase-contrast microscopy of A549 cells after 72h treatment with ATO, erlotinib or their combination at the indicated concentrations.*

5.4. Cell cycle alterations induced by ATO and erlotinib

To investigate alterations in cell cycle distribution induced by ATO and erlotinib, cell cycle analyses were performed by PI staining and flow cytometry. After 24 h treatment, a minor change in cell cycle distribution was observed (data not shown). Even after 48 h, ATO and erlotinib as single agents did not induce any distinct changes in the cell cycle (Figure 54). Only a slight increase in G1/G0 cells was measured after treatment with 10 μM ATO alone.

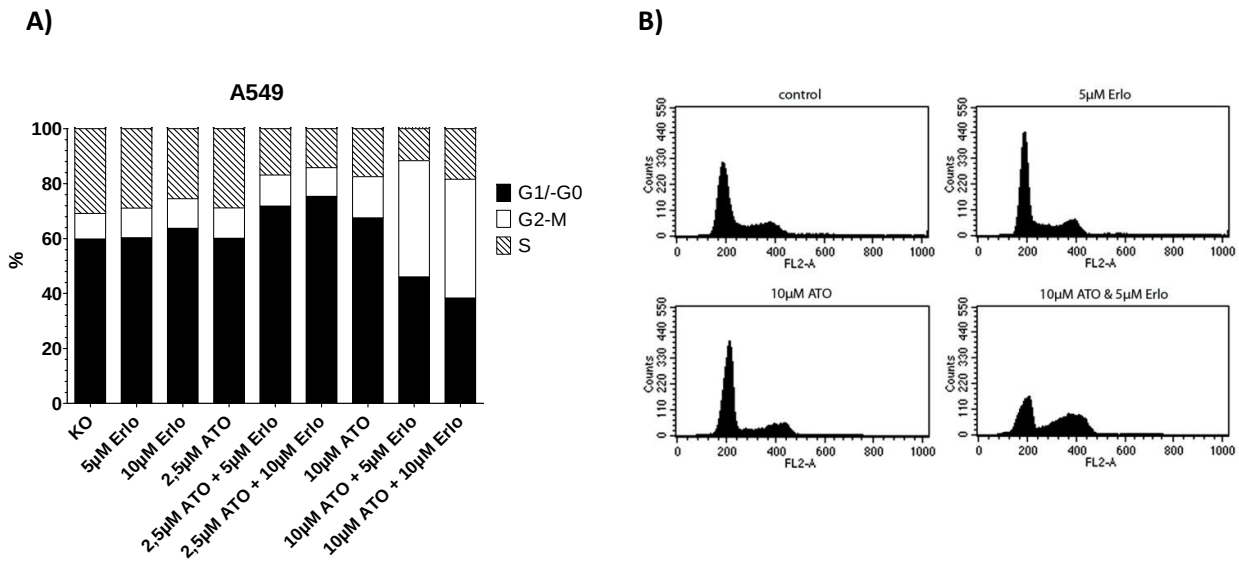

Figure 54. ***Influence of ATO and erlotinib as single agents and in combination on cell cycle distribution of A549 cells determined by FACS analyses after 48 h drug exposure.*** *A – Distribution of cells (%) in the indicated cell cycle phases after treatment with ATO and erlotinib. B – DNA histograms of A549 cells treated with 10µM ATO, 5µM erlotinib and their combination.*

With regard to the drug combination, also 2.5 µM ATO in combination with erlotinib only marginally increased the proportion of cells in G0/G1. In contrast, a distinct increase of G2/M cell cycle arrest was measured in cells treated with combination of 10 µM ATO and erlotinib (From 10% in G2/M arrested cells induced by 5 or 10 µM erlotinib and 15% induced by 10 µM ATO to 43% induced by drug combination). This was accompanied by a decrease of cells in G0/G1 and S phase (Figure 54 - B). This indicates that arresting cells in G2/M might be one of the major antiproliferative effects induced by the drug combination.

5.5. Role of the EGFR pathway

As already mentioned, EGFR plays an important role in cancer cell survival and proliferation, and both ATO as well as erlotinib are known for their interaction with this pathway. Such, stimulation of the EGFR pathway has been reported after ATO treatment, whereas erlotinib selectively inhibits the tyrosine kinase function of EGFR (see introduction). Consequently, the aim of the following experiments was to find out whether EGFR, or downstream players in the EGFR signaling, play the leading role in the observed synergistic antiproliferative activity induced by the combination of ATO and erlotinib. The strategy used in those experiments was inhibition of EGFR and other important protein kinase transducers, using diverse selective inhibitors in combination with ATO.

5.5.1. Stimulation of A549 with EGF

To determine whether EGFR stimulation with EGF has an impact on synergistic activity, A549 were pre-stimulated with EGF for 10 min before treatment with the drug combination. After 72 h incubation, MTT vitality assays were performed and CI values were calculated and compared to the treatment without stimulation. Generally, EGF-stimulated A549 cells became more resistant to treatment with ATO, erlotinib or their combination (Figure 55). Thus, single treatment with ATO had a reduced antiproliferative effect (IC_{50} > 25 µM) in comparison to the treatment without EGF stimulation (IC_{50} = 17.65 µM)(compare to Figure 45-A and Table 11). In general, the stimulation of the EGFR pathway had no disturbing effect on the synergism induced by drug combination (CI < 0.27). With regard to non-stimulated A549 cells, EGF-stimulated cells were 2.6-fold and 1.5-fold more resistant to the ATO co-treatment with 2.5 µM and 10 µM erlotinib, respectively.

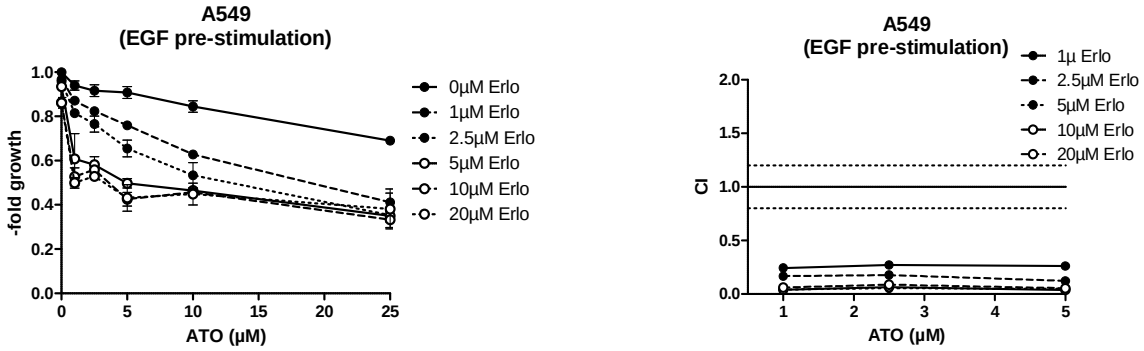

Figure 55. ***Vitality of A549 cells pre-stimulated with EGF for 10 min and then treated 72 h with ATO and erlotinib:*** *Viability diagram (left) and respective CI values (right) at indicated concentrations.*

Table 11

IC_{50} values of A549 treated with ATO, erlotinib or their combination

Cell line	EGF	ATO (µM) IC_{50}	Erlo (µM) IC_{50}	ATO with 2.5µM Erlo IC_{50}	RF	ATO with 10µM Erlo IC_{50}	RF
A549	Not-stimulated	17.65	>20	5.65	2.6	3.33	1.5
	Pre-stimulated	>25	>20	14.57		4.94	

RF – resistance factor

5.5.2. ATO in combination with other TKIs

To investigate whether ATO also synergizes with other TKI-inhibitors, gefitinib (EGFR), lapatinib (EGFR, Her2), sorafenib (Raf-1, BRAF, VEGFR-2, PDGFR-β, c-Kit, p38) and sunitinib (VEGFR 1-3, PDGFR α-β, c-Kit) were used (Figure 56). In these experiments, gefitinib single treatment had a weak effect on the proliferation of A549 cells (IC_{50} > 20 µM) which was comparable to anticancer effect of erlotinib (Table 12). Combination of ATO with gefitinib showed additive up to synergistic activities (Figure 56-A). In comparison to erlotinib, gefitinib in co-treatment with ATO showed additive activities at low concentrations, whereas a strong synergistic activity was observed at higher concentrations. Such, 25 µM gefitinib in co-treatment with all ATO concentrations showed the highest synergistic antiproliferative activity (all CI values < 0.09). In comparison to erlotinib and gefitinib, A549 were more sensitive to lapatinib (IC_{50} = 11.75 µM). This is because lapatinib unlike erlotinib or gefitinib inhibits the tyrosine kinase of both EGFR and Her2[218]. Low concentrations (0.5 - 1 µM) of lapatinib in combination with ATO had no antiproliferative effects, whereas ATO in co-treatment with 5 and 10 µM lapatinib induced a strong anticancer activity (Figure 56-B). With respect to ATO/erlotinib combination, lapatinib at low concentrations in co-treatment with ATO showed additive up to antagonistic effects, whereas at higher concentrations showed only synergistic activities.

Sorafenib and sunitinib are multi kinase inhibitors that inhibit the kinase activity of transmembrane receptors like PDGFR, VEGFR, c-KIT, Flt3[219]. Sorafenib was initially developed as Raf kinase inhibitor. Additionally, it has also been shown to have an inhibitory activity against ERK and p38 which are kinases downstream of EGFR[220]. Regarding the fact that A549 cells have a mutated Raf kinase, sorafenib was more toxic against this cell line (IC_{50} = 7.77 µM) in comparison to the other tested TKIs (Table 12). Combination treatment of sorafenib with ATO showed synergistic effects in all concentration combinations (Figure 56-C). In contrast, ATO in co-treatment with sunitinib showed only additive up to weak antagonistic activity (CI 0.7 – 1.5) (Figure 56-D). Treatment combinations of ATO with TKIs mentioned above indicate that pathways of EGFR and Her2 might be implicated in the synergistic antiproliferative activity of A549. Furthermore, synergistic activity of ATO with sorafenib but not sunitinib indicates that RAF/MEK/ERK pathway might be implicated.

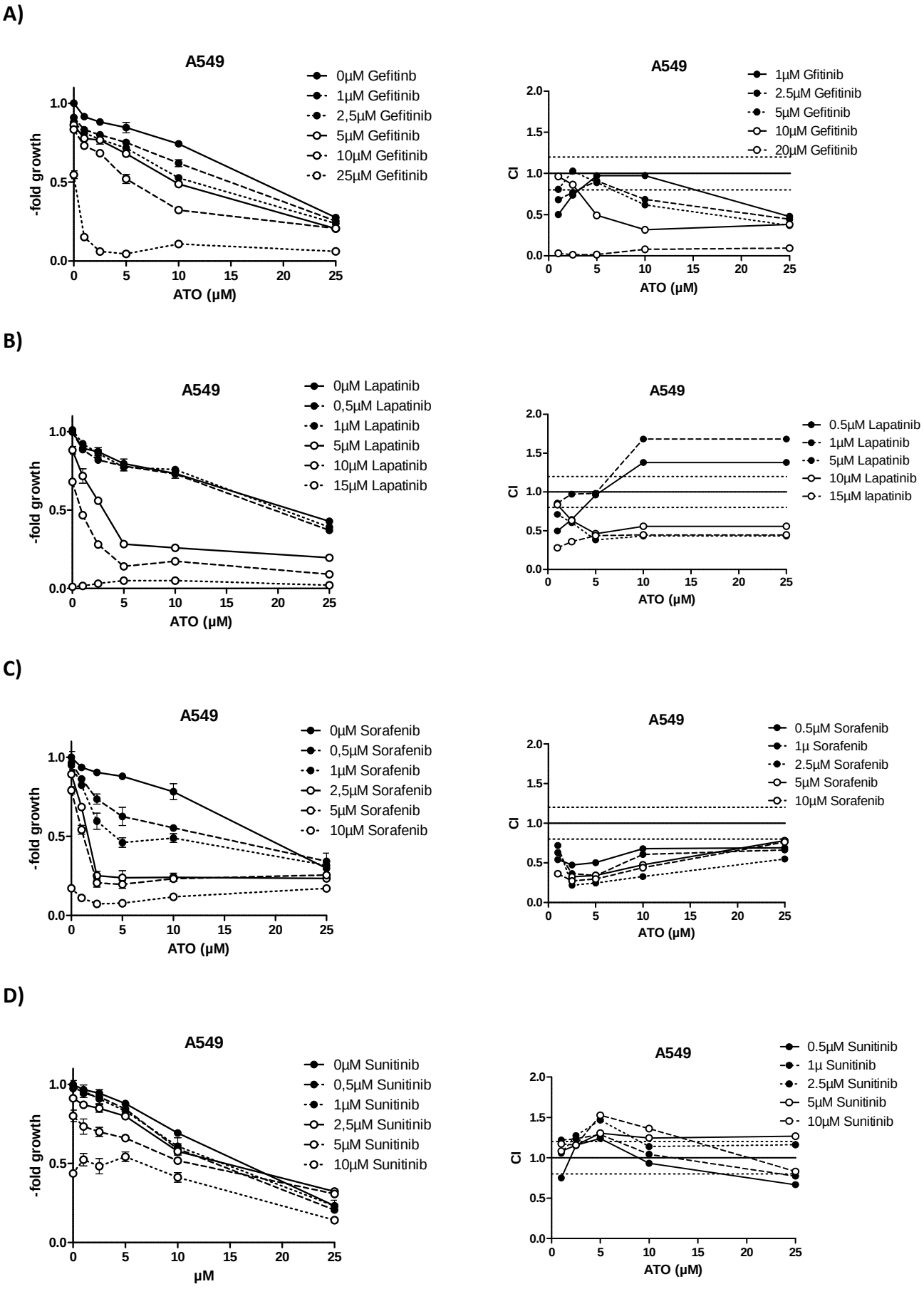

Figure 56. ***ATO in co-treatment with gefitinib, lapatinib, sorafenib and sunitinib against A549:*** *Viability diagrams (left) and they respective CI values (right) at indicated concentrations. Viability was measured by MTT assay after 72 h drug exposure.*

Table 12

IC_{50} values of different TKIs in A549

Cell line	Drug	IC_{50} (μM)
A549	Erlotinib	>20
	Gefitinib	>20
	Lapatinib	11.45
	Sorafenib	7.77
	Sunitinib	9.22

5.5.3. Impact of ATO in cells infected with dnEGFR adenovirus

Another experiment to study the role of EGFR in the observed synergism was done using adenoviruses to transfect A549 with dominant negative EGFR (dnEGFR) and further inhibit the activation of this pathway. As described in materials and methods, adenoviruses express a dnEGFR gene which was fused with the sequence for the GFP protein instead of the tyrosine kinase domain which makes it detectable with fluorescence microscopy but not-functional in signal transduction. Thus, a dimer containing the dnEGFR excludes the autophosphorylation step and leads to inactivation of the EGFR pathway. Additionally, adenoviruses containing only GFP gene were used as control. For optimal transduction, different MOIs of adenoviruses were used to infect A549 cells. Infected cells with both adenoviruses (dnEGFR-GFP and GFP only) at 1 MOI displayed no optimal expression of transduced genes (Figure 57). Expression of GFP protein transduced from 5 MOI viruses was strikingly increased in comparison to dnEGFR-GFP. Cells infected with 25 MOI dnEGFR-GFP adenoviruses had a much better protein expression than infection with 5 MOI, whereas 25 MOI viruses which transduced GFP showed an overexpression of the GFP protein. After infection (24 h) cells were seeded in 96-wells and treated with ATO. Then, MTT viability assays were performed and CI values were calculated to determine the effect of ATO treatment in cells transfected with dnEGFR-GFP and GFP as control, respectively. After 120 h incubation with 5 MOI viruses, transduced A549 with both dnEGFR-GFP and GFP proteins showed a considerable decrease in proliferation (Figure 58). 25 MOI GFP viruses, decreased cell viability up to 50%, whereas 25 MOI viruses with dnEGFR-GFP, had a dramatic antiproliferative impact with up to 85% decrease in cell viability. In general, the effects of ATO were only marginally influenced by infection with dnEGFR. Thus, in cells infected with 5 MOI dnEGFR-GFP adenoviruses, additive up to antagonistic effects were observed (CI 0.9 – 1.4), whereas cells infected with 25 MOI showed

additive up to synergistic effects (CI 0.9 – 0.7). However, also in virus-control cells, treatment with ATO had some additive effects and even some synergistic effects were observed in those cells infected with 25 MOI GFP only.

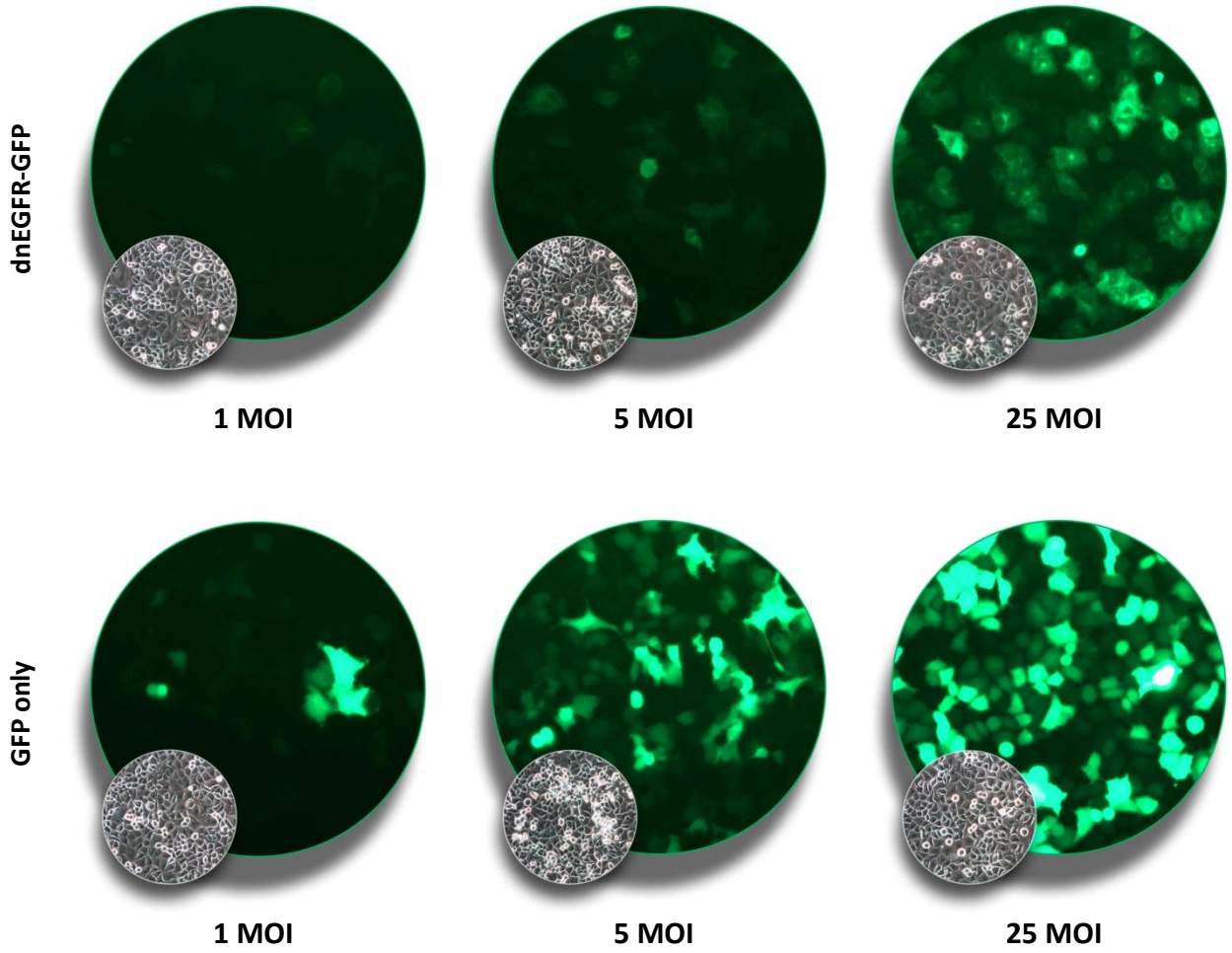

Figure 57. ***A549 cells transduced with dnEGFR-GFP and GFP using adenoviruses as transfectans*** **-** *Over panel shows cells infected with different MOIs of adenoviruses containing dnEGFR-GFP. Lower panel shows transfected cells with GFP. Fluorescent excitation of GFP (big cycles) represent the efficasity of transfection in comparison to phase contrast (small cycles).*

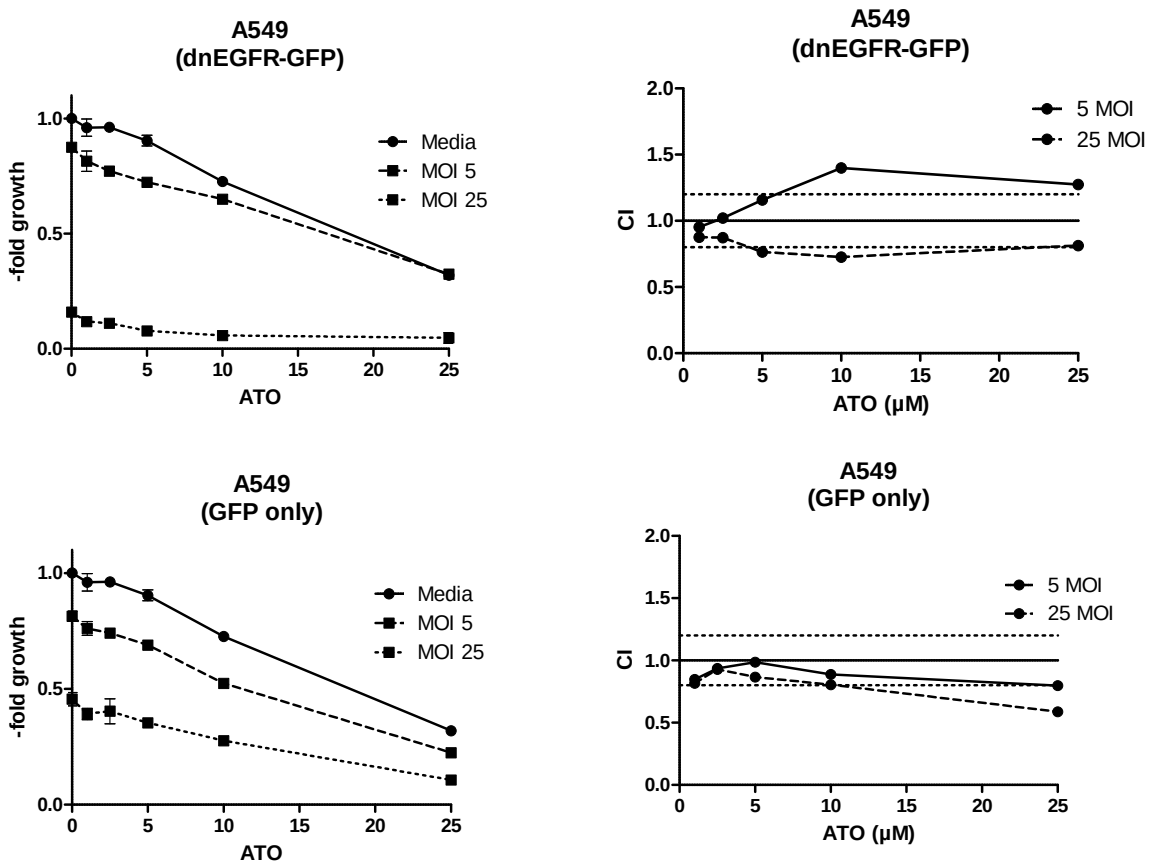

Figure 58. ***Viability of A549 infected with the respective adenovirus and treated with ATO.*** *Cell viability was measured by MTT assay after 72 h drug exposure. Respective CI values (Isobolograms) are shown on the right.*

5.5.4. Synergistic effects in cell models harboring EGFR mutations.

Specific mutations in tyrosine kinase of the EGFR lead to hypersensitivity of NSCLC cells against erlotinib. Some of these mutations (e.g. exon 19 deletions and mutations in exon 21) are referred to as activating mutations, as they seem to result in the increased kinase activity of the receptor. Others, such as mutations in exon 20 were associated with resistance to EGFR inhibitors[183]. To investigate the efficacy of the ATO/erlotinib combination in an EGFR mutant background, HCC827 (delE746-A750), H1650 (delE746-A750), and H1975 (L858R/T790M) were used. HCC827 cells are characterized by a drastic EGFR overexpression and activity which is indicated by a strong phosphorylation of EGFR (Figure 59). SW620 cells were used as a reference cell line with no expression of EGFR. In general the effects of EGFR mutations on ATO were minor resulting in comparable IC_{50} values of 5.1 µM, 6 µM, and 3.8 µM for HCC827, H1650, and H1975, respectively (Table 13). SW620 cells showed an intermediate resistance against ATO (IC_{50} = 8.42 µM). The exon 19 EGFR deletion (E746-A750) in the tyrosine kinase domain of EGFR, renders HCC827 cells hypersensitive to erlotinib (IC_{50}

= 30 nM) (Table 13). Additionally, H1650 cells were used in these experiments which harbor the same erlotinib-sensitizing deletion in exon 19 (E746-A750) but has lower expression levels of EGFR (Figure 59). This cell line has a loss of the PTEN tumor suppressor causing resistance against erlotinib (IC_{50} > 20 µM). H1975 cells contain a erlotinib-sensitizing mutation (L858R) together with a secondary mutation (T790M), which makes this cell line also resistant to erlotinib (IC_{50} > 20 µM). This resistance-inducing mutation is rarely (<5%) found in untreated EGFR mutant tumors, but is detected in more than 50% of patients who develop acquired resistance to EGFR TKI therapy[200,209,221]. As expected, SW620 cells which do not express EGFR were resistant to erlotinib (IC_{50} > 20 µM) (Table 13).

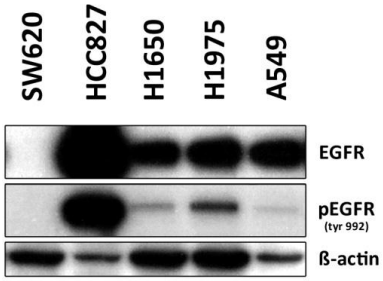

Figure 59. ***Western blot analysis of EGFR mutated cell lines***

With regard to the combination treatment, ATO and erlotinib showed predominantly antagonistic CI values (0.8 - 2) in erlotinib hypersensitive HCC827 cells (Figure 60-A). In contrast, drug combination in H1650 had synergistic activities in all concentrations tested with CI < 0.67 (Figure 60-B) and a 2.6-fold increase in toxicity of ATO combined with 2.5 µM erlotinib (IC_{50} = 2.4 µM) (Table 13). In H1975 cells, combination treatment with ATO and erlotinib lead to CI values between 0.5 and 1.2 (Figure 60-C). Such, 2.5 µM erlotinib in combination decreased ATO-IC_{50} up to 1.6 fold (IC_{50} =2.3 µM). Treatment of SW620 with the drug combination resulted mainly in synergistic CI values (0.8 – 0.5) (Figure 60-D) and 2.1-fold increase in ATO toxicity. This data indicate that EGFR mutations which make cells resistant against erlotinib have no impact on the synergistic activity of the drug combination. Moreover, combination of ATO with erlotinib can overcome erlotinib-resistance induced by EGFR mutations or PTEN loss. Interestingly, even in the absence of EGFR, SW620 responded synergistically to drug combination. This fact indicates that the EGFR pathway is not the only mechanism responsible for the observed synergism.

Table 13

IC_{50} values of EGFR mutated cells treated with ATO, erlotinib, and ATO/erlotinib combination

Cell line	EGFR mutation/additional changes	ATO (µM) IC_{50}	Erlo (µM) IC_{50}	ATO with 2.5µM Erlo IC_{50}	Fold decrease
HCC827	ΔE746-A750	5.1	0.03	-	-
H1650	ΔE746-A750/PTEN loss	6	>20	2.4	2.5
H1975	L858R/T790M	3.8	>20	2.3	1.6
SW620	EGFR absent	8.4	>20	4.2	2.1

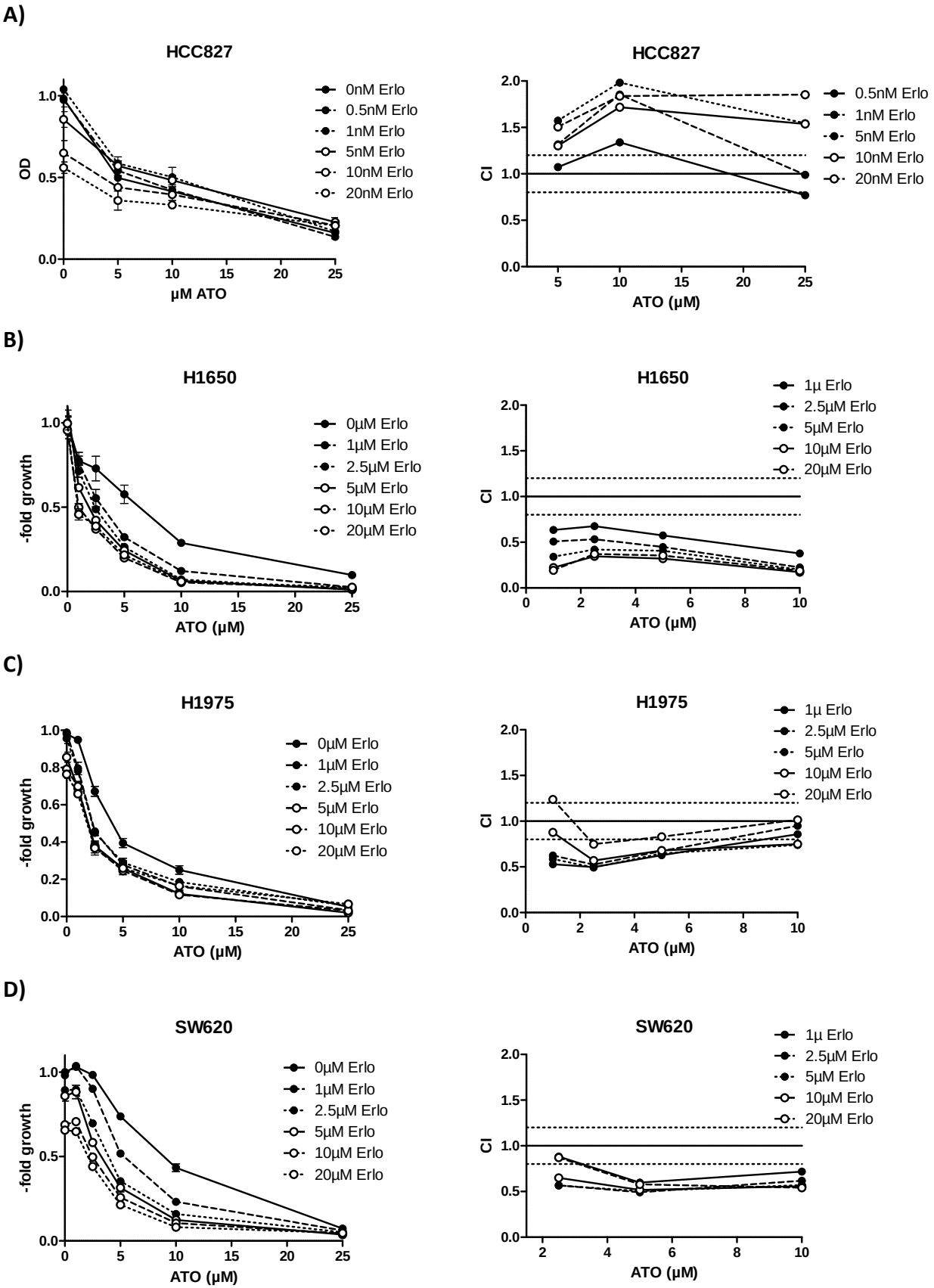

Figure 60. ***EGFR mutated cells treated with ATO and erlotinib*** **-** *Cell viability was measured by MTT assay after 72 h drug exposure (left panel). Respective CI values (Isobolograms) are shown in the right panel.*

5.5.5. Impact of inhibition of EGFR downstream kinases on ATO activity

There are several pathways regulated by EGFR and important protein kinases that transduce the signals. To investigate the role of EGFR signaling on the synergism, three key kinases downstream of EGFR were inhibited in A549 using specific small molecule inhibitors to study whether those pathways have an impact in antiproliferative activity in combination with ATO: 1) Mitogen-activated protein kinase (MEK), which is important in RAF/MEK/ERK signaling[222], was inhibited using U0126. 2) p38 MAP Kinase (MAPK) participates in a signaling cascade controlling cellular responses to cytokines and stress[223]. Activity of p38 was inhibited using SB203580. 3) Akt is the central kinase in PI3K signaling pathway and, thus, important for multiple cellular processes such as cell proliferation, apoptosis, transcription and cell migration[224]. Akt was inhibited by using the specific allosteric inhibitor MK-2206. Figure 61 A-B shows that inhibition of the MEK or of the p38 pathway had no impact on the proliferation of A549 cells.

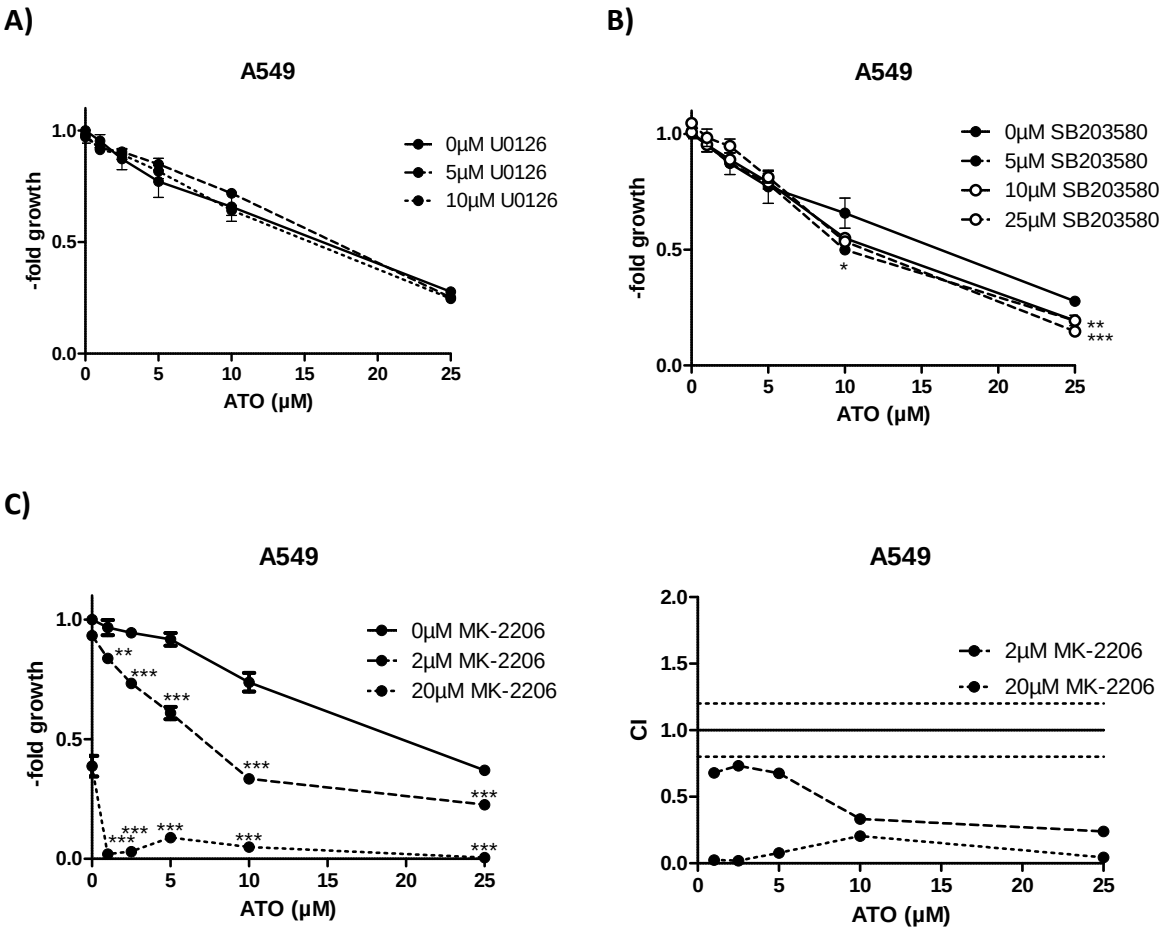

Figure 61. ***Combination treatments with ATO and kinase inhibitors (U0126, SB203580 and MK-2206) in A549 cells*** *- Cell viability was measured by MTT assay after 72 h drug exposure. C) Viability diagram (bottom left) and CI isobologram (bottom right) show effects of ATO in co-treatment with MK-2260 against A549 cells. For statistical analyses t-tests were performed (*p<0.05, **p<0.01, *** p<0.001).*

Also in combination with ATO, U0126 had no significant effects. In contrast, combination with SB203580 significantly (p = 0.04 – 0.003) enhanced the anticancer activity of ATO at concentrations higher than 5 µM resulting in CI values of 0.7 and 0.4 for 10 µM and 25 µM ATO, respectively (Figure 61-B). With regard to the role of Akt pathway, MK-2206 mono-treatment had a significant impact (p = 0.002 - 0.001) on the viability of A549 cells (IC = 16.7 µM). Moreover, combined with ATO, only synergistic activities in all concentrations used were observed (CI < 0.73) (Figure 61-C). This data suggest that p38 and especially the PI3K pathway are important in the synergistic activity of ATO with erlotinib.

5.6. c-Met receptor tyrosine kinase as a resistance factor against TKIs

Met is a transmembrane receptor protein with kinase activity essential in embryonic development and wound healing[225]. Like EGFR, also Met receptor is known to activate key oncogenic pathways (RAS, PI3K, STAT3, beta-catenin)[225]. Thus, enhanced Met expression and phosphorylation has been suggested as a factor for primary or acquired resistance against gefitinib[226]. To investigate the impact of amplified *MET* in the synergistic activity of ATO and erlotinib, the two NSCLC cell lines H2073 and H1993 originating from the same patient were used. The H2073 cell line was isolated from the primary lung tumor and harbor a basal Met expression and phosphorylation, whereas, the metastasis-derived cell line H1993 harbors *MET* amplification and consequently, a highly activated kinase function[227]. In our study, ATO mono-treatment had a lower toxicity against H2073 (IC_{50} = 7.53 µM) in comparison to H1993 (IC_{50} = 2.63 µM) (Table 14). Both cell lines were resistant against erlotinib single treatment (IC_{50} > 20 µM). Combination treatment with ATO and erlotinib in H2073 showed only synergistic CI values (Most CIs < 0.54). In contrast, H1993 treated with ATO/erlotinib combination showed mainly additive effects with CI values between 0.6 and 1.4 (Figure 62).

Table 14

IC_{50} values of NSCLC cells treated with ATO, erlotinib, and Met inhibitor

Cell line	MET	ATO (µM) IC_{50}	Erlo (µM) IC_{50}	PF-2341066 (µM) IC_{50}	RF
H1993	Met amplification	2.62	>20	2.82	3.45
H2073	Met basis expression	7.53	>20	9.73	

RF - Resistance factor

As a next step, ATO was combined with the Met inhibitor PF-2341066. As mono-treatment, Met inhibitor showed antiproliferative activity comparable to ATO in both cell lines (H2073 - IC_{50} = 7.53 µM and H1993 - IC_{50} = 2.82 µM). Thus, the *MET*-amplified H1993 was 3.45-fold more sensitive against Met inhibition than H2073. Combination of ATO with the Met inhibitor showed mainly antagonistic activities (CI values between 0.7 und 3). Together this data again indicate that: 1) an active EGFR pathway is necessary for the synergistic activity of ATO with erlotinib and 2) that cells which harbor mechanisms which render them independent to the regulation by EGFR exhibit no synergism after combining erlotinib with ATO.

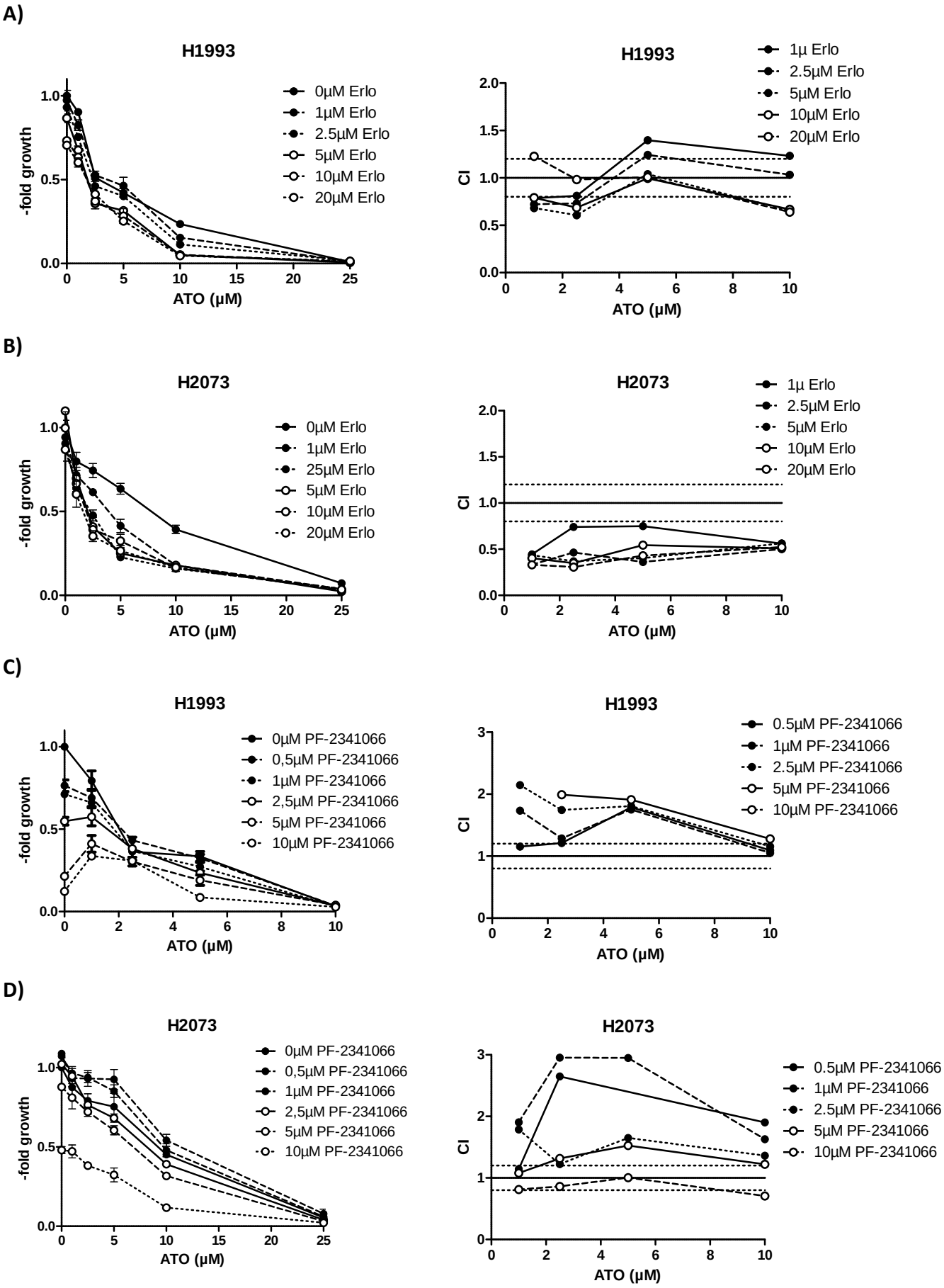

Figure 62. ***Viability of MET-amplified H1993 and basal MET-amplified H2073 cells measured with MTT assay after 72 h*** *- Combination effects of ATO/erlotinib and ATO/MET-Inhibitor are shown on the right.*

5.7. Arsenic accumulation in cells treated with ATO and erlotinib

One of the resistance factors in ATO therapy is increased cellular efflux of arsenic or its metabolites from the cells[228]. The aim of these experiments was to determine the effects of erlotinib in cellular arsenic uptake. To gain more insights in the cellular accumulation of arsenic, ICP-MS analyses were performed in different cell models that responded synergically to ATO/erlotinib combination. This sensitive method was used to determine the levels of arsenic taken up from cells after 3 h drug exposure with different ATO concentrations as single treatment and in combination with erlotinib (Figure 63).

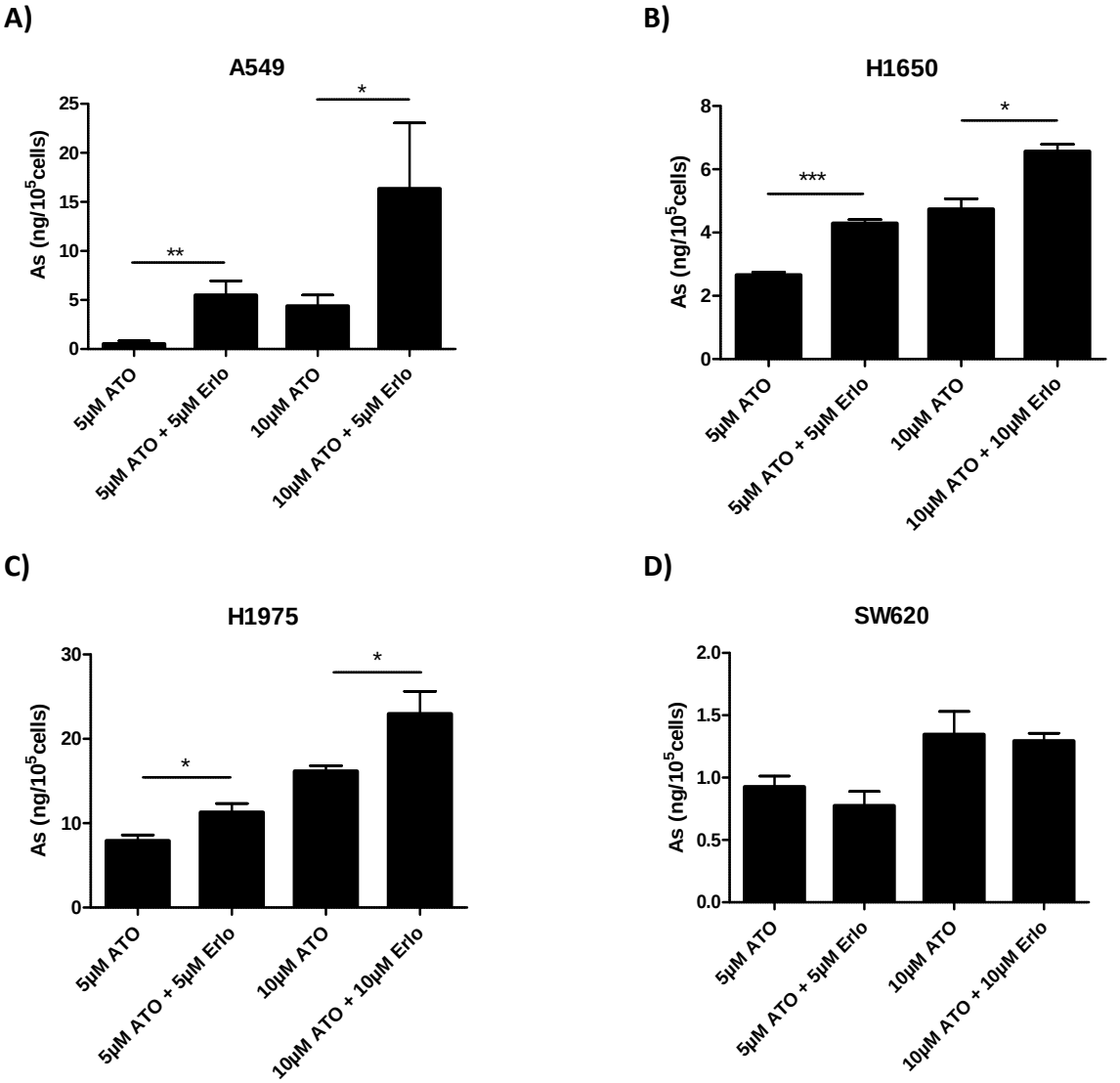

Figure 63. ***Accumulation levels of arsenic in cancer cell lines (A549, H1650, H1975 and SW620) after 3 h exposure with ATO alone, or in combination with erlotinib***. *Stastistical significance was calculated using t-test * p<0.05, **p<0.01, *** p<0.001.*

After ATO mono-treatment there was a dose-dependent uptake of arsenic levels in every cell line tested. In general, we observed a significant increase of arsenic in most cell lines upon erlotinib co-treatment. In A549 cells, this resulted in a 10.4-fold increase from 0.54 ng to 16.34 ng arsenic in 10^5 cells (Figure 63 – A). Similarly, a significant increase of arsenic levels was observed in the EGFR-mutated cells (H1650 and H1975) treated with drug combination compare to ATO single treatment. Although, this was to a lesser extend with up to 1.6-fold increase in H1650 and up to 1.4-fold increase in H1975, respectively (Figure 63 - B and C). Remarkably, the only exception from all four tested cells was the EGFR-negative cell line SW620, with no effects on arsenic accumulation in ATO co-treatment with erlotinib compare to single ATO treatment (Figure 63 - D). Erlotinib is reported to reverse the drug efflux function of MDR transporters[229-230]. Some of MDR transporters like MRP1 (ABCC1) and MRP2 (ABCC2) were implicated in arsenic export in various cancer cells[119,228]. Western blot analyses were performed to determine any relation of MRP1 and MRP2 expression levels to the accumulation levels and to synergistic effects of ATO/erlotinib combination. Consequently, enhanced accumulation of arsenic as presented above was in associated with the expression levels of MRP1 (Figure 64). A549 and H1650 showed an overexpression of MRP1 and compare to other tested cells, combination treatment showed also the highest synergistic effects in these cells. Synergistic activities were measured also in SW620 and H1975, however, in comparison to H1975 SW620 showed a very low expression of MRP1 and no significant increase of arsenic levels by erlotinib co-treatment. MRP2 was detected in every tested cell line, whereas A549 had the highest expression followed by SW620 and then other cell types tested. MRP1 correlate with a significant increase of arsenic accumulation by co-treatment with erlotinib, whereas MRP2 expression did not show any correlation with the intracellular accumulation levels of arsenic.

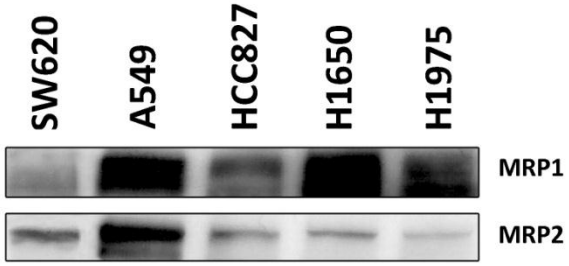

Figure 64 . ***Western blot analysis of MRP1 and MRP2 expression in SW620, HCC827, A549, H1650, and H1975.***

Furthermore, to study the role of MRP1 in synergistic activity of ATO/erlotinib combination, the NSCLC cell line SW1573 and its MRP1/P-gp-overexpressing subtype $SW1573_{2R160}$ were used (Figure 65). Generally, parental SW1573 was more sensitive to both ATO and erlotinib in comparison to the resistant $SW1573_{2R160}$ subline (Table 15). With respect to the drug combination, synergistic activity was observed in both cell line models. CI values were significantly lower in the ABC-transporter-overexpressing $SW1573_{2R160}$ subline (t-test p=0.015). This indicates that presence of MRP1 might render cells sensitive to the synergism of ATO and erlotinib.

Table 15

IC_{50} values of SW1573 and its MRP1/P-gp-overexpressing subtype treated with ATO, erlotinib and combination

Cell line	MRP1/P-gp	ATO (µM) IC_{50}	Erlo (µM) IC_{50}	ATO and 2.5 µM Erlo IC_{50}	Fold decrease
SW1573	Basis expression	5.3	7.3	2.5	2.1
$SW1573_{2R160}$	Overexpression	8.5	>20	3.6	2.3

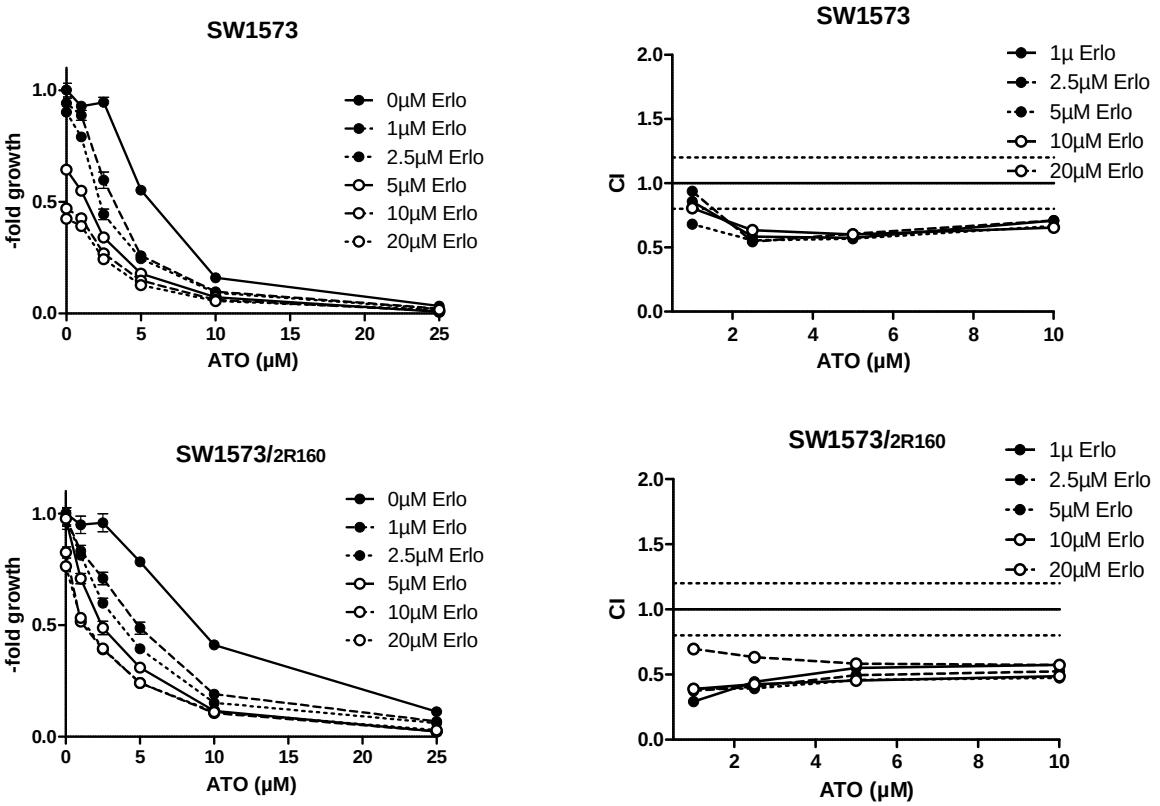

Figure 65. ***Viability and CI responses of SW1573 and MRP1/P-gp overexpressing subtype $SW1573_{2R160}$ treated with ATO and erlotinib.*** *Cell viability was measured by MTT assay after 72 h drug exposure. Respective CI values (Isobolograms) are shown on the right.*

A549 cells are characterized by high expression of MRP1 and MRP2 (Figure 64). Thus, the next step was to investigate whether inhibition of the MRP1 transport activity by the known modulator cyclosporin A (CSA) is able to reduce the synergistic effects of ATO with erlotinib[231-232]. As shown in Figure 66 – A, treatment with 1 µM CSA sensitized A549 significantly (up to 2.6-fold) against ATO and (1.2-fold) erlotinib mono-treatment (two-way ANOVA) (Table 16). Combination treatment with ATO, erlotinib, and CSA induced additive up to synergistic activities, whereas in A549 without CSA only synergistic activities were observed (Figure 66 - B and C). Taken together, results from $SW1573_{2R160}$ and CSA-treated A549 cells lead to the conclusion that inhibition of MRP1 by erlotinib might play a role in the synergistic activity of ATO with the EGFR TKI.

Table 16

IC_{50} values of treated A549 with CSA, ATO, and erlotinib

Cell line	CSA (1µM)	ATO (µM) IC_{50}	Erlo (µM) IC_{50}	ATO and 2.5 µM Erlo IC_{50}	Fold decrease
A549	Untreated	17.6	>20	5.6	3.14
	Treated	6.6	>20	4.1	1.6

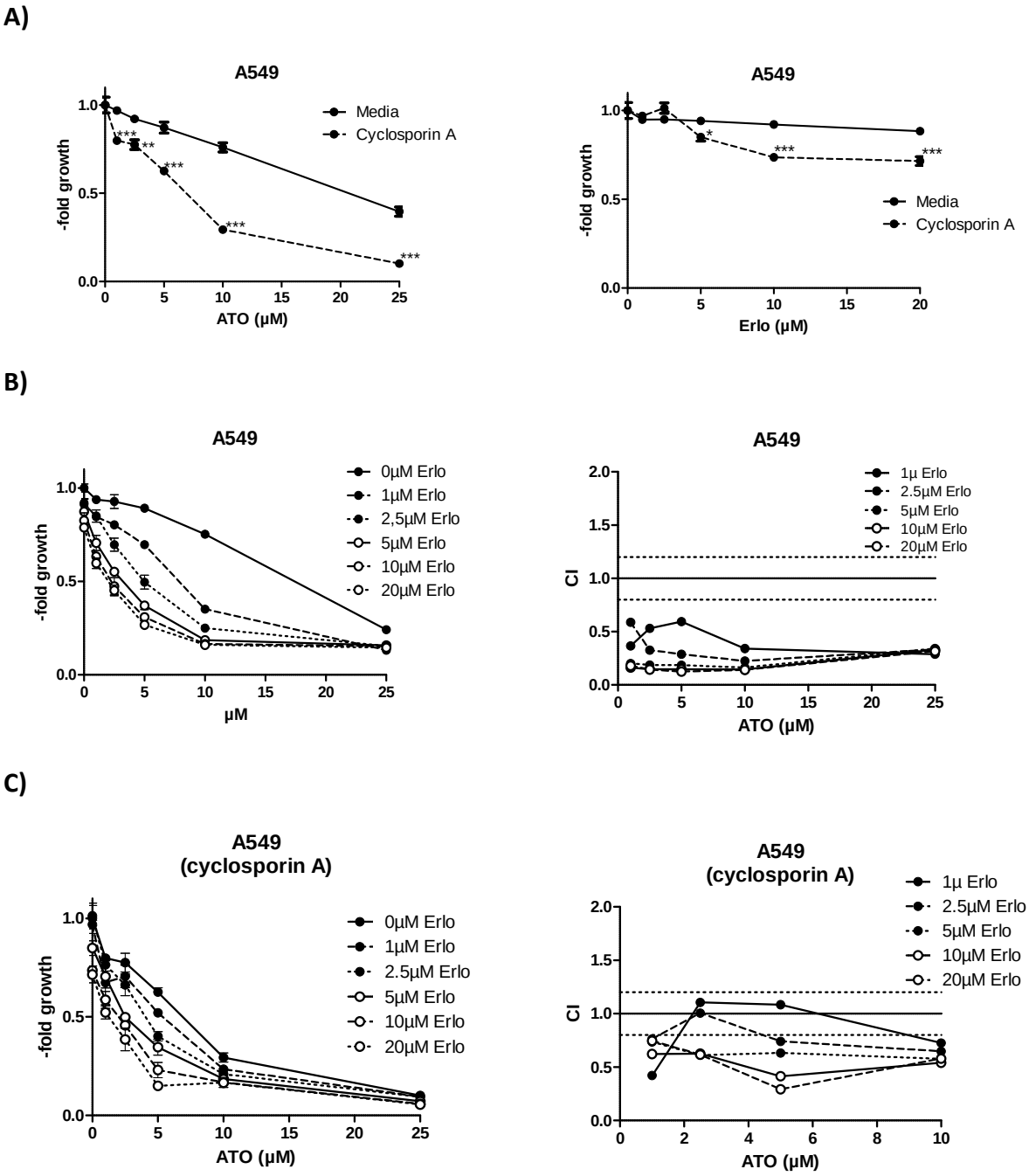

Figure 66. ***Viability and CI values of A549 cells treated with CSA, ATO and erlotinib. A*** *- Sensitizing activity of CSA against ATO and erlotinib.* ***B*** *- Cell viability and CI values of A549 treated with ATO and erlotinib and* ***C*** *- A549 cells treated with CSA, ATO and erlotinib. Cell viability was measured by MTT assay after 72 h drug exposure. Statistical significance was calculated with Two-way ANOVA *p<0.05, **p<0.01, ***p<0.001.*

5.7. Activity of ATO, erlotinib and their combination in A549 xenografts

Finally, we used A549 SCID mouse xenotransplantation models to test the efficacy of ATO and erlotinib *in vivo*. Two treatment settings were performed to test the anticancer activity of the combination: 1) treatment of small (not palpable) tumors (7 days after transplantation) and 2) treatment of palpable tumors (21 days after transplantation).

With regard to the toxicity, mice with small tumors that were receiving ATO showed a significant increase in body weight ($p<0.03$) and those treated with erlotinib a significant weight loss ($p<0.05$) (Figure 67 - A). In contrast, the combination of ATO with erlotinib was well tolerated without any change in body weight during therapy. Moreover, these effects were not observed in the second experiment using mice with palpable tumors. Here, no loss in body weight was observed, but treatment with erlotinib even resulted in gain of body weight (Figure 67 - D). Also a significant weight increase ($p<0.0001$) was measured during treatment with drug combination in comparison to mice treated with vehicle.

With regard to the anticancer activity, Figure 67 - B shows tumor volumes in mm^3 after treatment with the vehicles, ATO, erlotinib, and the ATO/erlotinib combination of mice in the first experiment. Mono-treatments with ATO or erlotinib in comparison to vehicle showed no tumor delay values (Td_{300}) at 300 mm^3 tumor volume from 32.7 to 32.8 and 29 days, respectively (Table 17). At 500 mm^3 tumor volume, mono-treatments even simulated tumor growth which resulted in reduced Td_{500} values (from 44.7 days in mice treated with vehicle to 40.3 and 34.8 days treated with ATO and erlotinib, respectively). In accordance to the *in vitro* data, also *in vivo* treatment with the drug combination induced a distinct delay in tumor growth (Td_{300} = 40 and Td_{500} = 53.8 days) compared to control (Td_{300} = 32.7 and Td_{500} = 44.7 days, respectively) (Figure 67 - B). With regard to the overall mean survival, none of the monotherapy had an impact on the lifespan (Figure 67 – C). In contrast, treatment with the drug combination resulted in long-term disease stabilization in one of the mice (prolong survival for 56 days), which led to an increase in the mean survival time in the combination group from 53 to 64 days. In the second experiment, (Figure 67 - E) no therapeutic effects were observed during treatment leading to Td_{500} values of 32.7 days for the control, 31.4 days for ATO, 35.3 days for erlotinib and 33.15 days for the combination, respectively. However, ATO and erlotinib had a slight stimulating long term effects on the tumor growth increasing the Td_{1000} values from 44.2 in control mice to 41 and 37.5 days in the ATO- and erlotinib-

treated groups, respectively. As a consequence, this resulted in reduced overall survival of both mono-treatment groups (mean 52 days for the control vs. 32 and 36 days for ATO and erlotinib, respectively) (Figure 67 - F). In contrast, the drug combination distinctly reduced tumor growth leading to an increased Td_{1000} value of 55 days and, thus, an increase in overall survival by 1.5-fold (to 76 days).

Table 17

Td values in mice treated with vehicle, ATO, erlotinib, and ATO/erlotinib

Experiment	Therapy (days after xenotransplantation)	Tumor volume (mm^3)	Vehicle (Td)	ATO (Td)	Erlo (Td)	ATO/Erlo (Td)
Small tumors	7 - 18	300	32.7	32.8	29	40
		500	44.7	40.3	34.8	53.8
Palpable tumors	21- 32	500	32.7	31.4	35.3	33.15
		1000	44.2	41	37.5	55

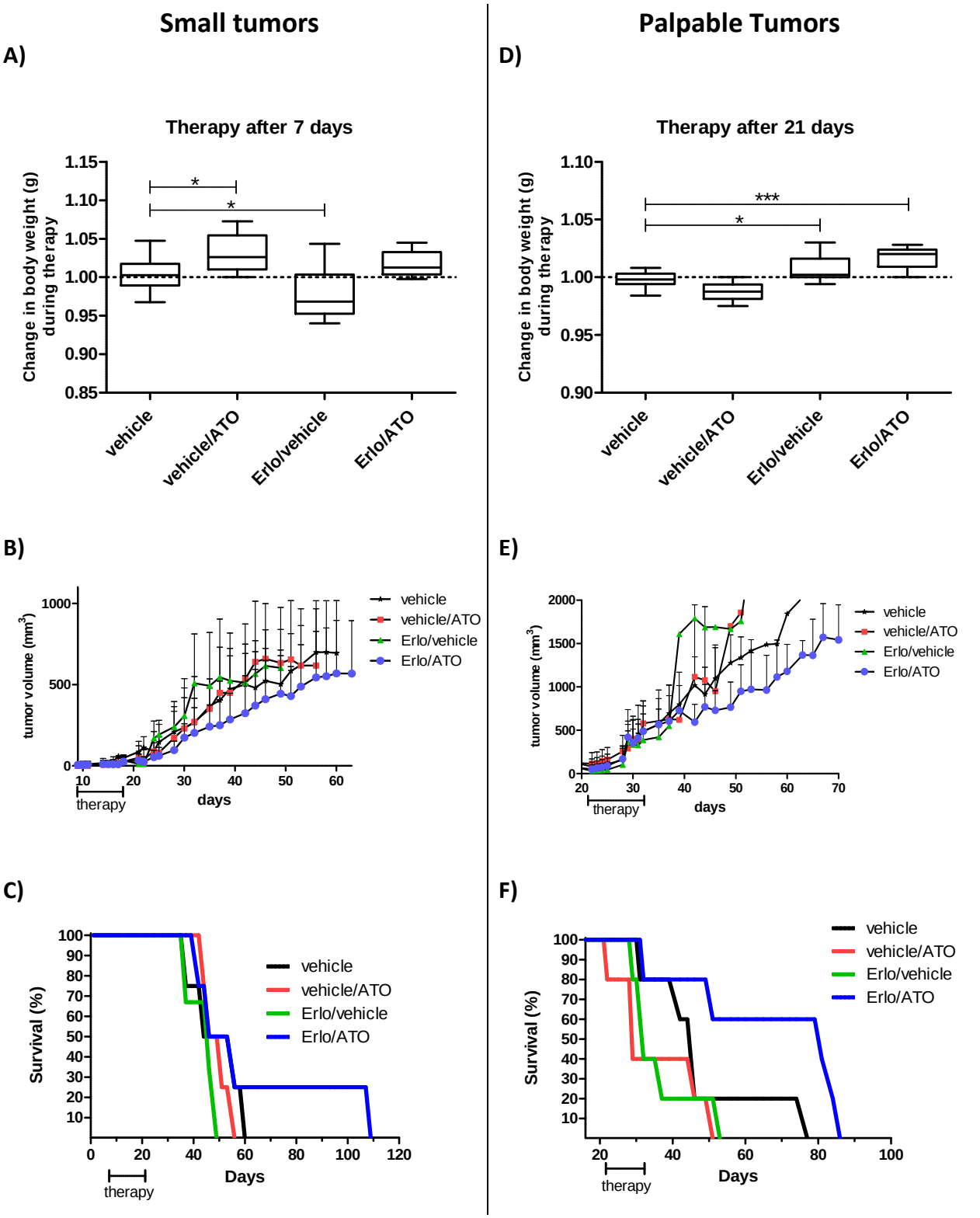

Figure 67. ***Anticancer activity of the ATO/erlotinib combination in vivo – A549*** *xenografts were grown in Balb/c SCID mice and treated with ATO (5 mg/kg; i.p.; dissolved in NaOH/PBS pH=7, five consecutive days per week) and/or erlotinib (25mg/kg; p.o.; dissolved in EtOH/H_2O; five consecutive days per week) for two weeks.* ***A*** *and* ***D*** *- change of body weight during therapy (two weeks);* ***B*** *and* ***E*** *- effect of treatment on tumor growth;* ***C*** *and* ***F*** *- effect of treatment on overall survival. Right column shows experiment of mice treated 7 days after xenotransplantation (small tumors), left column shows experiment of mice treated 21 days after xenotransplantation (palpable tumors). Stastistical significance was calculated using t-test * p<0.05, **p<0.01, *** p<0.001.*

6 Discussion

Arsenic has been used as a therapeutic agent to treat a variety of disorders for more than 2400 years[80]. Its antileukemic activity was first reported in the late 1800s. However, treatment of hematologic malignancies with arsenic experienced popularity in the 1930s. After oblivion for nearly 40 years, in the late 20th century arsenic in form of ATO was rediscovered as a potential remedy against APL[233]. Consequently, besides platinum-containing drugs, ATO is the only metal-containing chemotherapy approved by FDA (since 2000)[234]. Thus, ATO single treatment or in combination with other agents are intensively studied (especially against hematological malignancies). Promising effects were observed in non-APL hematologic malignancies especially in multiple myeloma (MM)[235]. Candidate drugs combined with ATO include signaling inhibitors (imatinib, PD184352, and LY294002 are inhibitors of BCR-ABL, MEK1, and PI3K, respectively), oxidative stress pathway modulators (ascorbic acid, 2-methoxyestradiol 2-ME, BSO), chemotherapeutic drugs (melphalan) or other agents (bortezomib, ATRA)[235]. Additionally, several studies investigated the application of ATO as a single agent against solid tumors. However, its therapeutic efficacy was so far widely limited.

ATO has been demonstrated to induce stimulation of EGFR-mediated signaling pathways[236]. Accordingly, ATO-induced differentiation of APL NB4 cells was shown to be enhanced by the EGFR inhibitor gefitinib[237]. Consequently, we combined in this study ATO with known EGFR inhibitor erlotinib to test their anticancer activity in non-hematologic malignancies. Generally, we found that the drug combination acts synergistically against various cancer cells *in vitro*. Interestingly, synergistic responses were observed mainly in cancer cells which showed resistance against ATO and erlotinib mono-treatments as well as in cells which were selected for resistance against cisplatin. Consequently, this combination regimen represents a potent therapy approach that could be used against cancers resistant to cisplatin. Furthermore, our *in vivo* studies show that anticancer activity of the drug combination was superior to either ATO or erlotinib mono-treatment of tumor-bearing mice. The mechanism underlying the observed synergism seem to be multifactorial.

6.1. Impact of ATO and erlotinib mono-treatment in various cancer cells

There is ample evidence proving that ATO targets several cancer cells via numerous mechanisms like induction of apoptosis, inhibition of proliferation, stimulation of differentiation, and inhibition of angiogenesis[141,238-239]. Stimulation of differentiation and apoptosis induction after ATO treatment are two best known modes of action in APL[240-241]. The chimeric protein PML-RARα initiates APL through both inhibition of differentiation and increased self-renewal of leukemic progenitor cells[115]. ATO induces the degradation of PML-RARα fusion protein and releases the maturation block of APL differentiation[115]. In APL, ATO in low concentrations (0.1 – 0.5 μM) induces differentiation, whereas apoptosis is induced at higher concentrations (0.5 – 2.0 μM)[242]. There are other similar oncogenic proteins targeted by ATO like Tax protein in T-cell leukemia virus type 1 and BCR-ABL fusion protein (philadelphia chromosome) in leukemia cells. Apoptosis induction of ATO has been shown to be multifactorial and not only limited to APL. ATO induces apoptosis by: 1) production of ROS, 2) depolarization of the mitochondrial membrane potential (ΔΨm), 3) down-regulation of Bcl-2 expression 4) opening of the permeability transition pore complex (PTPC) in mitochondrial membranes, 5) caspase cascade activation, etc[157,243-246]. We were interested on the cell viability impact of ATO in non-hematologic cancer cell lines. Overall, ATO mono treatment showed considerable anticancer effects but the IC_{50} values were in most cases above the clinical achievable concentration (5 μM)[242]. The highest resistance against ATO was observed in A549 cells (IC_{50} = 17.65 μM), whereas the highest sensitivity was observed in ovarian cancer cell line A2780 (IC_{50} = 1.83 μM) and thyroid cancer cell line SW579 (IC_{50} = 1.94 μM). A possible way to use arsenic against non-hematologic cancers in the clinics is reducing its toxicity and enhancing the anticancer activity by co-administration with other agents. The majority of combination regimens with ATO that revealed synergistic anticancer effects were reported in hematological malignancies[141]. Examples for combination studies with ATO in non-hematologic tumor cells were reported in NSCLC, in HCC or osteosarcoma cell lines as co-treatment with cisplatin, sorafenib, and radiation therapy, respectively[247-249]. According to our knowledge, this is the first study showing that combination of ATO with the EGFR-TKI erlotinib synergizes in non-hematological malignancies and represents a potent anticancer combination therapy against various cancer cell types.

Erlotinib is currently used for the treatment of locally advanced or metastatic NSCLC that has failed at least one prior chemotherapy regimen[250]. This drug represents also one of the most studied TKIs in NSCLCs. The best anticancer effects with erlotinib were observed in NSCLC with activating mutations in the tyrosine kinase domain of the EGFR[251]. In A549 and other cell lines tested in this study, erlotinib mono-treatment did not show any significant anticancer activity (IC_{50} > 20 µM)[252] which is in accordance with the wild-type EGFR status of these cell lines. Accordingly, the only exception was HCC827 cell line with a reported hypersensitivity against EGFR-TKIs based on a sensitizing deletion on exon 19 of the EGFR tyrosine kinase (△E746-A750)[253-254]. As a specific inhibitor of oncogenic EGFR, erlotinib was often chosen as co-therapy with other agents in cancers with elevated levels of EGFR. For example, a phase ll study has revealed that combination of erlotinib and the metal-drug carboplatin is active in patients with EGFR-positive ovarian cancer[255]. Other agents reported to be acting synergically with erlotinib in combination were gemcitabine, cisplatin or inhibitors of EGFR downstream transducers like Akt, MEK, Raf, and mTOR[256-261].

6.2. Impact of ATO and erlotinib in multi-drug resistant A549 cells

ATO and erlotinib in combination showed a strong synergistic effect in A549 after 72 h drug exposure. This multi-drug resistant NSCLC cell model was further investigated to determine the drug exposure time that is needed to induce a synergistic antiproliferative effect as well as impact of the drug combination on DNA synthesis, apoptosis induction and cell cycle distribution.

Previous studies have been shown that A549 represents a quite resistant cancer cell model against ATO mono-treatment based on expression of MDR proteins including the conjugate export drugs MRP1 and MRP2[262-264]. Data from our drug-pulsing experiments showed that at least 24 h drug exposure with ATO is necessary to induce a weak antiproliferative effect after 72 h incubation time. Increase in exposure time to 48 h lead to distinctly stronger anticancer effects in our study. In contrast, erlotinib was non-effective against A549 cells even after 72 h drug exposure and cell incubation time. The unresponsiveness of erlotinib could explain the expression of wtEGFR but also mutated *KRAS* in A549 cells[265]. But how long does the combination of tested drugs need to be exposed and induce a synergistic activity in A549? After 24 h drug exposure and cell incubation time, there was no activity in cell viability found. However, drug combination induced a significant decrease of DNA synthesis rate after 24 h

drug exposure. Consequently, a strong synergism in cell viability was measured after 48 h drug exposure. On the other hand, 6 h drug exposure was enough time to induce a synergistic activity. However, cells had to be cultured for another 72 h to detect the responsive activity. These data suggest that the tested drugs were incorporated inside the cells in the first 6 hours of drug exposure, but at least 48 h incubation are necessary to develop the full anticancer activity. This indicates that at least 1-2 cell cycle transits are needed for the activity of ATO.

Previous published data in A549 cells indicated that treatment of ATO (0 – 6 µM) after 48 h did not alter significantly the cell cycle distribution[262]. We confirmed this observation and further showed that 5 µM ATO in combination with erlotinib induced a slight increase of cells in G1/G0 phase. Moreover, ATO at 10 µM in co-treatment with 5 and 10 µM erlotinib induced a significant increase of cell populations with G2/M phase arrest. Apoptosis induction of ATO and erlotinib mono-treatment in A549 cells was marginally increased even after 72 h drug exposure. On the other hand, apoptosis of A549 cells was considerably increased after 48 h and strongly increased after 72 h after exposure to combination treatment with ATO and erlotinib. These observations led us to the conclusion that decreased cell viability measured after 48 h and 72 h by MTT assay is as a result of cytostatic (G2/M cell cycle arrest) and cytotoxic activities of the drug combination.

6.3. The role of EGFR pathway

The EGFR pathway plays an important role in growth, proliferation and survival of mammalian cells[266]. Aberrant activation of this pathway has been reported in various cancers which makes it an attractive target for therapy development (e.g. Erlotinib used in this study, is one of the designed TKIs to target EGFR)[183,200,267]. Also ATO was reported to interact with the EGFR pathway. Thus, induction of EGFR phosphorylation and MAP kinase pathway activation was reported in bladder cells after arsenic exposure[195]. In general, activation of this pathway by arsenic involves both EGFR-dependent as well as -independent events. For example, phosphorylation of the EGFR kinase domain via c-Src (MAP kinase pathway) was described as one mechanism of induced cell proliferation[195,268]. c-Src is a non-receptor kinase with SH2 and SH3 domains which can physically interact with EGFR, resulting in the phosphorylation of the EGFR at two unique sites (Tyr845, Tyr1101)[269]. Subsequently, ATO was also shown to increase levels of c-Src and to further stimulate the EGFR/ERK signaling[236]. Furthermore, epithelial cells in the lung of persons exposed to arsenic showed activation of the EGFR

pathway by increasing expression levels of EGFR ligand heparin binding-EGF[270]. Consequently, we hypothesized that stimulation of EGFR pathway by ATO could be a survival mechanism which can be blocked by administration of EGFR inhibitors.

Indeed, ATO co-treatment was synergistic with all tested EGFR inhibitors. Moreover, in accordance with the hypothesis of EGFR stimulation as a protection mechanism, co-treatment of A549 cells with EGF induced a considerable resistance against ATO as well as erlotinib. Notably, also the synergistic activity of the drug combination was weaker in the presence of EGF. This might be explained by the stimulation of additional EGFR-mediated cancer cell survival and proliferation pathways (e.g. stimulation of EGFR/Her2 heterodimers) in the presence of EGF that makes A549 cells more resistant to the drug combination compared to unstimulated cells.

The activity of EGFR-TKIs is often influenced by somatic mutations found in the EGFR kinase domain of NSCLCs. We analyzed different cell models containing sensitizing and/or resistance-mediating EGFR mutations to determine their role in the observed synergism of ATO with erlotinib. EGFR mutations are reported in ~10% of NSCLC in caucasian patients and in more than 40% of east-asian patients[271]. Nearly 95% of these EGFR mutations are sensitizing against TKIs (e.g. L858R or △E746-A750), whereas 5% of them are known to induce resistance (T790M)[200]. To test the efficacy of the drug combination against cells with activating EGFR mutations HCC827 (△E746-A750), H1975 (L858R/T790M), and H1650 (△E746-A750) cells were used. Combination treatment did not show synergistic activity at HCC827 cells which has only an EGFR sensitizing mutation. This observation may be explained by the fact that HCC827 are exclusively dependent on EGFR signaling for their survival and, thus, inhibitory effects are triggered already after treatment with very low concentrations of erlotinib (''oncogenic addiction''). Moreover, as the △E746-A750 mutation leads to constitutive (maximal) activation of the EGFR signaling pathway, it seems likely that in these cells ATO treatment is not able to further stimulate EGFR expression. These results are well in agreement with the hypothesis that the synergism of ATO with erlotinib is, at least in part, based on the inhibition of the enhanced EGFR signaling which allows cancer cells to survive ATO treatment.

With regard to resistance conferring EGFR mutations, in H1975 cells harboring a constitutive active EGFR with a second mutation (T790M) leading to erlotinib resistance, only a weak synergism was observed. The mechanism underlying the resistance by T790M mutation is

based on a steric modification of the erlotinib binding site which results in reduced affinity of the TKI for this kind of receptors and, therefore less effective EGFR inhibition[200,209,221,272]. Consequently, erlotinib is not able to inhibit the ATO-protective EGFR stimulation in these cells. In accordance with these observations, also cells with erlotinib resistance due to c-Met expression did not respond synergistically to the combination of ATO with erlotinib. In contrast even, antagonistic effects were observed in these experiments. Together, this indicates that a functional erlotinib-sensitive EGFR signaling is necessary for its synergistic effects with ATO.

Notably, a potent synergism of ATO with erlotinib was also found in H1650 cells, which again harbor the sensitizing EGFR mutation in △E746-A750 but are secondary resistant to erlotinib due to PTEN loss. PTEN is an important regulator of the PI3K/Akt pathway and such deletion of this protein has been linked with EGFR-TKI resistance[273-274]. As the results obtained, HCC827 cells indicate that a constitutive active EGFR (e.g. based on △E746-A750 mutation) is not associated with synergistic sensitivity to the drug combination and that PI3K/Akt pathway might play a role in the synergism of ATO with erlotinib. This fits also to the observation that no synergism is observed in c-Met overexpressing cells because the c-Met receptor is known to cause phosphorylation of ERBB3, which in turn activates the PI3K/Akt signaling pathway[275-277]. Thus, it can be hypothesized that the EGFR-independent activation of this pathway, renders c-Met overexpressing cells also resistant to the synergistic effects of the drug combination.

The assumption that the synergistic activity of ATO with erlotinib acts via the inhibition of the PI3K/Akt pathway is further supported by the potent synergistic activity of ATO with the Akt kinase inhibitor (MK-2206). The intrinsic activation of the PI3K/Akt/mTor pathway was recently reported for mesothelioma cells[278]. Notably, we observed a very strong synergistic response to the ATO/Erlotinib combination in several mesothelioma cell models (n=6), which is in good agreement with the assumption that the PI3K/Akt pathway of the EGFR signaling is important for the synergistic activity[278]. As also combination of ATO with inhibition of the PI3K/Akt pathway was recently suggested as anticancer strategy for HCC treatment, we conclude that this downstream signal pathway plays an important role in the synergism of ATO with erlotinib[279].

Nevertheless, Akt is not the only downstream transducer of EGFR. It has been shown that erlotinib inhibits phosphorylation of ERK (pERK) and further cyclin D1 after arsenic

exposure[270]. To test whether this pathway is involved in the synergistic activity of ATO with erlotinib, the effects of pERK inhibition via MEK on ATO were analyzed. However, the combination of ATO with an MEK inhibitor did not reveal any synergism. This indicates that interaction with phosphorylation of ERK is not the major player in the synergistic activity of ATO and erlotinib.

To gain more insights into the role of other RTKs and downstream transducers in anticancer activity of ATO, two other multi-kinase inhibitors (sorafenib and sunitinib) were used. Both TKIs inhibit similar RTKs like PDGFR, VEGFR and c-Kit but sorafenib additionally inhibits Raf and p38 kinases. Notably, ATO was synergistic in combination with sorafenib but not with sunitinib. This observation indicates that ATO synergizes based on the interaction with sorafenib-only targes (p38, Raf) but not with the RTKs which are inhibited by both drugs. The role of Raf in the observed synergism could be cell specific, considering the fact that A549 has a mutated Ras kinase which is upstream from Raf in the signaling. The role of p38 was further analyzed by combination of a p38 inhibitor with ATO. A weak but significant synergistic activity of this combination was observed which indicates that this kinase might play a role in the synergistic activity of ATO.

Surprisingly, ATO in co-treatment with erlotinib showed a synergistic effect in SW620 cell line which has no basal EGFR expression. This raised the question whether EGFR is the only factor responsible for the observed synergism or whether additional off-target effects of erlotinib are involved.

6.4. The role of ABC membrane transporters in increased intracellular ATO levels

Another hypothesis to explain the synergistic effect would be that the combination of the drugs could lead to increased accumulation of ATO or erlotinib inside the cells. Thus, pharmacological interactions between the two drugs might affect the accumulation levels of each other e.g. by competing for shared efflux mechanisms. Consequently, we measured cellular arsenic levels of cells treated with ATO alone or in combination with erlotinib. Out of four cell lines tested, three showed significantly higher arsenic accumulation in samples treated with the drug combination in comparison to the samples exposed to ATO mono-therapy. This suggests that erlotinib might inhibit cellular mechanisms leading to reduced levels of intracellular arsenic. Erlotinib represents an EGFR TKI interacting with the ATP-

binding domain of EGFR. Accordingly, it has been shown that EGFR-TKIs interact with MDR transporters as substrates or inhibitors[229] . Consequently, we tested if erlotinib affects MDR pumps which could lead to the increased ATO accumulation in the combination setting. For example, resistance to imatinib is related to P-gp overexpression while Gefitinib has been reported to interact with BCRP and P-gp[280]. Lapatinib and erlotinib have been shown to be P-gp and BCRP substrates. Moreover, the latter reverses P-gp- and BCRP-mediated MDR by direct inhibition of the drug efflux function[229-230]. In general, it is well known that the mode of action of erlotinib is reversible binding in ATP binding pockets of the receptor tyrosine kinase domain in the EGFR. Also ABC transporters (ATP-binding cassette) contain ATP binding pockets, which might be possible interaction targets of erlotinib. There is profound experimental evidence that suggests that arsenic uptake and efflux is mediated by several ABC membrane transporters such as MRP1 and MRP2, but possibly also others like suggested for MRP3 and P-gylcoprotein in the liver[119,123,125]. The MRPs belong to an ABC transporter subfamily (ABCC) with known substrate specificity for conjugates with glutathione- (GSH), glucuronide-, and sulfate-conjugated organic anions[281-282]. The formation of arsenic-GSH conjugates, such as arsenic triglutathione and dimethylarsenic diglutathione, is mediated by glutathion-S-transferase (GST) which results in more effective cellular and biliary excretion[125,283-284]. Therefore, arsenic-GSH conjugates are efficiently excreted as substrates of MRP1 and MRP2[285]. These reports are in accordance with our data showing that cells overexpressing P-gp und MRP1 ($SW1573_{2R160}$) were resistant against ATO and erlotinib mono-therapy but sensitive to their combination[286]. Furthermore, co-incubation of cyclosporine A as a modulator of P-gp and MRP1 sensitized MRP1 and MRP2 overexpressing A549 against both ATO and erlotinib and resulted in reduced synergistic activity. This again suggests that ATO and erlotinib are substrates of those MDR transporters.

Expression levels of MRP1 analyzed by Western blotting were in accordance with an increased ATO accumulation in response to co-treatment with erlotinib. Consequently, those cells that showed MRP1 overexpression were also more sensitive to the drug combination. This leads to the conclusion that MRP1 as one of the ABC transporters inhibited by erlotinib is a factor responsible for the synergism of ATO with erlotinib, at least in MRP1-overexpressing cell lines.

7 Conclusion

There is ample data for both the anticancer and the carcinogenic effect of arsenic in animal models as well as in human populations exposed to this metal. Skin hyperpigmentation has been shown to be a hallmark of arsenic chronic poisoning which represents also a pre-stage of skin cancer, whereas the anti-leukemic abilities led to approval of ATO for the treatment of APL. Apoptosis induction, cytostatic and many other modulation effects in cancer cells make ATO an attractive remedy in anticancer research and therapy. However, so far ATO has not been approved for the use in any solid tumor based on the fact that all clinical studies showed lack of activity in a mono-therapeutic setting. Consequently, aim of the study was to improve the anticancer activity of ATO against solid tumors by combination with EGFR inhibitors with a focus on the approved anti-NSCLC compound erlotinib. The underlying hypothesis was based on the recently published observation that chronic exposure to arsenic leads to activation of EGFR-mediated signaling pathways. Indeed we discovered a profound synergism of ATO and erlotinib in diverse solid tumor cell models. The underlying molecular mechanisms were demonstrated to be multifaceted and include on- as well as off-target effects of erlotinib, namely 1) inhibition of EGFR-mediated protection mechanism against ATO via the PI3K/AkT as well as the p38 MAPK pathways and 2) blockade of ATP-driven ATO efflux by members of the ABC transporter family. Importantly, this combination was shown to induce synergistic activity in cisplatin-resistant cells and thus can be used to overwhelm this resistance. Finally, *in vivo* xenograft experiments using a highly chemotherapy-resistant lung cancer model confirmed a profound anticancer activity of the investigated drug combination which resulted in significantly increased overall survival of the tumor-bearing mice.

Overall, we conclude that ATO in combination with erlotinib represents a promising treatment option for a variety of human solid tumor types as well as a feasible strategy to overcome intrinsic therapy resistance but also avoiding acquired treatment failure.

Abbreviations

ABC	ATP-binding cassette transporter
APL	Acute promyelocytic leukemia
AP1	Activator Protein 1
ATO	Arsenic trioxide
ATP	Adenosine triphosphate
Bcl-2	B-cell lymphoma 2
BCRP	Breast cancer resistance protein
BSA	Bovin serum albumin
CDK	Cyclin-dependent kinase
Cisplatin	cis-diamminedichloroplatinum(II)
DAPI	4',6-diamidino-2-phenylindole
DMSO	Dimethyl sulfoxide
DNA	Deoxyribonucleic acid
EGF	Epidermal growth factor
EGFR	Epidermal growth factor receptor
dnEGFR	Dominant-negative epidermal growth factor receptor
Erlo	Erlotinib
FACS	Fluorescence-activated cell sorting
FBS	Fetal bovine serum
FDA	Food and Drug Administration
GFP	Green fluorescent protein
GSH	Glutathione
GST	Glutathion-S-Transferase
HGF	Hepatocyte growth factor
HIF-1	Hypoxia inducible factor-1
IGF	Insulin-like growth factor
MAPK	Mitogen activated protein kinase
MDR	Multiple drug resistance
MOI	Multiplicity of infection
MRP	Multidrug resistance-associated protein
MTT	Dimethyl thiazolyl diphenyl tetrazolium salt

NFκB	Nuclear factor κB
NSLC	Non-small lung carcinoma
PBS	Phosphate buffered saline
PDGF	Platelet-derived growth factor
P-gp	p-glycoprotein
PI	Propidium iodide
PI3K	Phosphotidyl-inositol-3-OH kinase
PML	Promyelocytic leukemia protein
PMSF	Phenylmethanesulfonylfluoride
PVDF	Polyvinylidene fluoride
RARα	Retinoic acid receptor
Rb	Retinoblastoma protein
ROS	Reactive oxygen species
RTK	Receptor tyrosine kinase
SDS-PAGE	Sodium dodecyl sulfate polyacrylamide gel electrophoresis
STAT	Signal Transducer and Activator of Transcription
TBST	Tris-buffered saline with Tween
TNFβ	Tumor necrosis factor β
VEGF	Vascular endothelial growth factor

References

1 Ruddon, R. W. *Cancer biology*. 4th edn, (Oxford University Press, 2007).

2 Ferlay J, S. H., Bray F, Forman D, Mathers C and Parkin DM. in *Lyon, France: International Agency for Research on Cancer; 2010* (GLOBOCAN 2008, 2011).

3 WHO. *Cancer*, <http://www.who.int/cancer/en/> (2011).

4 Hejmadi, M. (Ventus Publishing ApS, 2009).

5 Pelengaris, S., Khan, M. & Blasco, M. A. *The molecular biology of cancer*. (Blackwell Pub., 2006).

6 Aggarwal, B. B. *et al.* Cancer is a Preventable Disease that Requires Major Lifestyle Changes. *Pharm Res-Dord* **25**, 2097-2116, doi:10.1007/s11095-008-9661-9 (2008).

7 Kryeziu, A. Graphics (Kapre, 2011).

8 Alberts, B. *Molecular biology of the cell*. 4th edn, (Garland Science, 2002).

9 Marian, B. *Krankheit, Krankheitsursachen und -bilder*. Third Edition edn, 420 (Facultas Universitätsverlag, 2010).

10 Knowles, M. A. & Selby, P. *Introduction to the cellular and molecular biology of cancer*. (Oxford University Press, 2005).

11 Kufe DW, P. R., Weichselbaum RR, et al., editors. (BC Decker Inc, 2003).

12 *Scitable by nature education*, <http://www.nature.com/scitable> (2011).

13 Hanahan, D. & Weinberg, R. A. Hallmarks of cancer: the next generation. *Cell* **144**, 646-674, doi:S0092-8674(11)00127-9 [pii]
10.1016/j.cell.2011.02.013 (2011).

14 Yamasaki, L. Role of the RB tumor suppressor in cancer. *Cancer Treat Res* **115**, 209-239 (2003).

15 Hanahan, D. & Weinberg, R. A. The hallmarks of cancer. *Cell* **100**, 57-70, doi:S0092-8674(00)81683-9 [pii] (2000).

16 Cheng, N., Chytil, A., Shyr, Y., Joly, A. & Moses, H. L. Transforming growth factor-beta signaling-deficient fibroblasts enhance hepatocyte growth factor signaling in mammary carcinoma cells to promote scattering and invasion. *Mol Cancer Res* **6**, 1521-1533, doi:6/10/1521 [pii]
10.1158/1541-7786.MCR-07-2203 (2008).

17 Davies, M. A. & Samuels, Y. Analysis of the genome to personalize therapy for melanoma. *Oncogene* **29**, 5545-5555, doi:onc2010323 [pii]
10.1038/onc.2010.323 (2010).

18 Tabernero, J. & Dienstmann, R. BRAF as a Target for Cancer Therapy. *Anti-Cancer Agent Me* **11**, 285-295 (2011).

19 Rosen, N. & Poulikakos, P. I. Mutant BRAF Melanomas-Dependence and Resistance. *Cancer Cell* **19**, 11-15, doi:10.1016/j.ccr.2011.01.008 (2011).

20 Avraham, R. & Yarden, Y. Feedback regulation of EGFR signalling: decision making by early and delayed loops. *Nat Rev Mol Cell Biol* **12**, 104-117, doi:nrm3048 [pii]
10.1038/nrm3048 (2011).

21 Stamenkovic, I. & Yu, Q. Merlin, a "magic" linker between extracellular cues and intracellular signaling pathways that regulate cell motility, proliferation, and survival. *Curr Protein Pept Sci* **11**, 471-484, doi:CPPS-61 [pii] (2010).

22 Youle, R. J. & Strasser, A. The BCL-2 protein family: opposing activities that mediate cell death. *Nat Rev Mol Cell Biol* **9**, 47-59, doi:nrm2308 [pii]
10.1038/nrm2308 (2008).

23 Yin, X. M. *et al.* Bid-deficient mice are resistant to Fas-induced hepatocellular apoptosis. *Nature* **400**, 886-891, doi:10.1038/23730 (1999).

24 Kaufmann, T. *et al.* The BH3-only protein bid is dispensable for DNA damage- and replicative stress-induced apoptosis or cell-cycle arrest. *Cell* **129**, 423-433, doi:S0092-8674(07)00380-7 [pii]

10.1016/j.cell.2007.03.017 (2007).
25 Adams, J. M. & Cory, S. The Bcl-2 apoptotic switch in cancer development and therapy. *Oncogene* **26**, 1324-1337, doi:1210220 [pii]
10.1038/sj.onc.1210220 (2007).
26 Levine, B. & Kroemer, G. Autophagy in the pathogenesis of disease. *Cell* **132**, 27-42, doi:S0092-8674(07)01685-6 [pii]
10.1016/j.cell.2007.12.018 (2008).
27 Brech, A., Ahlquist, T., Lothe, R. A. & Stenmark, H. Autophagy in tumour suppression and promotion. *Mol Oncol* **3**, 366-375, doi:S1574-7891(09)00079-9 [pii]
10.1016/j.molonc.2009.05.007 (2009).
28 White, E. & DiPaola, R. S. The double-edged sword of autophagy modulation in cancer. *Clin Cancer Res* **15**, 5308-5316, doi:1078-0432.CCR-07-5023 [pii]
10.1158/1078-0432.CCR-07-5023 (2009).
29 Grivennikov, S. I., Greten, F. R. & Karin, M. Immunity, inflammation, and cancer. *Cell* **140**, 883-899, doi:S0092-8674(10)00060-7 [pii]
10.1016/j.cell.2010.01.025 (2010).
30 Blasco, M. A. Telomeres and human disease: ageing, cancer and beyond. *Nat Rev Genet* **6**, 611-622, doi:10.1038/nrg1656 (2005).
31 Park, J. I. *et al.* Telomerase modulates Wnt signalling by association with target gene chromatin. *Nature* **460**, 66-72, doi:nature08137 [pii]
10.1038/nature08137 (2009).
32 Kang, H. J. *et al.* Ectopic expression of the catalytic subunit of telomerase protects against brain injury resulting from ischemia and NMDA-induced neurotoxicity. *J Neurosci* **24**, 1280-1287, doi:10.1523/JNEUROSCI.4082-03.2004
24/6/1280 [pii] (2004).
33 Masutomi, K. *et al.* The telomerase reverse transcriptase regulates chromatin state and DNA damage responses. *Proc Natl Acad Sci U S A* **102**, 8222-8227, doi:0503095102 [pii]
10.1073/pnas.0503095102 (2005).
34 Maida, Y. *et al.* An RNA-dependent RNA polymerase formed by TERT and the RMRP RNA. *Nature* **461**, 230-235, doi:nature08283 [pii]
10.1038/nature08283 (2009).
35 Carmeliet, P. Angiogenesis in life, disease and medicine. *Nature* **438**, 932-936, doi:nature04478 [pii]
10.1038/nature04478 (2005).
36 Hanahan, D. & Folkman, J. Patterns and emerging mechanisms of the angiogenic switch during tumorigenesis. *Cell* **86**, 353-364, doi:S0092-8674(00)80108-7 [pii] (1996).
37 Alison, M. *The cancer handbook*. 2nd edn, (John Wiley & Sons, 2007).
38 Baeriswyl, V. & Christofori, G. The angiogenic switch in carcinogenesis. *Semin Cancer Biol* **19**, 329-337, doi:S1044-579X(09)00064-9 [pii]
10.1016/j.semcancer.2009.05.003 (2009).
39 Kazerounian, S., Yee, K. O. & Lawler, J. Thrombospondins in cancer. *Cell Mol Life Sci* **65**, 700-712, doi:10.1007/s00018-007-7486-z (2008).
40 Talmadge, J. E. & Fidler, I. J. AACR centennial series: the biology of cancer metastasis: historical perspective. *Cancer Res* **70**, 5649-5669, doi:0008-5472.CAN-10-1040 [pii]
10.1158/0008-5472.CAN-10-1040 (2010).
41 Berx, G. & van Roy, F. Involvement of members of the cadherin superfamily in cancer. *Cold Spring Harb Perspect Biol* **1**, a003129, doi:cshperspect.a003129 [pii]
10.1101/cshperspect.a003129 (2009).
42 Frixen, U. H. *et al.* E-Cadherin-Mediated Cell Cell-Adhesion Prevents Invasiveness of Human Carcinoma-Cells. *J Cell Biol* **113**, 173-185 (1991).
43 Berx, G., Raspe, E., Christofori, G., Thiery, J. P. & Sleeman, J. P. Pre-EMTing metastasis? Recapitulation of morphogenetic processes in cancer. *Clin Exp Metastasis* **24**, 587-597, doi:10.1007/s10585-007-9114-6 (2007).

44 Klymkowsky, M. W. & Savagner, P. Epithelial-mesenchymal transition: a cancer researcher's conceptual friend and foe. *Am J Pathol* **174**, 1588-1593, doi:S0002-9440(10)61015-2 [pii] 10.2353/ajpath.2009.080545 (2009).

45 Micalizzi, D. S., Farabaugh, S. M. & Ford, H. L. Epithelial-mesenchymal transition in cancer: parallels between normal development and tumor progression. *J Mammary Gland Biol Neoplasia* **15**, 117-134, doi:10.1007/s10911-010-9178-9 (2010).

46 Taube, J. H. *et al.* Core epithelial-to-mesenchymal transition interactome gene-expression signature is associated with claudin-low and metaplastic breast cancer subtypes. *Proc Natl Acad Sci U S A* **107**, 15449-15454, doi:1004900107 [pii] 10.1073/pnas.1004900107 (2010).

47 Schmalhofer, O., Brabletz, S. & Brabletz, T. E-cadherin, beta-catenin, and ZEB1 in malignant progression of cancer. *Cancer Metastasis Rev* **28**, 151-166, doi:10.1007/s10555-008-9179-y (2009).

48 Yang, J. & Weinberg, R. A. Epithelial-mesenchymal transition: At the crossroads of development and tumor metastasis. *Developmental Cell* **14**, 818-829, doi:10.1016/j.devcel.2008.05.009 (2008).

49 Williams, E. D. *et al.* Epithelial-mesenchymal and mesenchymal - Epithelial transitions in carcinoma progression. *Journal of Cellular Physiology* **213**, 374-383, doi:10.1002/jcp.21223 (2007).

50 Zhou, S., Huang, C. & Wei, Y. The metabolic switch and its regulation in cancer cells. *Sci China Life Sci* **53**, 942-958, doi:10.1007/s11427-010-4041-1 (2010).

51 Gatenby, R. A. & Gillies, R. J. Why do cancers have high aerobic glycolysis? *Nat Rev Cancer* **4**, 891-899, doi:10.1038/nrc1478 (2004).

52 DeBerardinis, R. J., Lum, J. J., Hatzivassiliou, G. & Thompson, C. B. The biology of cancer: metabolic reprogramming fuels cell growth and proliferation. *Cell Metab* **7**, 11-20, doi:S1550-4131(07)00295-1 [pii] 10.1016/j.cmet.2007.10.002 (2008).

53 Guppy, M., Greiner, E. & Brand, K. The role of the Crabtree effect and an endogenous fuel in the energy metabolism of resting and proliferating thymocytes. *Eur J Biochem* **212**, 95-99 (1993).

54 Feron, O. Pyruvate into lactate and back: from the Warburg effect to symbiotic energy fuel exchange in cancer cells. *Radiother Oncol* **92**, 329-333, doi:S0167-8140(09)00336-3 [pii] 10.1016/j.radonc.2009.06.025 (2009).

55 Teng, M. W., Swann, J. B., Koebel, C. M., Schreiber, R. D. & Smyth, M. J. Immune-mediated dormancy: an equilibrium with cancer. *J Leukoc Biol* **84**, 988-993, doi:jlb.1107774 [pii] 10.1189/jlb.1107774 (2008).

56 Yang, L., Pang, Y. & Moses, H. L. TGF-beta and immune cells: an important regulatory axis in the tumor microenvironment and progression. *Trends Immunol* **31**, 220-227, doi:S1471-4906(10)00053-0 [pii] 10.1016/j.it.2010.04.002 (2010).

57 Shields, J. D., Kourtis, I. C., Tomei, A. A., Roberts, J. M. & Swartz, M. A. Induction of lymphoidlike stroma and immune escape by tumors that express the chemokine CCL21. *Science* **328**, 749-752, doi:science.1185837 [pii] 10.1126/science.1185837 (2010).

58 Mougiakakos, D., Choudhury, A., Lladser, A., Kiessling, R. & Johansson, C. C. Regulatory T cells in cancer. *Adv Cancer Res* **107**, 57-117, doi:S0065-230X(10)07003-X [pii] 10.1016/S0065-230X(10)07003-X (2010).

59 Ostrand-Rosenberg, S. & Sinha, P. Myeloid-derived suppressor cells: linking inflammation and cancer. *J Immunol* **182**, 4499-4506, doi:182/8/4499 [pii] 10.4049/jimmunol.0802740 (2009).

60 Blay, J. [Targeted therapies of cancer: not lost in translation]. *Bulletin du cancer*, 799-804 (2006).

61 Besse, B., Ropert, S. & Soria, J. C. Targeted therapies in lung cancer. *Ann Oncol* **18 Suppl 9**, ix135-142, doi:18/suppl_9/ix135 [pii]
10.1093/annonc/mdm308 (2007).

62 Berry, L. J., Moeller, M. & Darcy, P. K. Adoptive immunotherapy for cancer: the next generation of gene-engineered immune cells. *Tissue Antigens* **74**, 277-289, doi:TAN1336 [pii]
10.1111/j.1399-0039.2009.01336.x (2009).

63 Mouridsen, H. *et al.* Letrozole therapy alone or in sequence with tamoxifen in women with breast cancer. *N Engl J Med* **361**, 766-776, doi:361/8/766 [pii]
10.1056/NEJMoa0810818 (2009).

64 Lippert, T. H., Ruoff, H. J. & Volm, M. Current status of methods to assess cancer drug resistance. *Int J Med Sci* **8**, 245-253 (2011).

65 Gottesman, M. M., Fojo, T. & Bates, S. E. Multidrug resistance in cancer: role of ATP-dependent transporters. *Nat Rev Cancer* **2**, 48-58 (2002).

66 Heffeter, P. *et al.* Resistance against novel anticancer metal compounds: differences and similarities. *Drug Resist Updat* **11**, 1-16, doi:S1368-7646(08)00017-4 [pii]
10.1016/j.drup.2008.02.002 (2008).

67 Rao, V. V. *et al.* Choroid plexus epithelial expression of MDR1 P glycoprotein and multidrug resistance-associated protein contribute to the blood-cerebrospinal-fluid drug-permeability barrier. *Proc Natl Acad Sci U S A* **96**, 3900-3905 (1999).

68 Cordon-Cardo, C. *et al.* Expression of the multidrug resistance gene product (P-glycoprotein) in human normal and tumor tissues. *J Histochem Cytochem* **38**, 1277-1287 (1990).

69 Ambudkar, S. V. *et al.* Biochemical, cellular, and pharmacological aspects of the multidrug transporter. *Annu Rev Pharmacol Toxicol* **39**, 361-398, doi:10.1146/annurev.pharmtox.39.1.361 (1999).

70 Dilda, P. J. & Hogg, P. J. Arsenical-based cancer drugs. *Cancer Treat Rev* **33**, 542-564, doi:S0305-7372(07)00073-4 [pii]
10.1016/j.ctrv.2007.05.001 (2007).

71 Jedlitschky, G., Hoffmann, U. & Kroemer, H. K. Structure and function of the MRP2 (ABCC2) protein and its role in drug disposition. *Expert Opin Drug Metab Toxicol* **2**, 351-366, doi:10.1517/17425255.2.3.351 (2006).

72 Heffeter, P. *et al.* Intrinsic and acquired forms of resistance against the anticancer ruthenium compound KP1019 [indazolium trans-[tetrachlorobis(1H-indazole)ruthenate (III)] (FFC14A). *J Pharmacol Exp Ther* **312**, 281-289, doi:10.1124/jpet.104.073395
jpet.104.073395 [pii] (2005).

73 Fojo, T. & Bates, S. Strategies for reversing drug resistance. *Oncogene* **22**, 7512-7523, doi:10.1038/sj.onc.1206951
1206951 [pii] (2003).

74 Borst, P., Evers, R., Kool, M. & Wijnholds, J. A family of drug transporters: the multidrug resistance-associated proteins. *J Natl Cancer Inst* **92**, 1295-1302 (2000).

75 Chaney, S. G., Campbell, S. L., Bassett, E. & Wu, Y. Recognition and processing of cisplatin- and oxaliplatin-DNA adducts. *Crit Rev Oncol Hematol* **53**, 3-11, doi:S1040-8428(04)00162-3 [pii]
10.1016/j.critrevonc.2004.08.008 (2005).

76 Fink, D. *et al.* The role of DNA mismatch repair in platinum drug resistance. *Cancer Res* **56**, 4881-4886 (1996).

77 Meharg, A. A. *Venomous earth : how arsenic caused the world's worst mass poisoning*. (Macmillan, 2005).

78 Wolfe-Simon, F. *et al.* A Bacterium That Can Grow by Using Arsenic Instead of Phosphorus. *Science*, doi:science.1197258 [pii]
10.1126/science.1197258 (2010).

79 Davies, P. C. W. *et al.* Signatures of a Shadow Biosphere. *Astrobiology* **9**, 241-249, doi:DOI 10.1089/ast.2008.0251 (2009).

80 Waxman, S. & Anderson, K. C. History of the development of arsenic derivatives in cancer therapy. *Oncologist* **6 Suppl 2**, 3-10 (2001).

81 <www.iupac.org> (

82 Frankenberger, W. T. *Environmental chemistry of arsenic*. (Marcel Dekker, 2002).

83 Henke, K. R. *Arsenic : environmental chemistry, health threats, and waste treatment*. (Wiley, 2009).

84 Nriagu, J. O. *Arsenic in the environment*. (Wiley, 1994).

85 Aronson, S. M. Arsenic and old myths. *R I Med* **77**, 233-234 (1994).

86 Nriagu, J. O. *Arsenic in the environment*. (Wiley, 1994).

87 Azcue, J. M., Nriagu, J. O. & Schiff, S. Role of Sediment Porewater in the Cycling of Arsenic in a Mine-Polluted Lake. *Environ Int* **20**, 517-527 (1994).

88 Lugli, A. *et al.* The medical mystery of Napoleon Bonaparte: an interdisciplinary expose. *Adv Anat Pathol* **18**, 152-158, doi:10.1097/PAP.0b013e31820ca329 00125480-201103000-00004 [pii] (2011).

89 Nations, G. o. B. U. (Government of Bangladesh & United Nations, 2010).

90 Saha, K. C. Melanokeratosis from arsenic contaminated tubewell water. *Indian J Dermatol* **29**, 37-46 (1984).

91 Porosnicu, M. *et al.* Co-treatment with As2O3 enhances selective cytotoxic effects of STI-571 against Brc-Abl-positive acute leukemia cells. *Leukemia* **15**, 772-778 (2001).

92 Guha Mazumder, D. N. *et al.* Chronic arsenic toxicity from drinking tubewell water in rural West Bengal. *Bull World Health Organ* **66**, 499-506 (1988).

93 Smith, A. H., Lingas, E. O. & Rahman, M. Contamination of drinking-water by arsenic in Bangladesh: a public health emergency. *Bull World Health Organ* **78**, 1093-1103 (2000).

94 Kapaj, S., Peterson, H., Liber, K. & Bhattacharya, P. Human health effects from chronic arsenic poisoning--a review. *J Environ Sci Health A Tox Hazard Subst Environ Eng* **41**, 2399-2428, doi:V525102618555865 [pii] 10.1080/10934520600873571 (2006).

95 Tokar, E. J., Qu, W. & Waalkes, M. P. Arsenic, stem cells, and the developmental basis of adult cancer. *Toxicol Sci* **120 Suppl 1**, S192-203, doi:kfq342 [pii] 10.1093/toxsci/kfq342 (2011).

96 Bode, A. M. & Dong, Z. The paradox of arsenic: molecular mechanisms of cell transformation and chemotherapeutic effects. *Crit Rev Oncol Hematol* **42**, 5-24, doi:S1040842801002153 [pii] (2002).

97 Huang, M. *et al.* Risk assessment of low-level cadmium and arsenic on the kidney. *J Toxicol Environ Health A* **72**, 1493-1498, doi:916457084 [pii] 10.1080/15287390903213095 (2009).

98 Guha Mazumder, D. N. Arsenic and non-malignant lung disease. *J Environ Sci Health A Tox Hazard Subst Environ Eng* **42**, 1859-1867, doi:783095615 [pii] 10.1080/10934520701566926 (2007).

99 Saha, K. C. Diagnosis of arsenicosis. *J Environ Sci Health A Tox Hazard Subst Environ Eng* **38**, 255-272 (2003).

100 Haque, R. *et al.* Arsenic in drinking water and skin lesions: dose-response data from West Bengal, India. *Epidemiology* **14**, 174-182, doi:10.1097/01.EDE.0000040361.55051.54 (2003).

101 Steinmaus, C., Yuan, Y., Bates, M. N. & Smith, A. H. Case-control study of bladder cancer and drinking water arsenic in the western United States. *Am J Epidemiol* **158**, 1193-1201 (2003).

102 Chen, C. L. *et al.* Ingested arsenic, cigarette smoking, and lung cancer risk: a follow-up study in arseniasis-endemic areas in Taiwan. *JAMA* **292**, 2984-2990, doi:292/24/2984 [pii] 10.1001/jama.292.24.2984 (2004).

103 Tsai, S. Y., Chou, H. Y., The, H. W., Chen, C. M. & Chen, C. J. The effects of chronic arsenic exposure from drinking water on the neurobehavioral development in adolescence. *Neurotoxicology* **24**, 747-753, doi:S0161-813X(03)00029-9 [pii] 10.1016/S0161-813X(03)00029-9 (2003).

104 Baker, B. A., Topliff, A. R., Messing, R. B., Durkin, D. & Johnson, J. S. Persistent neuropathy and hyperkeratosis from distant arsenic exposure. *J Agromedicine* **10**, 43-54 (2005).

105 Mukherjee, S. C. *et al.* Neuropathy in arsenic toxicity from groundwater arsenic contamination in West Bengal, India. *J Environ Sci Health A Tox Hazard Subst Environ Eng* **38**, 165-183 (2003).

106 Hopenhayn, C. *et al.* Arsenic exposure from drinking water and birth weight. *Epidemiology* **14**, 593-602, doi:10.1097/01.ede.0000072104.65240.69 (2003).

107 Jones, M. R., Tellez-Plaza, M., Sharrett, A. R., Guallar, E. & Navas-Acien, A. Urine arsenic and hypertension in US adults: the 2003-2008 National Health and Nutrition Examination Survey. *Epidemiology* **22**, 153-161, doi:10.1097/EDE.0b013e318207fdf2 (2011).

108 Milton, A. H., Hasan, Z., Rahman, A. & Rahman, M. Non-cancer effects of chronic arsenicosis in Bangladesh: preliminary results. *J Environ Sci Health A Tox Hazard Subst Environ Eng* **38**, 301-305 (2003).

109 Diaz-Villasenor, A., Burns, A. L., Hiriart, M., Cebrian, M. E. & Ostrosky-Wegman, P. Arsenic-induced alteration in the expression of genes related to type 2 diabetes mellitus. *Toxicol Appl Pharmacol* **225**, 123-133, doi:S0041-008X(07)00380-8 [pii]
10.1016/j.taap.2007.08.019 (2007).

110 Zhu, J., Chen, Z., Lallemand-Breitenbach, V. & de The, H. How acute promyelocytic leukaemia revived arsenic. *Nat Rev Cancer* **2**, 705-713, doi:Doi 10.1038/Nrc887 (2002).

111 Kwong, Y. L. & Todd, D. Delicious poison: arsenic trioxide for the treatment of leukemia. *Blood* **89**, 3487-3488 (1997).

112 Chan, P. C. & Huff, J. Arsenic carcinogenesis in animals and in humans: Mechanistic, experimental, and epidemiological evidence. *Environ Carcin Eco R* **15**, 83-122 (1997).

113 Forkner, C. E. & Scott, T. T. M. Arsenic as a therapeutic agent in chronic myelogenous leukemia - Preliminary report. *J Amer Med Assoc* **97**, 0003-0005 (1931).

114 Duan, X. M., Xu, J. S. & Xin, X. M. [Anti-tumor effects of ailing-1 on human megakaryoblastic leukemia cells]. *Zhongguo Zhong Xi Yi Jie He Za Zhi* **17**, 97-98 (1997).

115 de The, H. & Chen, Z. Acute promyelocytic leukaemia: novel insights into the mechanisms of cure. *Nat Rev Cancer* **10**, 775-783, doi:nrc2943 [pii]
10.1038/nrc2943 (2010).

116 Soignet, S. L. *et al.* Complete remission after treatment of acute promyelocytic leukemia with arsenic trioxide. *N Engl J Med* **339**, 1341-1348, doi:10.1056/NEJM199811053391901 (1998).

117 Soignet, S. L. *et al.* United States multicenter study of arsenic trioxide in relapsed acute promyelocytic leukemia. *J Clin Oncol* **19**, 3852-3860 (2001).

118 Devesa, V. *et al.* Comprehensive analysis of arsenic metabolites by pH-specific hydride generation atomic absorption spectrometry. *J Anal Atom Spectrom* **19**, 1460-1467, doi:10.1039/b407388f (2004).

119 Drobna, Z. *et al.* Metabolism of arsenic in human liver: the role of membrane transporters. *Arch Toxicol* **84**, 3-16, doi:10.1007/s00204-009-0499-7 (2010).

120 Thomas, D. J. Unraveling arsenic--glutathione connections. *Toxicol Sci* **107**, 309-311, doi:kfn257 [pii]
10.1093/toxsci/kfn257 (2009).

121 Jungwirth, U. *et al.* Anticancer Activity of Metal Complexes: Involvement of Redox Processes. *Antioxid Redox Signal*, doi:10.1089/ars.2010.3663 (2011).

122 Dean, M., Hamon, Y. & Chimini, G. The human ATP-binding cassette (ABC) transporter superfamily. *J Lipid Res* **42**, 1007-1017 (2001).

123 Salerno, M., Petroutsa, M. & Garnier-Suillerot, A. The MRP1-mediated effluxes of arsenic and antimony do not require arsenic-glutathione and antimony-glutathione complex formation. *J Bioenerg Biomembr* **34**, 135-145 (2002).

124 Vernhet, L., Allain, N., Bardiau, C., Anger, J. P. & Fardel, O. Differential sensitivities of MRP1-overexpressing lung tumor cells to cytotoxic metals. *Toxicology* **142**, 127-134 (2000).

125 Leslie, E. M., Haimeur, A. & Waalkes, M. P. Arsenic transport by the human multidrug resistance protein 1 (MRP1/ABCC1). Evidence that a tri-glutathione conjugate is required. *J Biol Chem* **279**, 32700-32708, doi:10.1074/jbc.M404912200 M404912200 [pii] (2004).

126 Lazo, G. *et al.* Use of arsenic trioxide (As2O3) in the treatment of acute promyelocytic leukemia (APL). The MD Anderson experience. *Blood* **98**, 595a-596a (2001).

127 Zhang, P. The use of arsenic trioxide (As2O3) in the treatment of acute promyelocytic leukemia. *J Biol Reg Homeos Ag* **13**, 195-200 (1999).

128 Chen, G. Q. *et al.* Use of arsenic trioxide (As2O3) in the treatment of acute promyelocytic leukemia (APL) .1. As2O3 exerts dose-dependent dual effects on APL cells. *Blood* **89**, 3345-3353 (1997).

129 Faber, J. & Armstrong, S. A. Mixed lineage leukemia translocations and a leukemia stem cell program. *Cancer Res* **67**, 8425-8428, doi:67/18/8425 [pii] 10.1158/0008-5472.CAN-07-0972 (2007).

130 Zhu, J. *et al.* Arsenic-induced PML targeting onto nuclear bodies: implications for the treatment of acute promyelocytic leukemia. *Proc Natl Acad Sci U S A* **94**, 3978-3983 (1997).

131 Kinjo, K. *et al.* Arsenic trioxide (As2O3)-induced apoptosis and differentiation in retinoic acid-resistant acute promyelocytic leukemia model in hGM-CSF-producing transgenic SCID mice. *Leukemia* **14**, 431-438 (2000).

132 Lallemand-Breitenbach, V. *et al.* Retinoic acid and arsenic synergize to eradicate leukemic cells in a mouse model of acute promyelocytic leukemia. *J Exp Med* **189**, 1043-1052 (1999).

133 Lin, R. J. *et al.* Role of the histone deacetylase complex in acute promyelocytic leukaemia. *Nature* **391**, 811-814, doi:10.1038/35895 (1998).

134 Grignani, F. *et al.* The acute promyelocytic leukemia-specific PML-RAR alpha fusion protein inhibits differentiation and promotes survival of myeloid precursor cells. *Cell* **74**, 423-431, doi:0092-8674(93)80044-F [pii] (1993).

135 Raelson, J. V. *et al.* The PML/RAR alpha oncoprotein is a direct molecular target of retinoic acid in acute promyelocytic leukemia cells. *Blood* **88**, 2826-2832 (1996).

136 Nervi, C. *et al.* Caspases mediate retinoic acid-induced degradation of the acute promyelocytic leukemia PML/RARalpha fusion protein. *Blood* **92**, 2244-2251 (1998).

137 Tallman, M. S. Arsenic trioxide: its role in acute promyelocytic leukemia and potential in other hematologic malignancies. *Blood Rev* **15**, 133-142, doi:10.1054/blre.2001.0160 S0268-960X(01)90160-2 [pii] (2001).

138 Lallemand-Breitenbach, V. *et al.* Role of promyelocytic leukemia (PML) sumolation in nuclear body formation, 11S proteasome recruitment, and As2O3-induced PML or PML/retinoic acid receptor alpha degradation. *J Exp Med* **193**, 1361-1371 (2001).

139 Muller, S., Matunis, M. J. & Dejean, A. Conjugation with the ubiquitin-related modifier SUMO-1 regulates the partitioning of PML within the nucleus. *EMBO J* **17**, 61-70, doi:10.1093/emboj/17.1.61 (1998).

140 Shen, T. H., Lin, H. K., Scaglioni, P. P., Yung, T. M. & Pandolfi, P. P. The mechanisms of PML-nuclear body formation. *Mol Cell* **24**, 331-339, doi:S1097-2765(06)00661-7 [pii] 10.1016/j.molcel.2006.09.013 (2006).

141 Miller, W. H., Jr., Schipper, H. M., Lee, J. S., Singer, J. & Waxman, S. Mechanisms of action of arsenic trioxide. *Cancer Res* **62**, 3893-3903 (2002).

142 Guo, A. *et al.* The function of PML in p53-dependent apoptosis. *Nat Cell Biol* **2**, 730-736, doi:10.1038/35036365 (2000).

143 Yedjou, C. G. & Tchounwou, P. B. Modulation of p53, c-fos, RARE, cyclin A, and cyclin D1 expression in human leukemia (HL-60) cells exposed to arsenic trioxide. *Mol Cell Biochem* **331**, 207-214, doi:10.1007/s11010-009-0160-z (2009).

144 Yoda, A. *et al.* Arsenic trioxide augments Chk2/p53-mediated apoptosis by inhibiting oncogenic Wip1 phosphatase. *J Biol Chem* **283**, 18969-18979, doi:M800560200 [pii] 10.1074/jbc.M800560200 (2008).

145 Kim, Y. J. *et al.* Arsenic trioxide-induced apoptosis in TM4 Sertoli cells: The potential involvement of p21 expression and p53 phosphorylation. *Toxicology* **285**, 142-151, doi:S0300-483X(11)00163-6 [pii]
10.1016/j.tox.2011.04.013 (2011).

146 Zhao, S., Zhang, J., Zhang, X., Dong, X. & Sun, X. Arsenic trioxide induces different gene expression profiles of genes related to growth and apoptosis in glioma cells dependent on the p53 status. *Mol Biol Rep* **35**, 421-429, doi:10.1007/s11033-007-9102-6 (2008).

147 Shen, L. *et al.* As2O3 induces apoptosis of the human B lymphoma cell line MBC-1. *J Biol Regul Homeost Agents* **14**, 116-119 (2000).

148 Hamadeh, H. K., Vargas, M., Lee, E. & Menzel, D. B. Arsenic disrupts cellular levels of p53 and mdm2: a potential mechanism of carcinogenesis. *Biochem Biophys Res Commun* **263**, 446-449, doi:10.1006/bbrc.1999.1395
S0006-291X(99)91395-5 [pii] (1999).

149 Huang, C., Ma, W. Y., Li, J. & Dong, Z. Arsenic induces apoptosis through a c-Jun NH2-terminal kinase-dependent, p53-independent pathway. *Cancer Res* **59**, 3053-3058 (1999).

150 Carney, D. A. Arsenic trioxide mechanisms of action--looking beyond acute promyelocytic leukemia. *Leuk Lymphoma* **49**, 1846-1851, doi:904755977 [pii]
10.1080/10428190802464745 (2008).

151 Emadi, A. & Gore, S. D. Arsenic trioxide - An old drug rediscovered. *Blood Rev* **24**, 191-199, doi:S0268-960X(10)00022-6 [pii]
10.1016/j.blre.2010.04.001.

152 Chou, W. C. *et al.* Role of NADPH oxidase in arsenic-induced reactive oxygen species formation and cytotoxicity in myeloid leukemia cells. *Proc Natl Acad Sci U S A* **101**, 4578-4583, doi:10.1073/pnas.0306687101
0306687101 [pii] (2004).

153 Drobna, Z., Styblo, M. & Thomas, D. An Overview of Arsenic Metabolism and Toxicity. *Current Protocols*, doi:10.1002/0471140856.tx0431s42 (2009).

154 Chen, M. J., Yang, P. Y., Ye, Y. Z., Hu, D. N. & Chen, M. F. Arsenic trioxide induces apoptosis in uveal melanoma cells through the mitochondrial pathway. *Am J Chin Med* **38**, 1131-1142, doi:S0192415X10008524 [pii] (2010).

155 Emadi, A. & Gore, S. D. Arsenic trioxide - An old drug rediscovered. *Blood Rev* **24**, 191-199, doi:S0268-960X(10)00022-6 [pii]
10.1016/j.blre.2010.04.001 (2010).

156 McBride, H. M., Neuspiel, M. & Wasiak, S. Mitochondria: More than just a powerhouse. *Curr Biol* **16**, R551-R560, doi:10.1016/j.cub.2006.06.054 (2006).

157 Qin, D. Y., Huang, R. & Wu, T. In vitro arsenic trioxide induces apoptosis in T cells of asthmatic patients by a Bcl-2 related mechanism. *Yao Xue Xue Bao* **43**, 35-43 (2008).

158 Akao, Y. *et al.* Arsenic induces apoptosis in B-cell leukaemic cell lines in vitro: activation of caspases and down-regulation of Bcl-2 protein. *Br J Haematol* **102**, 1055-1060 (1998).

159 Wang, Z. G. *et al.* Arsenic trioxide and melarsoprol induce programmed cell death in myeloid leukemia cell lines and function in a PML and PML-RARalpha independent manner. *Blood* **92**, 1497-1504 (1998).

160 Hideshima, T. *et al.* NF-kappa B as a therapeutic target in multiple myeloma. *Journal of Biological Chemistry* **277**, 16639-16647, doi:10.1074/jbc.M200360200 (2002).

161 Chen, F., Castranova, V., Shi, X. L. & Demers, L. M. New insights into the role of nuclear factor-kappa B, a ubiquitous transcription factor in the initiation of diseases. *Clin Chem* **45**, 7-17 (1999).

162 Mattson, M. P., Culmsee, C., Yu, Z. & Camandola, S. Roles of nuclear factor kappaB in neuronal survival and plasticity. *J Neurochem* **74**, 443-456 (2000).

163 Lemarie, A. *et al.* Arsenic trioxide induces apoptosis of human monocytes during macrophagic differentiation through nuclear factor-kappaB-related survival pathway down-regulation. *J Pharmacol Exp Ther* **316**, 304-314, doi:jpet.105.092874 [pii]
10.1124/jpet.105.092874 (2006).

164 Roussel, R. R. & Barchowsky, A. Arsenic inhibits NF-kappaB-mediated gene transcription by blocking IkappaB kinase activity and IkappaBalpha phosphorylation and degradation. *Arch Biochem Biophys* **377**, 204-212, doi:10.1006/abbi.2000.1770 S0003-9861(00)91770-3 [pii] (2000).

165 Hess, J., Angel, P. & Schorpp-Kistner, M. AP-1 subunits: quarrel and harmony among siblings. *J Cell Sci* **117**, 5965-5973, doi:10.1242/jcs.01589 (2004).

166 Ameyar, M., Wisniewska, M. & Weitzman, J. B. A role for AP-1 in apoptosis: the case for and against. *Biochimie* **85**, 747-752, doi:S0300908403001524 [pii] (2003).

167 Dong, Z., Birrer, M. J., Watts, R. G., Matrisian, L. M. & Colburn, N. H. Blocking of tumor promoter-induced AP-1 activity inhibits induced transformation in JB6 mouse epidermal cells. *Proc Natl Acad Sci U S A* **91**, 609-613 (1994).

168 Dong, Z., Watts, R., Sun, Y., Zhan, S. & Colburn, N. Progressive elevation of ap-1 activity during preneoplastic-to-neoplastic progression as modeled in mouse jb6 cell variants. *Int J Oncol* **7**, 359-364 (1995).

169 Hu, Y., Jin, X. & Snow, E. T. Effect of arsenic on transcription factor AP-1 and NF-kappaB DNA binding activity and related gene expression. *Toxicol Lett* **133**, 33-45, doi:S0378427402000838 [pii] (2002).

170 Simeonova, P. P. *et al.* Arsenic mediates cell proliferation and gene expression in the bladder epithelium: association with activating protein-1 transactivation. *Cancer Res* **60**, 3445-3453 (2000).

171 Cavigelli, M. *et al.* The tumor promoter arsenite stimulates AP-1 activity by inhibiting a JNK phosphatase. *EMBO J* **15**, 6269-6279 (1996).

172 Lim, Y. & Matsui, W. Hedgehog signaling in hematopoiesis. *Crit Rev Eukaryot Gene Expr* **20**, 129-139, doi:4755276625828a95,0d2b29cf60372388 [pii] (2010).

173 Hofmann, I. *et al.* Hedgehog signaling is dispensable for adult murine hematopoietic stem cell function and hematopoiesis. *Cell Stem Cell* **4**, 559-567, doi:S1934-5909(09)00152-0 [pii] 10.1016/j.stem.2009.03.016 (2009).

174 Kim, B. M. & Choi, M. Y. New insights into the role of Hedgehog signaling in gastrointestinal development and cancer. *Gastroenterology* **137**, 422-424, doi:S0016-5085(09)00990-1 [pii] 10.1053/j.gastro.2009.06.021 (2009).

175 Jiang, J. & Hui, C. C. Hedgehog signaling in development and cancer. *Dev Cell* **15**, 801-812, doi:S1534-5807(08)00484-X [pii] 10.1016/j.devcel.2008.11.010 (2008).

176 Ruiz i Altaba, A. Gli proteins and Hedgehog signaling: development and cancer. *Trends Genet* **15**, 418-425, doi:S0168-9525(99)01840-5 [pii] (1999).

177 Beauchamp, E. M. *et al.* Arsenic trioxide inhibits human cancer cell growth and tumor development in mice by blocking Hedgehog/GLI pathway. *J Clin Invest* **121**, 148-160, doi:42874 [pii] 10.1172/JCI42874 (2011).

178 Kim, J., Lee, J. J., Gardner, D. & Beachy, P. A. Arsenic antagonizes the Hedgehog pathway by preventing ciliary accumulation and reducing stability of the Gli2 transcriptional effector. *Proc Natl Acad Sci U S A* **107**, 13432-13437, doi:1006822107 [pii] 10.1073/pnas.1006822107 (2010).

179 Raju, G. P. Arsenic: a potentially useful poison for Hedgehog-driven cancers. *J Clin Invest* **121**, 14-16, doi:45692 [pii] 10.1172/JCI45692 (2011).

180 Li, Y. M. & Broome, J. D. Arsenic targets tubulins to induce apoptosis in myeloid leukemia cells. *Cancer Res* **59**, 776-780 (1999).

181 Roboz, G. J. *et al.* Arsenic trioxide induces dose- and time-dependent apoptosis of endothelium and may exert an antileukemic effect via inhibition of angiogenesis. *Blood* **96**, 1525-1530 (2000).

182 Sibilia, M. *et al.* The epidermal growth factor receptor: from development to tumorigenesis. *Differentiation* **75**, 770-787, doi:S0301-4681(09)60170-5 [pii]

10.1111/j.1432-0436.2007.00238.x (2007).
183 Gazdar, A. F. Epidermal growth factor receptor inhibition in lung cancer: the evolving role of individualized therapy. *Cancer Metastasis Rev* **29**, 37-48, doi:10.1007/s10555-010-9201-z (2010).
184 Guiu, S., Coudert, B., Favier, L., Arnould, L. & Fumoleau, P. [Management of metastatic HER2-positive breast cancer: present and future]. *Bull Cancer* **97**, 365-383, doi:bdc.2010.1040 [pii] 10.1684/bdc.2010.1040 (2010).
185 Schlessinger, J. Ligand-induced, receptor-mediated dimerization and activation of EGF receptor. *Cell* **110**, 669-672, doi:S0092867402009662 [pii] (2002).
186 Stover, D. R., Becker, M., Liebetanz, J. & Lydon, N. B. Src Phosphorylation of the Epidermal Growth-Factor Receptor at Novel Sites Mediates Receptor Interaction with Src and P85-Alpha. *Journal of Biological Chemistry* **270**, 15591-15597 (1995).
187 Jorissen, R. N. *et al.* Epidermal growth factor receptor: mechanisms of activation and signalling. *Exp Cell Res* **284**, 31-53, doi:S0014482702000988 [pii] (2003).
188 Quesnelle, K. M., Boehm, A. L. & Grandis, J. R. STAT-mediated EGFR signaling in cancer. *J Cell Biochem* **102**, 311-319, doi:10.1002/jcb.21475 (2007).
189 Silva, C. M. Role of STATs as downstream signal transducers in Src family kinase-mediated tumorigenesis. *Oncogene* **23**, 8017-8023, doi:10.1038/sj.onc.1208159 (2004).
190 Quinlan, M. P. & Settleman, J. Isoform-specific ras functions in development and cancer. *Future Oncol* **5**, 105-116, doi:10.2217/14796694.5.1.105 (2009).
191 Vanhaesebroeck, B. & Alessi, D. R. The PI3K-PDK1 connection: more than just a road to PKB. *Biochem J* **346 Pt 3**, 561-576 (2000).
192 Dowling, R. J., Topisirovic, I., Fonseca, B. D. & Sonenberg, N. Dissecting the role of mTOR: lessons from mTOR inhibitors. *Biochim Biophys Acta* **1804**, 433-439, doi:S1570-9639(09)00359-8 [pii] 10.1016/j.bbapap.2009.12.001 (2010).
193 Dunlop, E. A. & Tee, A. R. Mammalian target of rapamycin complex 1: signalling inputs, substrates and feedback mechanisms. *Cell Signal* **21**, 827-835, doi:S0898-6568(09)00016-3 [pii] 10.1016/j.cellsig.2009.01.012 (2009).
194 Eblin, K. E., Bredfeldt, T. G., Buffington, S. & Gandolfi, A. J. Mitogenic signal transduction caused by monomethylarsonous acid in human bladder cells: role in arsenic-induced carcinogenesis. *Toxicol Sci* **95**, 321-330, doi:kfl160 [pii] 10.1093/toxsci/kfl160 (2007).
195 Simeonova, P. P., Wang, S., Hulderman, T. & Luster, M. I. c-Src-dependent activation of the epidermal growth factor receptor and mitogen-activated protein kinase pathway by arsenic. Role in carcinogenesis. *J Biol Chem* **277**, 2945-2950, doi:10.1074/jbc.M109136200 M109136200 [pii] (2002).
196 Qian, Y., Castranova, V. & Shi, X. New perspectives in arsenic-induced cell signal transduction. *J Inorg Biochem* **96**, 271-278, doi:S0162013403002356 [pii] (2003).
197 Eguchi, R. *et al.* Arsenic trioxide induces apoptosis through JNK and ERK in human mesothelioma cells. *J Cell Physiol* **226**, 762-768, doi:10.1002/jcp.22397 (2011).
198 Yingchun, L. *et al.* E3 ubiquitin ligase Cbl-b potentiates the apoptotic action of arsenic trioxide by inhibiting the PI3K/Akt pathway. *Braz J Med Biol Res* **44**, 105-111, doi:S0100-879X2010007500142 [pii] (2011).
199 Rocha-Lima, C. M., Soares, H. P., Raez, L. E. & Singal, R. EGFR targeting of solid tumors. *Cancer Control* **14**, 295-304 (2007).
200 Sharma, S. V., Bell, D. W., Settleman, J. & Haber, D. A. Epidermal growth factor receptor mutations in lung cancer. *Nat Rev Cancer* **7**, 169-181, doi:nrc2088 [pii] 10.1038/nrc2088 (2007).
201 Giaccone, G. *et al.* Gefitinib in combination with gemcitabine and cisplatin in advanced non-small-cell lung cancer: a phase III trial--INTACT 1. *J Clin Oncol* **22**, 777-784, doi:10.1200/JCO.2004.08.001

JCO.2004.08.001 [pii] (2004).

202 Herbst, R. S. *et al.* Gefitinib in combination with paclitaxel and carboplatin in advanced non-small-cell lung cancer: a phase III trial--INTACT 2. *J Clin Oncol* **22**, 785-794, doi:10.1200/JCO.2004.07.215
JCO.2004.07.215 [pii] (2004).

203 Thatcher, N. *et al.* Gefitinib plus best supportive care in previously treated patients with refractory advanced non-small-cell lung cancer: results from a randomised, placebo-controlled, multicentre study (Iressa Survival Evaluation in Lung Cancer). *Lancet* **366**, 1527-1537, doi:S0140-6736(05)67625-8 [pii]
10.1016/S0140-6736(05)67625-8 (2005).

204 Yang, C. H. *et al.* Final Overall Survival (Os) Results from a Phase Iii, Randomised, Open-Label, First-Line Study of Gefitinib (G) V Carboplatin/Paclitaxel (C/P) in Clinically Selected Patients with Advanced Non-Small Cell Lung Cancer (Nsclc) in Asia (Ipass). *Annals of Oncology* **21**, 1-2 (2010).

205 Mok, T. S. *et al.* Gefitinib or Carboplatin-Paclitaxel in Pulmonary Adenocarcinoma. *New Engl J Med* **361**, 947-957, doi:Doi 10.1056/Nejmoa0810699 (2009).

206 Lee, D. H. *et al.* Randomized Phase III trial of gefitinib versus docetaxel in non-small cell lung cancer patients who have previously received platinum-based chemotherapy. *Clin Cancer Res* **16**, 1307-1314, doi:1078-0432.CCR-09-1903 [pii]
10.1158/1078-0432.CCR-09-1903 (2010).

207 Gazdar, A. F. Epidermal growth factor receptor inhibition in lung cancer: the evolving role of individualized therapy. *Cancer Metastasis Rev* **29**, 37-48, doi:10.1007/s10555-010-9201-z.

208 Stamos, J., Sliwkowski, M. X. & Eigenbrot, C. Structure of the epidermal growth factor receptor kinase domain alone and in complex with a 4-anilinoquinazoline inhibitor. *J Biol Chem* **277**, 46265-46272, doi:10.1074/jbc.M207135200
M207135200 [pii] (2002).

209 Pao, W. *et al.* Acquired resistance of lung adenocarcinomas to gefitinib or erlotinib is associated with a second mutation in the EGFR kinase domain. *PLoS Med* **2**, e73, doi:05-PLME-RA-0027R1 [pii]
10.1371/journal.pmed.0020073 (2005).

210 Daub, H., Specht, K. & Ullrich, A. Strategies to overcome resistance to targeted protein kinase inhibitors. *Nat Rev Drug Discov* **3**, 1001-1010, doi:nrd1579 [pii]
10.1038/nrd1579 (2004).

211 Godin-Heymann, N. *et al.* Oncogenic activity of epidermal growth factor receptor kinase mutant alleles is enhanced by the T790M drug resistance mutation. *Cancer Res* **67**, 7319-7326, doi:67/15/7319 [pii]
10.1158/0008-5472.CAN-06-4625 (2007).

212 Pao, W. *et al.* KRAS mutations and primary resistance of lung adenocarcinomas to gefitinib or erlotinib. *PLoS Med* **2**, e17, doi:04-PLME-RA-0242R1 [pii]
10.1371/journal.pmed.0020017 (2005).

213 Zucali, P. A. *et al.* Role of cMET expression in non-small-cell lung cancer patients treated with EGFR tyrosine kinase inhibitors. *Ann Oncol* **19**, 1605-1612, doi:mdn240 [pii]
10.1093/annonc/mdn240 (2008).

214 Rho, J. K. *et al.* The role of MET activation in determining the sensitivity to epidermal growth factor receptor tyrosine kinase inhibitors. *Mol Cancer Res* **7**, 1736-1743, doi:1541-7786.MCR-08-0504 [pii]
10.1158/1541-7786.MCR-08-0504 (2009).

215 Izdebska, M., Grzanka, A., Szczepanski, M. A. & Litwiniec, A. [Selected mechanisms of the therapeutic effect of arsenic trioxide in cancer treatment]. *Postepy Hig Med Dosw (Online)* **62**, 463-467, doi:868643 [pii] (2008).

216 Campbell, R. A. *et al.* Antimyeloma effects of arsenic trioxide are enhanced by melphalan, bortezomib and ascorbic acid. *Br J Haematol* **138**, 467-478, doi:BJH6675 [pii]
10.1111/j.1365-2141.2007.06675.x (2007).

217 Fischer, H. *et al.* Fibroblast growth factor receptor-mediated signals contribute to the malignant phenotype of non-small cell lung cancer cells: therapeutic implications and synergism with epidermal growth factor receptor inhibition. *Mol Cancer Ther* **7**, 3408-3419, doi:7/10/3408 [pii]
10.1158/1535-7163.MCT-08-0444 (2008).

218 Burris, H. A., 3rd. Dual kinase inhibition in the treatment of breast cancer: initial experience with the EGFR/ErbB-2 inhibitor lapatinib. *Oncologist* **9 Suppl 3**, 10-15 (2004).

219 Wilhelm, S. M. *et al.* BAY 43-9006 exhibits broad spectrum oral antitumor activity and targets the RAF/MEK/ERK pathway and receptor tyrosine kinases involved in tumor progression and angiogenesis. *Cancer Res* **64**, 7099-7109, doi:64/19/7099 [pii]
10.1158/0008-5472.CAN-04-1443 (2004).

220 Atil, B. Molecular determinants of the Anti-Cancer Activity of Ruthenium Compound KP1339. (2010).

221 Kobayashi, S. *et al.* EGFR mutation and resistance of non-small-cell lung cancer to gefitinib. *N Engl J Med* **352**, 786-792, doi:352/8/786 [pii]
10.1056/NEJMoa044238 (2005).

222 Trujillo, J. I. MEK inhibitors: a patent review 2008 - 2010. *Expert Opin Ther Pat* **21**, 1045-1069, doi:10.1517/13543776.2011.577068 (2011).

223 Shi, Y. & Gaestel, M. In the cellular garden of forking paths: how p38 MAPKs signal for downstream assistance. *Biol Chem* **383**, 1519-1536, doi:10.1515/BC.2002.173 (2002).

224 Chen, Y., Wang, B. C. & Xiao, Y. PI3K: A potential therapeutic target for cancer. *J Cell Physiol*, doi:10.1002/jcp.23038 (2011).

225 Trusolino, L., Bertotti, A. & Comoglio, P. M. MET signalling: principles and functions in development, organ regeneration and cancer. *Nat Rev Mol Cell Bio* **11**, 834-848, doi:Doi 10.1038/Nrm3012 (2010).

226 Kosaka, T., Yamaki, E., Mogi, A. & Kuwano, H. Mechanisms of Resistance to EGFR TKIs and Development of a New Generation of Drugs in Non-Small-Cell Lung Cancer. *J Biomed Biotechnol*, doi:Artn 165214
Doi 10.1155/2011/165214 (2011).

227 Benedettini, E. *et al.* Met activation in non-small cell lung cancer is associated with de novo resistance to EGFR inhibitors and the development of brain metastasis. *Am J Pathol* **177**, 415-423, doi:S0002-9440(10)60096-X [pii]
10.2353/ajpath.2010.090863 (2010).

228 Vernhet, L. *et al.* Resistance of human multidrug resistance-associated protein 1-overexpressing lung tumor cells to the anticancer drug arsenic trioxide. *Biochem Pharmacol* **61**, 1387-1391, doi:S0006-2952(01)00606-2 [pii] (2001).

229 Colabufo, N. A. *et al.* EGFR tyrosine kinase inhibitors and multidrug resistance: perspectives. *Front Biosci* **16**, 1811-1823, doi:3823 [pii] (2011).

230 Shi, Z. *et al.* Erlotinib (Tarceva, OSI-774) antagonizes ATP-binding cassette subfamily B member 1 and ATP-binding cassette subfamily G member 2-mediated drug resistance. *Cancer Res* **67**, 11012-11020, doi:67/22/11012 [pii]
10.1158/0008-5472.CAN-07-2686 (2007).

231 Kuhne, A. *et al.* Influx and efflux transport as determinants of melphalan cytotoxicity: Resistance to melphalan in MDR1 overexpressing tumor cell lines. *Biochemical Pharmacology* **78**, 45-53, doi:DOI 10.1016/j.bcp.2009.03.026 (2009).

232 Konsoula, Z. & Jung, M. Involvement of P-glycoprotein and Multidrug Resistance Associated Protein 1 on the Transepithelial Transport of a Mercaptoacetamide-Based Histone-Deacetylase Inhibitor in Caco-2 Cells. *Biol Pharm Bull* **32**, 74-78 (2009).

233 Antman, K. H. Introduction: the history of arsenic trioxide in cancer therapy. *Oncologist* **6 Suppl 2**, 1-2 (2001).

234 Jungwirth, U. *et al.* Anticancer activity of metal complexes: involvement of redox processes. *Antioxid Redox Signal* **15**, 1085-1127, doi:10.1089/ars.2010.3663.

235 Takahashi, S. Combination therapy with arsenic trioxide for hematological malignancies. *Anticancer Agents Med Chem* **10**, 504-510, doi:BSP/ACAMC/E-Pub/ 00081 [pii].

236 Liu, Z. M. & Huang, H. S. As2O3-induced c-Src/EGFR/ERK signaling is via Sp1 binding sites to stimulate p21(WAF1/CIP1) expression in human epidermoid carcinoma A431 cells. *Cellular Signalling* **18**, 244-255, doi:DOI 10.1016/j.cellsig.2005.04.006 (2006).

237 Noh, E. K. *et al.* Gefitinib enhances arsenic trioxide (AS2O3)-induced differentiation of acute promyelocytic leukemia cell line. *Leuk Res* **34**, 1501-1505, doi:S0145-2126(10)00097-4 [pii] 10.1016/j.leukres.2010.02.016 (2010).

238 Liu, L., Chen, B. A. & Qin, S. K. [Anti-angiogenesis effect of arsenic trioxide plus cinobufacin on human hepatocarcinoma transplantation model nude mice]. *Zhongguo Zhong Xi Yi Jie He Za Zhi* **31**, 67-72 (2011).

239 Alimoghaddam, K. *et al.* Anti-leukemic and anti-angiogenesis efficacy of arsenic trioxide in new cases of acute promyelocytic leukemia. *Leuk Lymphoma* **47**, 81-88, doi:Q68622625N084430 [pii] 10.1080/10428190500300373 (2006).

240 Lengfelder, E., Hofmann, W. K. & Nowak, D. Impact of arsenic trioxide in the treatment of acute promyelocytic leukemia. *Leukemia*, doi:leu2011245 [pii] 10.1038/leu.2011.245 (2011).

241 Zhang, X. *et al.* [The impact of arsenic trioxide or all-trans retinoic acid treatment on coagulopathy in acute promyelocytic leukemia]. *Zhonghua Nei Ke Za Zhi* **40**, 829-833 (2001).

242 Chen, G. Q. *et al.* Use of arsenic trioxide (As2O3) in the treatment of acute promyelocytic leukemia (APL): I. As2O3 exerts dose-dependent dual effects on APL cells. *Blood* **89**, 3345-3353 (1997).

243 Rojewski, M. T., Baldus, C., Knauf, W., Thiel, E. & Schrezenmeier, H. Dual effects of arsenic trioxide (As2O3) on non-acute promyelocytic leukaemia myeloid cell lines: induction of apoptosis and inhibition of proliferation. *Br J Haematol* **116**, 555-563, doi:3298 [pii] (2002).

244 Park, W. H. *et al.* Arsenic trioxide-mediated growth inhibition in MC/CAR myeloma cells via cell cycle arrest in association with induction of cyclin-dependent kinase inhibitor, p21, and apoptosis. *Cancer Res* **60**, 3065-3071 (2000).

245 Park, J. W. *et al.* Arsenic trioxide induces G2/M growth arrest and apoptosis after caspase-3 activation and bcl-2 phosphorylation in promonocytic U937 cells. *Biochem Biophys Res Commun* **286**, 726-734, doi:10.1006/bbrc.2001.5416 S0006-291X(01)95416-6 [pii] (2001).

246 Larochette, N. *et al.* Arsenite induces apoptosis via a direct effect on the mitochondrial permeability transition pore. *Exp Cell Res* **249**, 413-421, doi:10.1006/excr.1999.4519 S0014-4827(99)94519-6 [pii] (1999).

247 Li, H., Zhu, X., Zhang, Y., Xiang, J. & Chen, H. Arsenic trioxide exerts synergistic effects with cisplatin on non-small cell lung cancer cells via apoptosis induction. *J Exp Clin Cancer Res* **28**, 110, doi:1756-9966-28-110 [pii] 10.1186/1756-9966-28-110 (2009).

248 Wu, J., Luo, R. C., Zhang, H. & Cui, Y. Z. [Inhibitory effect of sorafenib combined with arsenic trioxide on hepatocellular carcinoma cells]. *Nan Fang Yi Ke Da Xue Xue Bao* **28**, 639-641 (2008).

249 Chiu, H. W., Lin, W., Ho, S. Y. & Wang, Y. J. Synergistic effects of arsenic trioxide and radiation in osteosarcoma cells through the induction of both autophagy and apoptosis. *Radiat Res* **175**, 547-560, doi:10.1667/RR2380.1 [pii] 10.1667/RR2380.1.

250 Muir, V. J. & Dhillon, S. Erlotinib: as maintenance monotherapy in non-small-cell lung cancer. *BioDrugs* **25**, 139-146, doi:10.2165/11206910-000000000-00000.

251 Soria, J. C., Mok, T. S., Cappuzzo, F. & Janne, P. A. EGFR-mutated oncogene-addicted non-small cell lung cancer: Current trends and future prospects. *Cancer Treat Rev*, doi:S0305-7372(11)00218-0 [pii] 10.1016/j.ctrv.2011.10.003 (2011).

252 Kurtze, I., Sonnemann, J. & Beck, J. F. KRAS-mutated non-small cell lung cancer cells are responsive to either co-treatment with erlotinib or gefitinib and histone deacetylase inhibitors or single treatment with lapatinib. *Oncol Rep* **25**, 1021-1029, doi:10.3892/or.2011.1160.

253 Wang, W. *et al.* Crosstalk to stromal fibroblasts induces resistance of lung cancer to epidermal growth factor receptor tyrosine kinase inhibitors. *Clin Cancer Res* **15**, 6630-6638, doi:1078-0432.CCR-09-1001 [pii]
10.1158/1078-0432.CCR-09-1001 (2009).

254 Yeo, W. L. *et al.* Erlotinib at a dose of 25 mg daily for non-small cell lung cancers with EGFR mutations. *J Thorac Oncol* **5**, 1048-1053, doi:10.1097/JTO.0b013e3181dd1386.

255 Hirte, H. *et al.* A phase II study of erlotinib (OSI-774) given in combination with carboplatin in patients with recurrent epithelial ovarian cancer (NCIC CTG IND.149). *Gynecol Oncol* **118**, 308-312, doi:S0090-8258(10)00361-6 [pii]
10.1016/j.ygyno.2010.05.005.

256 Xie, X. *et al.* Combining EGFR and mTOR blockade for the treatment of epithelioid sarcoma. *Clin Cancer Res* **17**, 5901-5912, doi:1078-0432.CCR-11-0660 [pii]
10.1158/1078-0432.CCR-11-0660.

257 Bartholomeusz, C. *et al.* Gemcitabine Overcomes Erlotinib Resistance in EGFR-Overexpressing Cancer Cells through Downregulation of Akt. *J Cancer* **2**, 435-442.

258 Diep, C. H., Munoz, R. M., Choudhary, A., Von Hoff, D. D. & Han, H. Synergistic effect between erlotinib and MEK inhibitors in KRAS wild-type human pancreatic cancer cells. *Clin Cancer Res* **17**, 2744-2756, doi:1078-0432.CCR-10-2214 [pii]
10.1158/1078-0432.CCR-10-2214.

259 Martinelli, E. *et al.* Synergistic antitumor activity of sorafenib in combination with epidermal growth factor receptor inhibitors in colorectal and lung cancer cells. *Clin Cancer Res* **16**, 4990-5001, doi:1078-0432.CCR-10-0923 [pii]
10.1158/1078-0432.CCR-10-0923.

260 Herchenhorn, D. *et al.* Phase I/II study of erlotinib combined with cisplatin and radiotherapy in patients with locally advanced squamous cell carcinoma of the head and neck. *Int J Radiat Oncol Biol Phys* **78**, 696-702, doi:S0360-3016(10)00008-8 [pii]
10.1016/j.ijrobp.2009.08.079.

261 Hirai, H. *et al.* MK-2206, an allosteric Akt inhibitor, enhances antitumor efficacy by standard chemotherapeutic agents or molecular targeted drugs in vitro and in vivo. *Mol Cancer Ther* **9**, 1956-1967, doi:1535-7163.MCT-09-1012 [pii]
10.1158/1535-7163.MCT-09-1012.

262 Walker, A. M., Stevens, J. J., Ndebele, K. & Tchounwou, P. B. Arsenic trioxide modulates DNA synthesis and apoptosis in lung carcinoma cells. *Int J Environ Res Public Health* **7**, 1996-2007 (2010).

263 Munic, V., Hlevnjak, M. & Erakovic Haber, V. Characterization of rhodamine-123, calcein and 5(6)-carboxy-2',7'-dichlorofluorescein (CDCF) export via MRP2 (ABCC2) in MES-SA and A549 cells. *Eur J Pharm Sci* **43**, 359-369, doi:S0928-0987(11)00141-2 [pii]
10.1016/j.ejps.2011.05.003 (2011).

264 Pham, A. N. *et al.* Pharmacogenomics approach reveals MRP1 (ABCC1)-mediated resistance to geldanamycins. *Pharm Res* **26**, 936-945, doi:10.1007/s11095-008-9796-8 (2009).

265 Naumov, G. N. *et al.* Combined vascular endothelial growth factor receptor and epidermal growth factor receptor (EGFR) blockade inhibits tumor growth in xenograft models of EGFR inhibitor resistance. *Clin Cancer Res* **15**, 3484-3494, doi:1078-0432.CCR-08-2904 [pii]
10.1158/1078-0432.CCR-08-2904 (2009).

266 Oda, K., Matsuoka, Y., Funahashi, A. & Kitano, H. A comprehensive pathway map of epidermal growth factor receptor signaling. *Mol Syst Biol* **1**, 2005 0010, doi:msb4100014 [pii]
10.1038/msb4100014 (2005).

267 Grossmann, A. H. & Samowitz, W. S. Epidermal growth factor receptor pathway mutations and colorectal cancer therapy. *Arch Pathol Lab Med* **135**, 1278-1282, doi:10.5858/arpa.2011-0047-RA (2011).

268 Luster, M. I. & Simeonova, P. P. Arsenic and urinary bladder cell proliferation. *Toxicol Appl Pharmacol* **198**, 419-423, doi:10.1016/j.taap.2003.07.017 S0041008X04000808 [pii] (2004).

269 Tice, D. A., Biscardi, J. S., Nickles, A. L. & Parsons, S. J. Mechanism of biological synergy between cellular Src and epidermal growth factor receptor. *P Natl Acad Sci USA* **96**, 1415-1420 (1999).

270 Andrew, A. S., Mason, R. A., Memoli, V. & Duell, E. J. Arsenic activates EGFR pathway signaling in the lung. *Toxicol Sci* **109**, 350-357, doi:kfp015 [pii] 10.1093/toxsci/kfp015 (2009).

271 Sos, M. L. *et al.* PTEN loss contributes to erlotinib resistance in EGFR-mutant lung cancer by activation of Akt and EGFR. *Cancer Res* **69**, 3256-3261, doi:0008-5472.CAN-08-4055 [pii] 10.1158/0008-5472.CAN-08-4055 (2009).

272 Yun, C. H. *et al.* The T790M mutation in EGFR kinase causes drug resistance by increasing the affinity for ATP. *Proc Natl Acad Sci U S A* **105**, 2070-2075, doi:0709662105 [pii] 10.1073/pnas.0709662105 (2008).

273 Yamasaki, F. *et al.* Acquired resistance to erlotinib in A-431 epidermoid cancer cells requires down-regulation of MMAC1/PTEN and up-regulation of phosphorylated Akt. *Cancer Res* **67**, 5779-5788, doi:67/12/5779 [pii] 10.1158/0008-5472.CAN-06-3020 (2007).

274 Mellinghoff, I. K. *et al.* Molecular determinants of the response of glioblastomas to EGFR kinase inhibitors. *N Engl J Med* **353**, 2012-2024, doi:353/19/2012 [pii] 10.1056/NEJMoa051918 (2005).

275 Engelman, J. A. *et al.* MET amplification leads to gefitinib resistance in lung cancer by activating ERBB3 signaling. *Science* **316**, 1039-1043, doi:1141478 [pii] 10.1126/science.1141478 (2007).

276 Sattler, M., Reddy, M. M., Hasina, R., Gangadhar, T. & Salgia, R. The role of the c-Met pathway in lung cancer and the potential for targeted therapy. *Ther Adv Med Oncol* **3**, 171-184, doi:10.1177/1758834011408636 10.1177_1758834011408636 [pii].

277 Benedettini, E. *et al.* Met activation in non-small cell lung cancer is associated with de novo resistance to EGFR inhibitors and the development of brain metastasis. *Am J Pathol* **177**, 415-423, doi:S0002-9440(10)60096-X [pii] 10.2353/ajpath.2010.090863.

278 Hoda, M. A. *et al.* Temsirolimus inhibits malignant pleural mesothelioma growth in vitro and in vivo: synergism with chemotherapy. *J Thorac Oncol* **6**, 852-863, doi:10.1097/JTO.0b013e31820e1a25 (2011).

279 Liu, Z. M., Tseng, J. T., Hong, D. Y. & Huang, H. S. Suppression of TG-interacting factor sensitizes arsenic trioxide-induced apoptosis in human hepatocellular carcinoma cells. *Biochem J* **438**, 349-358, doi:BJ20101653 [pii] 10.1042/BJ20101653 (2011).

280 Elkind, N. B. *et al.* Multidrug transporter ABCG2 prevents tumor cell death induced by the epidermal growth factor receptor inhibitor Iressa (ZD1839, Gefitinib). *Cancer Res* **65**, 1770-1777, doi:65/5/1770 [pii] 10.1158/0008-5472.CAN-04-3303 (2005).

281 Suzuki, T., Nishio, K. & Tanabe, S. The MRP family and anticancer drug metabolism. *Curr Drug Metab* **2**, 367-377 (2001).

282 Carew, M. W. & Leslie, E. M. Selenium-dependent and -independent transport of arsenic by the human multidrug resistance protein 2 (MRP2/ABCC2): implications for the mutual detoxification of arsenic and selenium. *Carcinogenesis* **31**, 1450-1455, doi:bgq125 [pii] 10.1093/carcin/bgq125 (2010).

283 Wang, H. F. & Lee, T. C. Glutathione S-transferase pi facilitates the excretion of arsenic from arsenic-resistant Chinese hamster ovary cells. *Biochem Biophys Res Commun* **192**, 1093-1099, doi:S0006-291X(83)71529-9 [pii]
10.1006/bbrc.1993.1529 (1993).

284 Sakurai, T. *et al.* Role of glutathione in dimethylarsinic acid-induced apoptosis. *Toxicol Appl Pharmacol* **198**, 354-365, doi:10.1016/j.taap.2003.10.015
S0041008X04000821 [pii] (2004).

285 Chen, X., Zhang, M. & Liu, L. X. The overexpression of multidrug resistance-associated proteins and gankyrin contribute to arsenic trioxide resistance in liver and gastric cancer cells. *Oncol Rep* **22**, 73-80 (2009).

286 Faneyte, I. F., Kristel, P. M. & van de Vijver, M. J. Determining MDR1/P-glycoprotein expression in breast cancer. *Int J Cancer* **93**, 114-122, doi:10.1002/1097-0215(20010701)93:1<114::AID-IJC1309>3.0.CO;2-J [pii] (2001).

Ich habe mich bemüht, sämtliche Inhaber der Bildrechte ausfindig zu machen und ihre Zustimmung zur Verwendung der Bilder in dieser Arbeit eingeholt. Sollte dennoch eine Urheberrechtsverletzung bekannt werden, ersuche ich um Meldung bei mir.

Curriculum vitae

Personal Data:

Name:	Kushtrim KRYEZIU
Address:	Hauffgasse 16/9a, 1110 Wien
Date of Birth:	16.01.1985
Place of Birth:	Kapre, KOSOVO
Family status:	married
Citizenship:	Kosovar
Telephone:	+43 676 4485193
E-mail:	kushtrim-kryeziu@live.at

Education:

2010	Diploma thesis at the Institute for Cancer Research (ICR) Department of Medicine I, Medical University of Vienna, Borschkegasse 8a, A-1090 Vienna, Supervision by Univ.-Prof. Mag. Dr. Renee Schröder (University of Vienna, Department of Biochemistry and Cell biology), a. o. Univ.-Prof. Dr. Walter Berger (ICR) and Univ. Ass. Mag. Dr. Petra Heffeter (ICR)
2004 – 2010	University of Vienna, Austria (Genetics and Microbiology) specialization in molecular genetics and pathology.
2003 – 2004	University of Pristina, Kosovo (Biology)
2002	School leaving examination (Matura) at secondary school Dragash
1998 – 2002	Secondary school (Gymnasium) in Dragash, Kosovo
1990 – 1998	Primary school in Kapre and Bollobrad, Kosovo

Language skills:

Albanian (native), German (advanced), English (advanced)